GEOCHEMICAL FINGERPRINTING OF SPECULAR HEMATITE FROM PREHISTORIC MINES AND ARCHAEOLOGICAL SITES IN SOUTHERN AFRICA

by

ADAM VICTOR KIEHN

(Under the Direction of George A. Brook)

ABSTRACT

Specularite ore was collected from five prehistoric mining regions in Botswana and the Northern Cape Province of South Africa and 172 samples were analyzed by instrumental neutron activation analysis. A fingerprinting methodology was developed using the geochemical signatures of specularite sources represented by first-row transition metals. A validation set of 15 samples was chosen and underwent the fingerprinting process to test the validity of the method. A deductive elemental limit series analysis reduced the number of possible sources for each validation sample. Discriminant function analysis then correctly classified 14 of 15 validation samples and 6 of 7 specularite artifacts from archaeological sites in Botswana.

INDEX WORDS: Specularite, Hematite, Geochemistry, Provenance, Geoarchaeology, INAA

# GEOCHEMICAL FINGERPRINTING OF SPECULAR HEMATITE FROM PREHISTORIC MINES AND ARCHAEOLOGICAL SITES IN SOUTHERN AFRICA

by

ADAM VICTOR KIEHN

B.S., University of Wisconsin-Madison, 2004

A Thesis Submitted to the Graduate Faculty of The University of Georgia in Partial Fulfillment of the Requirements for the Degree

MASTER OF SCIENCE

ATHENS, GEORGIA

2008

# GEOCHEMICAL FINGERPRINTING OF SPECULAR HEMATITE FROM PREHISTORIC MINES AND ARCHAEOLOGICAL SITES IN SOUTHERN AFRICA

by

ADAM VICTOR KIEHN

| | |
|---|---|
| Major Professor: | George A. Brook |
| Committee: | Samuel Swanson |
| | Ervan Garrison |

Electronic Version Approved:

Maureen Grasso
Dean of the Graduate School
The University of Georgia
May 2008

# DEDICATION

I would like to dedicate this thesis to everyone who has helped along the way and given me a push to finally get it finished. My family has been behind me every step of the way to give me the confidence and drive to finish the work, and without their urging this work may not have come to fruition. Whitney, my fiancé, has also stuck with me through all of the lab drudgery that followed the fun fieldwork in Africa in the last 2-plus years, even during her own thesis work while in another state. And, of course, I would not have been able to do any of this without the opportunities, encouragement, advice, and means that George has given to me, even when I've been a "bottleneck" at times in the last 4 years. Thank you.

# ACKNOWLEDGEMENTS

I would like to acknowledge and say, "Thank you," to the many people and organizations that contributed time, effort, expertise, and funding to make this project successful. Funding was provided from the National Science Foundation to the University of Georgia (#9520982 and #0313826) and the University of Missouri (#0504015). My studies were made possible by assistantships from the University of Georgia Graduate School and Department of Geology.

Dr. George Brook, my Major Professor and advisor is responsible for making this project possible and helping in some way at nearly every stage with funding, advice, guidance, motivation and most especially during the six-week trip to Southern Africa to collect all of the specularite samples in 2005. Dr. Sam Swanson and Dr. Ervan Garrison also provided much essential guidance and expertise to my studies and laboratory methods.

All of my graduate student colleagues have lent valuable advice and diversions. Fuyuan Liang also gave laboratory help and advice, and Sheldon Skaggs ran my XRD samples and gave me a place to stay on my return trips to Athens when finally finishing this thesis.

Michael Glascock, Rachel Popelka-Filcoff, and Jonathan Dake of the University of Missouri granted funding, knowledge, and effort in processing so many samples by INAA.

Laboratory space and equipment was provided by Drs. Paul Schroeder and Michael Roden in Dept. of Geology and Dr. David Leigh in the Dept. of Geography at UGA.

Eugene Marais provided housing and guidance that made the trip possible and aided an attempt to sample a prehistoric mine in Klein Aus, Namibia.

Archaeological and Geologic specularite samples from the Tsodilo Hills and Toteng Site in Botswana were obtained with the help and knowledge of Alec Campbell of Gaborone, Botswana; Larry Robbins of Michigan State University, Mike Murphy of Kalamazoo Valley Community College; Bob Hitchcock of the University of Nebraska-Lincoln; Grace Babutsi and Abel Abednico Mabuse of the University of Botswana; and, of course, George Brook. Alec Campbell also provided housing and guided us to the Sebilong and Dikgatlampi mines near Gaborone.

David Morris and Leon Jacobson of the McGregor Museum in Kimberley, South Africa provided archaeological specularite sample MACG-01 and helped us find and obtain permission to sample the Blinkklipkop specularite mine.

Catrien Van Waarden housed us while in Francistown, Botswana and guided us to the Matsiloje specularite mine.

David R. Cohen of the University of Califronia-Berkeley provided archaeological specularite samples from AK-47 site in Thamaga, Botswana.

## TABLE OF CONTENTS

## LIST OF TABLES

## LIST OF FIGURES

## CHAPTER 1 INTRODUCTION

Archaeological occurrences and early historic accounts indicate that in Southern Africa specularite was heavily exploited and highly valued as a cosmetic from the Early Iron Age through the 19th century (Burchell, 1822; Thackeray et al., 1983). It was prepared for use by grinding and mixing with grease then applied to the hair and body, giving the wearer a glittering or shimmering appearance. The glittery powder is very difficult to remove completely from skin and other surfaces it contacts, much like the modern cosmetic glitter popular among young women in recent years.

Specular hematite or specularite ($Fe_2O_3$) is a mineral with steel gray to black color, metallic luster, tabular or platy crystals, and a specular or micaceous habit. It can occur in igneous, metamorphic, and sedimentary geologic settings, but the most desirable crystals, such as those sampled for this study, are most commonly found in hydrothermal vein deposits and metamorphosed hematite-rich sedimentary rocks. Specularite from these deposits is chemically and geologically similar to other pigments, such as red and yellow ochre, so similar fingerprinting methods might prove successful with these too.

Being able to provenance archaeological materials is crucial to understanding why people procured, processed and used them. In the case of specularite, there have been very few attempts to provenance archaeological finds. In Australia the isotopic and magnetic characteristics of sedimentary hematite have been used successfully to fingerprint sources (Jercher et al., 1998; Smith and Fankhauser, 1996; Smith et al., 1998; Smith and Pell, 1997). However, specularite in Southern Africa has not been fingerprinted despite widespread archaeological occurrence. The ability to source specularite, which is common at archaeological sites, could provide answers to such contentious questions as how prehistoric groups in the Kalahari region interacted (Denbow

and Wilmsen, 1986; Robbins et al., 2000; Robbins et al., 1998b). This study is an attempt to geochemically characterize and fingerprint specularite deposits from mines in Botswana and nearby in the Northern Cape Province of South Africa by applying multivariate discriminant analysis to chemical compositions determined by Instrumental Neutron Activation Analysis (INAA). In an attempt to determine their provenance, archaeological samples of specularite were subjected to the same methods once the feasibility of these techniques was proven.

### *1.1 OBJECTIVES AND ASSUMPTIONS*

The main goal of this study is to determine if archaeological specularite can be traced to prehistoric mines based on its geochemical signature. To achieve this, the study has these main objectives:

1) Begin building a database of prehistoric specularite mine locations in Botswana and NW South Africa and their geochemical compositions using geologic samples.
2) Develop a methodology for fingerprinting specularite mines using these samples.
3) Use the methodology to test if the geochemical signatures can distinguish between mines at the regional scale.
4) Apply these methods to specularite samples from archaeological contexts.
5) Assess the potential of these methods to make inferences about trade patterns based on the probable sources of the archaeological specularite.

To achieve these objectives, specularite ore was collected from 5 prehistoric specularite mining areas: Sebilong and Dikgatlampi near Gaborone in southeastern Botswana, Matsiloje near Francistown in northeastern Botswana, Tsodilo Hills in northwestern Botswana, and Blinkklipkop near Postmasburg in northwestern South Africa. Specularite from these mining

areas was compared to test whether there is enough variation to separate potential sources at the regional scale, where the mining areas are separated by dozens to hundreds of kilometers. Finally, seven archaeological samples from 5 different sites were analyzed and classified based on the geologic source training set.

There are two separate approaches to the process of provenance determination dependent on the nature of the material its sources: (1) The source based approach; (2) the artifact based approach (Glascock and Neff, 2003; Neff, 2000). The spatial distribution of sources and compositional heterogeneity of the material being sourced determine whether a source-grouping or artifact-grouping based approach is most appropriate.

Approach 1 is appropriate if the sources are few, spatially discrete, and widely separated such as lithic quarries and mines or obsidian flows. This approach starts with sampling and analysis of the raw materials from the sources. The data from the analysis is used to characterize the sources and form reference groups for classification, and then the artifacts are analyzed and compared to the source groups to determine provenance. Approach 2 is more appropriate if the sources are more numerous and not as easily delineated from each other. In this approach the finished artifacts are first analyzed and statistical methods are used to recognize patterns in the data. These observations are then compared to the raw material sources which are sampled as widely as possible to determine possible associations. In this study a source-based approach is used because the known specularite sources are few and far between.

Additionally, all provenance studies make some implicit assumptions. The violation of any of these assumptions could cause the study to fail in meeting its objectives, but success would show that these assumptions do indeed hold. According to the provenance postulate, the sourcing of materials requires that “there exist some qualitative or quantitative chemical or

mineralogical difference between natural sources that exceeds the qualitative or quantitative variation within each source" (Weigand et al., 1977). It has been shown previously that the provenance postulate holds true for fine-grained hematite and ochre when examined using geochemical and elemental methods (Erlandson et al., 1999; Kiehn et al., 2007; Popelka-Filcoff, 2006; Popelka-Filcoff et al., 2007). This postulate of greater "between group variance" than "within group variance" is applied in this study of specularite.

Provenance studies are also limited by the fact that an artifact cannot be definitely assigned to a single source until all possible sources have been identified and analyzed. However, in this study no attempt is made to define the range of variability among all possible sources; instead, samples of specularite ore from a handful of different mines and mining areas are tested to determine if they can be differentiated on the basis of geochemical characteristics. A few specularite artifacts were then sourced, with the full knowledge that not all possible sources were known or were sampled. This was done to show the feasibility of the techniques developed for answering archaeological research questions.

An important assumption made in this study is that the geochemical fingerprinting process implemented here is based on the geochemical signature of specularite and not other minerals found in the rock samples. As a result, the methods of fingerprinting used in this study are based on geochemical signatures rather than mineralological or petrographic analyses. In order to reliably source specularite this way, there must be a unique homogeneous geochemical signature for the hematite mined from each source. This signature should be apparent only in elements found primarily, or at least an order of magnitude greater, in hematite and other related heavy minerals than in associated silicate or carbonate minerals. Even if an element is geochemically significant (e.g. as a substitute for iron in hematite), it cannot be used reliably to

fingerprint hematite if it is found at similar or higher concentrations in other common minerals found at the mine. This assumption will be called the representative Specularite Signature assumption when referred to in the future.

## *1.2 GLOSSARY*

- FINGERPRINTING – Process of characterizing sources to identify unique inherent properties of each source that can be used to determine provenance.
- DISCRIMINANT FUNCTION ANALYSIS (DFA) – A two stage multivariate statistical operation that develops linear functions of multiple independent variables to maximize the ratio of between-groups variance to within-groups variance to best separate groups identified in a training set, then uses those functions to classify other cases with one of the groups. Discussed in more detail in Chapter 3.2.5.
- ELEMENTAL LIMIT SERIES ANALYSIS (ELSA) – A graphical statistical method developed for this study that uses the presence or absence of elements in the composition of a material to deductively reduce the number of possible sources. Discussed in more detail in Chapter 3.2.4.
- ELEMENTAL LIMIT SERIES (ELS) -The array of boxes representing the composition of an individual sample or group of samples compared during ELSA.
- TM – Transition Metal model abbreviation, which uses the first-row transition elements to identify geochemical signatures for specularite sources.
- ALR – Abbreviation for Additive Log Ratio transformation of the raw compositional data. Explained in further detail in Chapter 3.2.1

## *1.3 LITERATURE REVIEW*

Previously published literature relevant to fingerprinting specular hematite either deals with the characterization of hematite and iron oxides in general, which may help to lend insights into patterns in the composition of specularite, or are provenance studies on a a variety of

archaeological materials. Despite numerous provenance studies, only a handful have examined the potential of fingerprinting iron oxides and none have focused on specularite.

Geochemical and compositional provenance studies have been conducted on a wide range of materials, both natural and man-made (see for examples, Cackler et al., 1999; Glascock and Neff, 2003; Glascock et al., 2004; Neff, 2000; Weinstein-Evron and Ilani, 1994; Yong et al., 2005). Provenance studies have ranged from highly successful obsidian source fingerprinting (Glascock, 2002), to occasionally successful pottery studies (Glascock et al., 2004; Yong et al., 2005), and studies with less promising results on soapstone artifacts (Luckenbach et al., 1975; Moffat and Buttler, 1986). Despite several provenance studies on mineralogically and chemically similar ochre, there have been no published attempts to geochemically fingerprint specularite sources.

Studies using the geochemistry of obsidian to source artifacts in Central and North America and Europe have been some of the most accurate and successful provenance studies to date (see Glascock, 2002; Glascock and Neff, 2003; Tykot, 2002; and references therein). Nearly 100% of 421 obsidian artifacts from Chichen Itza analyzed using INAA were confidently associated with a single source from a database of potential sources in Mexico and Guatemala (Glascock, 2002). The chemistry of obsidian allows the delineation of nearly all sources on compositional plots showing only a few trace elements, the importance of which were suggested by principal components analysis. The Chichen Itza study was an extension of and used the database built by a previous study that successfully sourced over 90% of nearly 1200 obsidian artifacts from throughout Mesoamerica (Glascock et al., 1994).

Luckenbach et al. (1975) used INAA to successfully fingerprint soapstone artifacts in Virginia, but a follow-up study by Moffat and Buttler (1986) failed to produce reliable results

consistent with the archaeological record in Europe. Both studies used normalized rare-earth element plots and compared the graphical patterns of artifacts and known sources. The technique is based mainly on the signatures imparted by several geologic processes, which limits its ability to distinguish between sources formed by similar processes. Moffat and Buttler uncovered this problem because their source samples showed a great deal of overlap for the few REEs found at detectable levels. Thus, although REE patterns were useful for provenance of Virginia steatites (Luckenbach et al., 1975), Moffat and Buttler concluded that the most reliable provenance method for Shetland steatite was the examination of hand samples.

Cackler et al. (1999) attempted to use geochemical fingerprinting to distinguish between sources in a single chert deposit in northern Belize using INAA with simple and multivariate statistics. This study was built on and tested previous work by Tobey (1986) that used k-means cluster analysis to identify 4 distinct clusters from 80 samples spread amongst 10 sources. Tobey then used discriminant analysis to determine provenance of 160 artifacts from 10 sites and found that most could be attributed to the same cluster. Cackler et al. added an additional 101 source and 14 artifacts to Tobey's data and used cluster analysis to identify 3 clusters rather than 4. These clusters correlate to chert types and not actual quarries, so although many of the artifacts could be associated with one cluster, actual geographic sources could not be identified. Cackler et al, attribute this finding to the homogeneous nature of the single chert formation that all samples were drawn from. This allowed an incomplete sampling of a homogeneous source to mimic groupings within a heterogeneous source. Cackler et al. also point out the danger of using cluster and discriminant analysis to ferret out groups without sound reasoning for the specified groups.

There have been several attempts to characterize and fingerprint sedimentary ochre sources in Australia using various geochemical and magnetic techniques. Multiple types and colors of ochre have been used in these provenance studies. The mixed mineralogy, which includes goethite, clays, Fe-poor minerals, and amorphous phases, complicated the sourcing problem for these studies.

Weinstein-Evron and Ilani (1994) compared 93 Natufian ochre artifacts from el-Wad Cave, Israel to seven iron oxide veins within 10 km of the cave using XRD and ICP-AES to determine mineralogy and geochemistry. They used only simple statistics and determined that the composition of the artifacts and veins were very similar, but that the veins were too similar to each other to determine an exact source for any of the artifacts. Interestingly, most of the ochre artifacts were nearly all hematite and jasperoid, but the source veins were mainly jasperoid and goethite with rare hematite. Heating experiments showed that the yellow-red source goethite could be transformed into deep-red hematite by roasting at 300ºC for 2 hours, but these heat-treated ochre samples were not characterized as part of the provenance study. The authors speculate that heating ochre to improve color could have been a step toward ceramic and metallurgic technology.

Tankersley and others (1995) qualitatively compared red ochre artifacts from the Hell Gap Site, Wyoming to several possible North American ochre sources including the nearby Paleoindian ochre mining site of Powars II, Wyoming. The study used XRD and SEM to characterize the mineralogy, fabric, and biological components of the ochres. The researchers concluded that the ochre artifacts were most similar to the specular and earthy hematite mined at Powars II. This study does not offer quantitative analysis or large sample numbers, but serves as

a starting point and proves that there is great inter-source variability between the sources sampled.

Erlandson et al. (1999) characterized two prehistoric red ochre mines and six other natural red ochre occurrences in western North America using particle induced X-ray emission (PIXE) analysis. They employed principal components analysis to examine their data and concluded that each source was geochemically distinct. Source homogeneity was tested by analyzing four split samples from each of three sources which showed rather low variation between samples. However, original sample size is not given and the split samples were apparently split after crushing and homogenization so the hand-sample scale variation, not mine homogeneity, was actually tested. The researchers correctly conclude that more samples must be analyzed to truly test whether inter-source variation exceeds intra-source variation and that these sources are actually geochemically distinct. Despite these limitations, their analyses do suggest that homogeneous, geographically and geochemically discrete hematite sources can be differentiated and used to interpret mining and trade patterns in prehistory.

Popelka-Filcoff has recently conducted research on geochemically fingerprinting ochre sources in North and South America, and worked with others to follow up on the findings of Erlandson et al (Erlandson et al., 1999; Popelka-Filcoff, 2006; Popelka-Filcoff et al., 2007; Popelka-Filcoff et al., 2005). Popelka-Filcoff's work uses an artifact based approach, and shows several distinct groupings of unprovenanced artifacts from Peru (Popelka-Filcoff et al., 2007). Popelka-Filcoff established the feasibility of ochre provenance with data from previous studies augmented by INAA analysis on ochre artifacts from Peru with multivariate statistics. Results and conclusions from these studies on ochre artifacts closely agree with results from specularite studies presented here and previously (Kiehn et al., 2007; Popelka-Filcoff et al., 2007). In

particular, first-row transition metals and REEs are reliable and useful for fingerprinting the iron oxides, and discriminant function analysis is useful after log-ratio transformation of the compositional data.

Clarke (1976) qualitatively characterized red and white ochre from the Wilgie Mia pigment mine exploited by Aborigines in western Australia. Spectrographic analysis determined the relative elemental composition of the red ochre and electron probe analysis determined that the red ochre was mostly hematite and the white ochre was mostly huntite. Clarke also used optical microscopy to compare pigments from this source to a few nearby rock painting sites.

Smith and Pell (1997) used the $\delta^{18}O$ signatures of sedimentary quartz grains found in Australian red ochre to distinguish between potential sources in different geologic provinces. They used the $\delta^{18}O$ of quartz because it is less susceptible to alteration than the $\delta^{18}O$ signal of hematite and reflects the sedimentary processes that formed ochre which can identify the sample's geologic province. The researchers also suggest that this technique could be used on vein quartz associated with specularite, where the signal could identify material from different vein systems. Smith and Pell finally conclude that this technique alone would not be enough to source archaeological hematite, but should be used to screen potential sources before moving on to mineralogical and elemental analysis.

Jercher et al. (1998) characterized several Australian ochre sources using Rietveld X-ray diffraction and X-ray fluorescence analyses to quantitatively characterize their samples mineralogically and geochemically. They note that the most useful elements for fingerprinting ochre sources are the transition metals that can substitute readily for Fe in the hematite unit cell. These transition metal concentrations were also normalized by the iron content to allow comparison between sources. Problems noted by the authors are that the data collected from the

two analytical methods could not be compared quantitatively because of variable water content and amorphous phases, and that only one sample was analyzed and assumed as representative for each of 6 sources. The researchers reached the conclusions that a nested multi-technique approach has potential for fingerprinting the Australian ochre sources, but that many more samples from as many sources as possible are needed to build a complete and representative source database for truly reliable attributions.

Smith et al. (1998) built on these previous studies (Jercher et al., 1998; Smith and Fankhauser, 1996; Smith and Pell, 1997) and applied their nested techniques in an ochre provenance study at Puritjarra Rock Shelter, central Australia. They analyzed artifacts and source samples by low power microscopy, XRD, and ICP-MS to group samples by fabric and mineralogy before applying principal components and cluster analysis to their geochemical data. Their findings showed that Karrku ochre mine, located 150 km to the north, was the principal source of the artifacts from c. 32,000 – 13,000 BP, but that later a significant number of artifacts began appearing from Ulpunyali, 65 km to the southeast and local sources. The study also synthesized these findings with the known settlement patterns and regional archaeology in a rather complete interaction study. They noted that these methods could not yet be extended to actual rock art pigments because of binder and mixing complications, but overall this serves as an exemplary case study of provenance used to interpret interaction and settlement patterns.

Mooney et al. (2002) attempted to use mineral magnetics to characterize and fingerprint Australian ochre sources as a less expensive and intensive alternative to the previous isotopic and geochemical methods. The unburned and unprocessed ochre samples from the same sources that Smith and Pell (1997) used, along with several additional sources, were characterized by magnetic susceptibility, isothermal and anhysteretic remanent magnetism, and hysteresis loops

using multivariate statistics. Their findings were in line with the isotopic study (Smith and Pell, 1997), in that several sources could be ruled out for some samples, although confident provenance of an exact source for most samples was precluded by incomplete sampling and source characteristic overlap. This method appears to be a suitable alternative to more intensive techniques for Australian ochre sources that were already differentiable on the basis of mineralogy.

Previous studies determined which elements are most reliable and useful for fingerprinting specularite and other heavy minerals commonly associated with it. Preliminary analyses of specularite from mines in Southern Africa (Kiehn et al., 2007) and previous literature indicate that transition metals (TM) and rare earth elements (REE) have unique signatures associated with genetic and metamorphic processes (Harding, 2004; Popelka-Filcoff, 2006; Popelka-Filcoff et al., 2007; Smith and Fankhauser, 1996; Wernicke and Lippolt, 1994). While analyses using REE or a combined TM and REE model can both be successful in discriminating sources, the TM has a firmer theoretical basis because the mechanisms and processes that determine their presence are better understood, and generally more successful (Kiehn et al., 2007; Popelka-Filcoff et al., 2007).

A few studies illustrate the archaeological contexts of specularite. Humphreys (1974) noted four occurrences of ostrich egg shells filled with specularite discovered by plowing on farms in the Northern Cape, South Africa as well as one intact egg shell full of specularite in a burial at Driekopseiland. Jacobson (1977) reports the discovery of small ceramic vessels containing specularite on a farm in Namibia, more than 100 km from the nearest known occurrence of specularite. Two of the three Khoi style vessels were half filled with specularite.

The discovery of four other vessels containing specularite is also noted, although locations and contexts are omitted.

In summary, the published literature indicates that hematite meets assumptions for the provenance postulate and can be fingerprinted with limited success using other methods such as XRD and mineralogical comparisons. Specularite was highly valued by the people who mined and exchanged it, possibly due to the limited number of sources, which makes the source-based approach used in this study the most appropriate. Previous research also suggests that a model based on minor and trace transition metals may have discriminating potential. Also, previous provenance studies on simple or monominerallic substances have generally been more successful than those on more complex or heterogeneous rocks, providing hope for the present study.

# CHAPTER 2 BACKGROUND

## *2.1 STUDY REGIONS*

The specularite sources sampled for fingerprinting are spread widely across Southern Africa, from northern Botswana to northern South Africa. These areas are by no means a complete sample of all possible sources of archaeological specularite, nor were they likely being exploited simultaneously. Despite these limitations, the five mining regions examined will serve well as subjects to test the viability of fingerprinting specularite sources in the subcontinent.

Many of the samples collected for this study come from mines known to archaeologists at the Tsodilo Hills in northwestern Botswana. Archaeologists and early European explorers documented exploitation of specularite deposits for cosmetic purposes at Sebilong and Dikgatlampi in southeastern Botswana and at Blinkklipkop in the Northern Cape, South Africa. In addition to these sites, samples from previously undocumented prehistoric workings in the Matsiloje Range of northeastern Botswana were analyzed. The different geologic character of the specularite deposits and their wide geographic separation make these regions ideal for testing a a variety of fingerprinting methods. The remainder of this section will briefly summarize the relevant geologic and archaeological history as presented in previous literature for southern Africa and for each of the source areas.

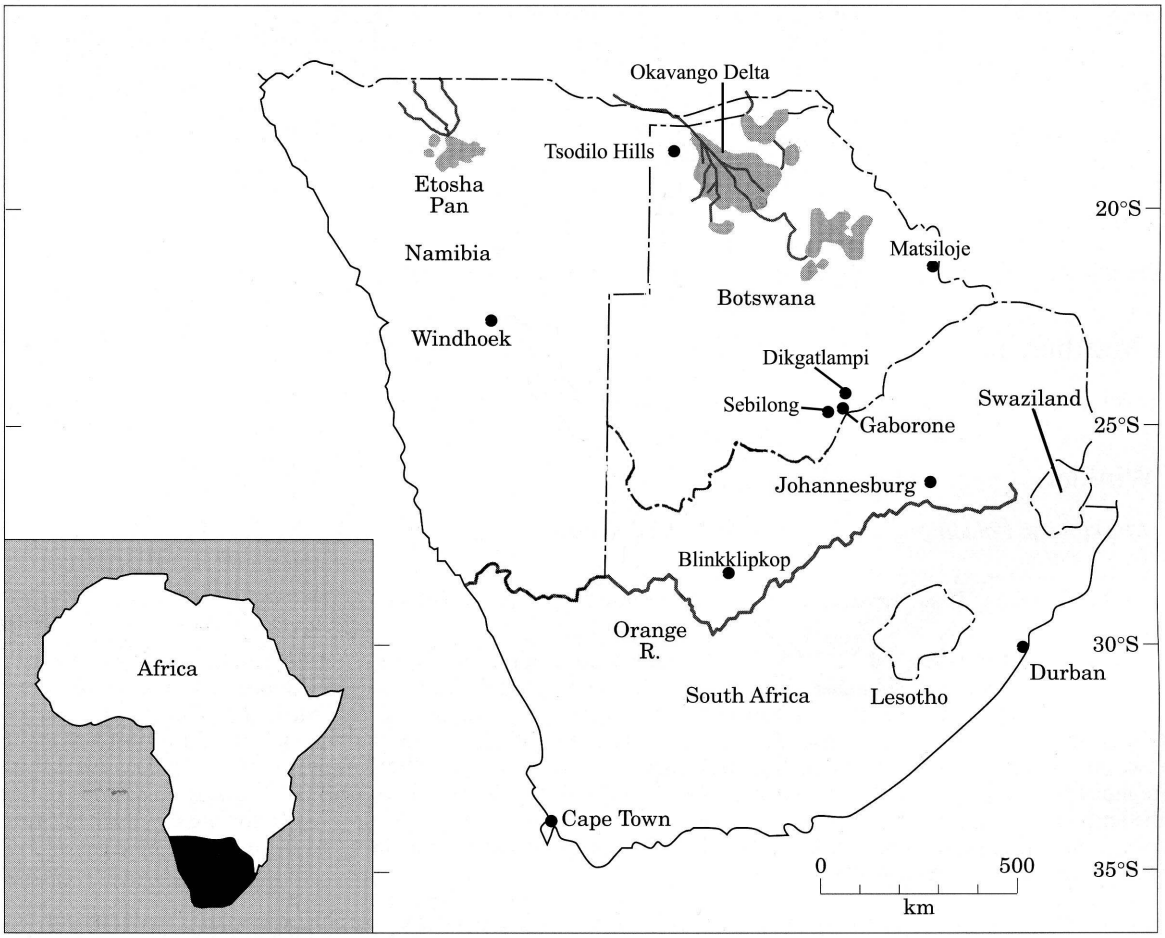


Figure 1. Prehistoric specularite mines in southern Africa examined in this research.

## *2.2 GEOLOGY AND ARCHAEOLOGY OF SPECULARITE SOURCES*

### *2.2.1 TSODILO HILLS*

The Tsodilo Hills are located in northwestern Botswana near the Okavango River; they are surrounded by sand dunes and plains. This area has proven to be one of the most interesting archaeological localities in Southern Africa, in part because hills in the region are rare, the nearest being about 200 km away. Evidence of human activity in this small area in the Kalahari Desert includes two Early Iron Age (EIA) villages, thousands of rock paintings in rock shelters and caves dating back to the Middle (MSA) and Late Stone Age (LSA), and numerous mica

schist and specularite mines (Campbell et al., 1994; Denbow and Wilmsen, 1986; Robbins, 1990; Robbins et al., 2000; Robbins et al., 1996, 1998b; Robbins et al., 1994).

There are four named hills at Tsodilo: Male, Female, Child, and North (Robbins et al., 1998b). Male Hill rises 410 m above the surrounding landscape and Female Hill is 300 m high; the other two hills are 40 m high or less. The Hills have formed in compositionally mature Precambrian quartzites and schists that have been extensively faulted and altered.

Evidence for occasional specularite mining at Tsodilo Hills dates to before 5300±160 B.P. at Rhino Cave (Robbins et al., 1996). However, radiocarbon dates from soot deposits formed during fire-spalling indicate that intensive specularite mining began ca. A.D. 800 and lasted until about A.D. 1025, a period coinciding with occupation of the EIA villages of Nqoma and Divuyu on Female Hill. The large scale of production from the mines at this time implies that specularite from the Tsodilo Hills was being traded or distributed beyond local populations. Ostrich-eggshell and ceramic containers have been found with specularite in them in Swaziland and Namibia, respectively (Humphreys, 1974; Jacobson, 1977). The Namibian find has no known source of specularite within 100 km or more, demonstrating long distance transport (Beaumont, 1973). Glass beads and marine shells dating to around 900 A.D., found at Nqoma, are also evidence that these people had trade networks extending as far as the Indian Ocean (Denbow and Wilmsen, 1986).

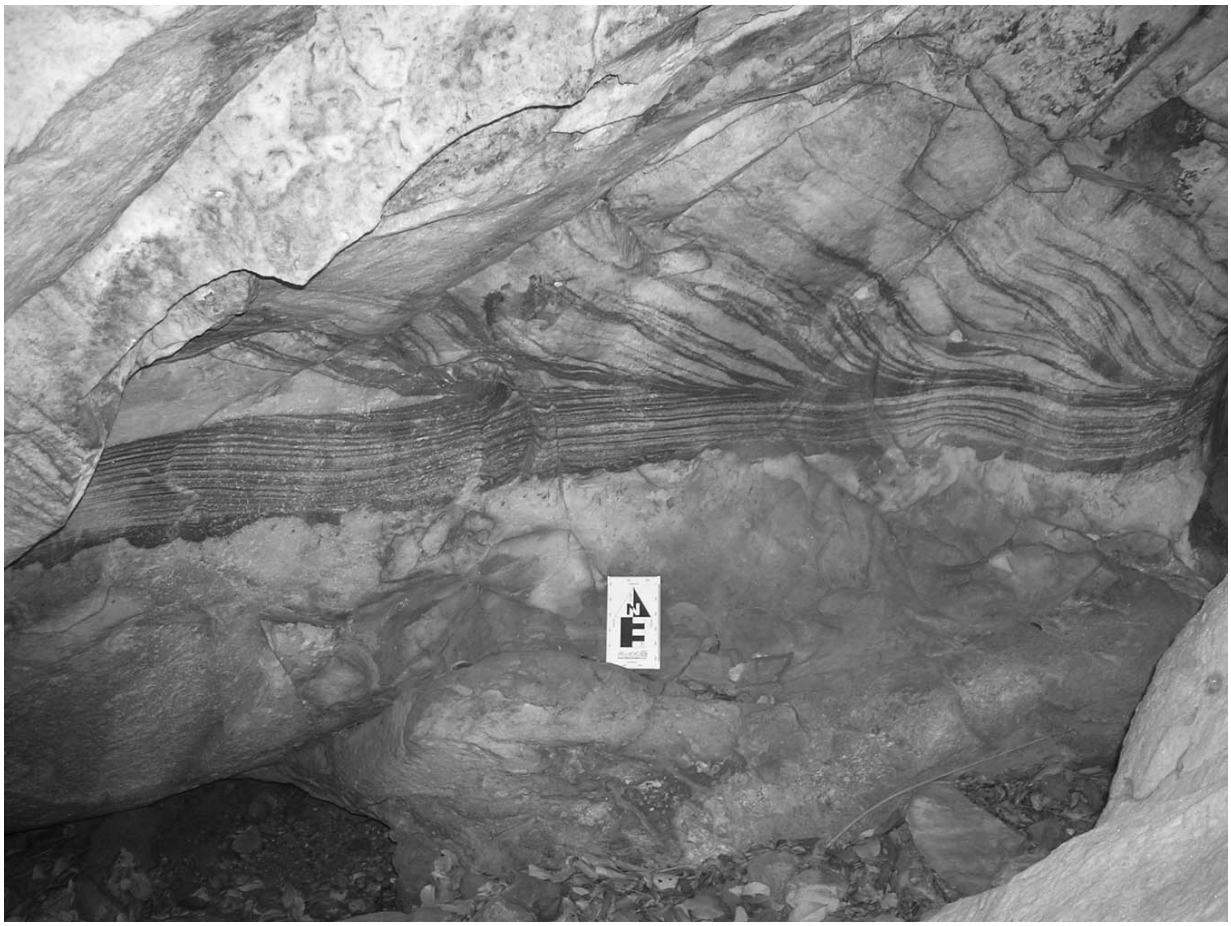

Figure 2. Hematite concentrated on remnant cross-bedding planes in Precambrian quartzite at Mike Main Mine in Female Hill, Tsodilo Hills, Botswana.

### *2.2.2 MATSILOJE*

The Matsiloje mine is located in a range of steep-sided hills rising from the plains of northeastern Botswana. The Matsiloje Range is near Botswana's border with Zimbabwe and is approximately 40 km east-southeast of Francistown. It reaches up to 200 m above the surrounding plain and is about 1 km wide. The Range is formed of Archean metasedimentary and metavolcanic rocks running roughly north-south for about 20 km (Key, 1976), and is composed mostly of folded and faulted amphibolites, banded ironstones, and quartz schists belonging to the Lady Mary Formation of the Tati Schist Group.

There are several abandoned gold mines in the Range which like the ancient specularite mine are associated with fault zones. While fine-grained specularite is available throughout exposures of this banded ironstone, specularite crystals are concentrated in altered zones. The ancient specularite mine examined here is at the top of the ridge in a saddle that is used today and likely in the period of the workings, as a low pass through the hills. The mining site appears to be exclusively above-ground and roughly comparable in scale to many of the workings at Tsodilo. This site has not been excavated and is otherwise undocumented so exact dates are unavailable, although many dolerite hammerstones and suggestions of historical European workings were found, suggesting exploitation had begun by the late prehistoric.

### *2.2.3 SEBILONG AND DIKGATLAMPI*

Sebilong and Dikgatlampi are located approximately 40 km WSW and 60 km NNW of Gaborone, respectively, in southeastern Botswana. The topography of the area generally consists of plains and flat alluvial valleys interrupted by sharp hills and tablelands. The Sebilong mine is located on a cliff face at the edge of a plateau in the Sesitajwane Hills between Thamaga and Moshupa (Campbell and Main, 2003). The plateau is composed of the Mannyelanong Formation of the early to mid-Proterozoic Waterberg Group. This formation is mainly cross-bedded red quartz sandstones and is brecciated and altered in zones where coarse-grained specularite is concentrated in and near quartz veins (Aldiss et al., 1989).

Fire-spalling was used to extract a large amount of specularite, as evidenced by the tailings that form a scree slope from the workings near the top of the 80 m high cliff to the base where slag from iron-smithing has been found (Campbell and Main, 2003). The site has not been excavated but thermoluminescence (TL) dating and historical accounts place the workings between the 14$^{th}$ and 19$^{th}$ centuries, with evidence for iron smelting at the base of the cliff dating

to the latter part of the period. This region, near the village of Thamaga, has several other hills and ridges similar to the one exploited at Sebilong that have more unreported prehistoric mining sites (Campbell, pers. comm.).

The Dikgatlampi workings are located in one of a series of low hills rising from a plain 8 km SE of the village of Lentsweletau. There are roughly two dozen pits in a two hectare area. The pits exploit specularite found in brecciated zones of the sandstone and conglomerate that form the hill. As at Sebilong, these rocks belong to the Mannyelanong Formation of the Waterberg Group (Aldiss et al., 1989; Campbell and Main, 2003). Preliminary excavation of one of the pits revealed pottery and metal tools thought to date to the 17$^{th}$ century, however no direct dates are available. Also no evidence for iron working or prehistoric settlement has been found at the site, but more ancient workings cannot be completely ruled out (Campbell and Main, 2003; Cohen, 1977).

### *2.2.4 BLINKKLIPKOP*

Blinkklipkop is one the best-documented specularite mines in southern Africa. It is located 5 km NE of Upington in the Northern Cape Province of South Africa and is one of many specularite workings in the area, several of which are rather extensive like Blinkklipkop. Other names applied to Blinkklipkop have been Gatkoppies, Sebilo, and Tsanstabane. The mine is located in the rather high relief hills underlain by rocks belonging to the Transvaal Supergroup. Blinkklipkop is near the geologic contact of the Campbellrand and the Asbestos Hills Subgroups in brecciated banded iron formation rocks where concentrations of specularite are associated with vein quartz (Harding, 2004).

The specularite deposits are in the Blinkklip Breccia that formed syndepositionally and postdepositionally from the Asbestos Hill Banded Ironstone formation dated to 2432 +/- 31 Ma

(Trendall et al., 1990; von Plehwe-Leisen and Klemm, 1995). The breccia is formed of consolidated clasts of chemically precipitated banded ironstones that were broken by karstic collapse of the underlying Campbellrand dolomite. The clasts were cemented by iron-rich ooze in sinkholes and then overlain by subsequent banded iron formations (von Plehwe-Leisen and Klemm, 1995).

There are numerous accounts of this particular mine from early 19$^{th}$ and 20$^{th}$ century explorers and missionaries including descriptions of the former extent of the subterranean workings, much of which have since collapsed (Thackeray et al., 1983). Currently, a man-made cave about 5 m high extends about 10 m into the hillside. Past accounts describe a number of narrow inclined tunnels stretching for nearly 100 yards into the hillside from the cave (Thackeray et al., 1983; Wagner, 1928). Radiocarbon dates from excavations show that the mine was being worked at 1200 B.P. and during several episodes afterward, although even earlier exploitation cannot be ruled out (Thackeray et al., 1983). This pattern is very similar to the Doornfontein mine 12 km NW of Blinkklipkop which indicates a significant demand for specularite during this period (Beaumont and Boshier, 1974).

### *2.3 ARCHAEOLOGICAL SAMPLES*

Due diligence must be taken with the alteration or destruction of archaeological material in provenance studies as with any other scientific study. This is especially true of the archaeological specularite processed in this research because it is generally found in very limited quantities, often only a few dozen grams. While there are dozens of archaeological samples available from the Tsodilo Hills (Miller and van der Merwe, 1994; Murphy et al., 1994; Robbins et al., 2000; Robbins et al., 1996, 1998b), only a few were chosen for this proof-of-method study rather than potentially crushing samples and losing valuable data before these methods showed success.

Fewer archaeological samples were available from the other regions so nearly all of these were used in this study.

In total, seven archaeological samples were prepared for INAA from five separate archaeological sites (Table 1, Figure 1, Figure 3). Rhino Cave and Nqoma are both in the Tsodilo Hills, so the labels in Figure 3 are omitted, and sample MACG-01 has no provenance.

Samples AK47-01 and AK47-02 are from site AK47 in Thamaga, Botswana (provided by David R. Cohen, UC-Berkeley). The proximity of the Sebilong and Dikgatlampi mines, 10 km and ca. 50 km away, respectively, make these the most likely sources for these samples.

Sample MACG-01 was acquired from the McGregor Museum in Kimberley, South Africa and is of unknown provenience. The sample was provided by David Morris and Leon Jacobson, who both suggested that it was taken from the Blinkklipkop mine which was also sampled as a geologic source. Morris and Jacobson based their assessment on the proximity of the mine and the general resemblance of the specimen to deposits at Blinkklipkop, which has seen extensive excavation and distribution of materials during history and prehistory (Morris and Beaumont, 2004; Thackeray et al., 1983).

Sample NQOM-01 was excavated from the Nqoma site in the Tsodilo Hills (Phaladi, 1991). Nqoma is an Early Iron Age site on Female Hill and is also described in Section 2.2.1. This sample is obviously expected to come from one of the specularite deposits in the Tsodilo Hills.

Samples TSRC-01 and TSRC-01 were both excavated from Rhino Cave in Tsodilo Hills which has MSA and LSA artifacts and rock art (Robbins et al., 1996). As with NQOM-01, these samples probably came from one of the local mines.

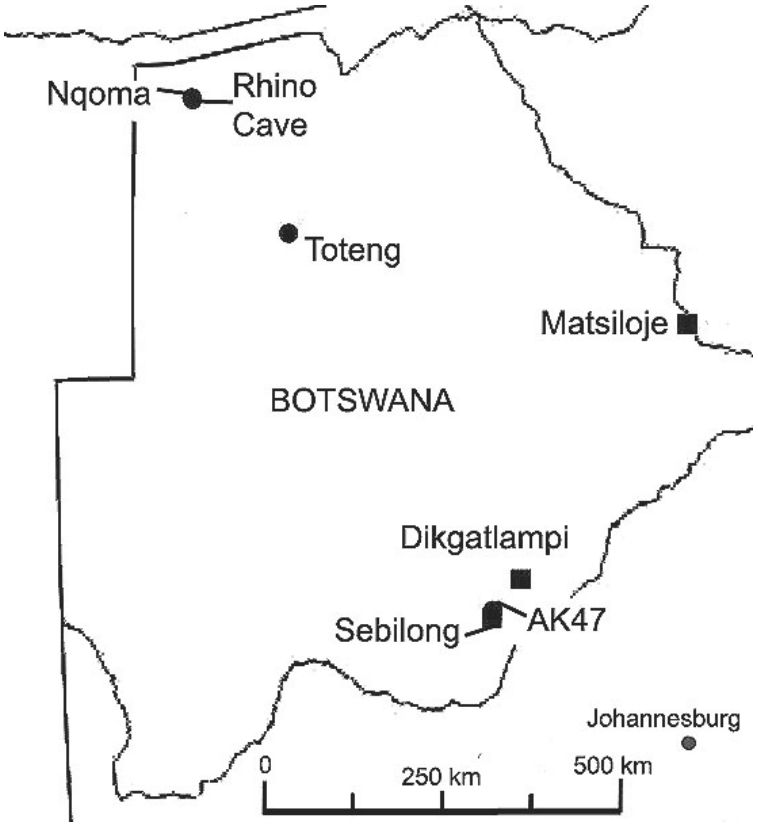


Figure 3. Map of Botswana showing locations of archaeological specularite samples in relation to selected possible geologic sources.

Sample TOTG-01 is from an open-air archaeological site at Toteng near the Nchabe River that flows into Lake Ngami. This site is dozens of kilometers from the nearest specularite outcrops (Robbins et al., 1998a) and the most obvious source is the Tsodilo Hills.

So, the three samples from archaeological sites at Tsodilo are most likely to have been obtained from the Tsodilo Hills mines, and the sample from Toteng may also be from Tsodilo despite the hills being about 400 km to the north. If distance to source is a major factor, the samples from Thamaga should match either the Sebilong or Dikgatlampi mines, while MACG-01 may have been obtained at Blinkklipkop.

Table 1. List of archaeological specularite samples and provenience information

| Sample ID | Mass (g) | Location | Site | Provenience |
|---|---|---|---|---|
| AK47-01 | 0.728 | Thamaga, Botswana | AK47 | Square F4-8 |
| AK47-02 | 0.729 | Thamaga, Botswana | AK47 | Square E6-1 |
| MACG-01 | 0.88 | South Africa | Unknown | Unknown |
| NQOM-01 | 0.464 | Tsodilo Hills, Botswana | Nqoma | Square 80W 34S, 0-10 cm |
| TSRC-01 | 0.527 | Tsodilo Hills, Botswana | Rhino Cave | Square 3, 95-100 cm |
| TSRC-02 | 1.022 | Tsodilo Hills, Botswana | Rhino Cave | Square 3, 50-55 cm, gravel area |
| TOTG-01 | 0.605 | Toteng, Botswana | Toteng | Gulley surface collection with Late Stone Age material |

# CHAPTER 3 METHODOLOGY

## *3.1 LABORATORY METHODS*

Heavy minerals, including specular hematite, were concentrated in order to reduce spurious variation introduced by non-hematite minerals in hematite-poor geologic samples to avoid violating the Specularite Signature assumption. Most archaeological samples are already very rich in hematite, but those that are not must also be concentrated in the same way before analysis. The archaeological samples were only subjected to INAA and not thin sectioning or XRD analysis due to their small sizes.

Hand samples of about 50-300 grams each were crushed using a Plattner mortar then ground to a monominerallic grain size with a mullite mortar and pestle. The actual grain size distribution depended on the rock, but was generally between fine and coarse sand sizes. The heavy mineral fraction was obtained by gravity separation in Tygon tubing filled with sodium polytungstate solution with density greater than 2.9 $g/cm^3$. Once the samples had completely settled, the tubing was clamped between the settled grains at the bottom and the remaining suspended material to separate the light and heavy fractions. The bottom clamp was opened over a Buchner funnel with filter paper over a vacuum flask, releasing the heavy fraction which was rinsed several times with deionized water to remove and recover the Na-polytungstate solution from the sample. The sample was then washed from the filter paper with ethanol or acetone and allowed to dry at room temperature. The light fraction was recovered in the same manner.

The heavy mineral fractions were inspected and described at before crushing and heavy mineral separation with 10-45x binocular magnification. The mineralogy of the samples at this scale was recorded and any trace or accessory minerals noted as well, along with miscellaneous observations. This description is relatively limited, and only quartz, hematite, and muscovite

mica were present in most samples, and kyanite was noted in only a handful of the Tsodilo Hills samples (Table 29). In nearly all of the 172 samples, the same minerals were present in the concentrated sample as the original rock, just in different proportions. More detailed thin-section petrography and XRD revealed the same mineralogy (Chapter 4.1), with the addition of fine-grained garnet in some of the Tsodilo Hills samples that was not visible at this scale.

If there appeared to be at least 0.5 g of hematite total, but less than about 30% by volume in the sample, the heavy mineral concentration was repeated before submitting the samples for INAA analysis to further concentrate the hematite. The powdered sample was again described and judged subjectively on the amount of non-hematite minerals remaining in the powder after heavy mineral separation based on the color. This data is summarized and reported in Table 29 in the Appendix. Generally, the remaining heavy mineral fraction weighed a few grams, but ranged from 0.5 – 15 grams depending on the size of the original hand sample and its relative hematite content, easily enough for INAA, which required only 100 mg (Glascock, pers. comm., 2005). The large samples were ground to a fine powder using a corundum mortar and pestle to homogenize the material and reduce variability of the INAA readings (following M. Glascock, pers. comm., 2005).

Contamination by the heavy mineral concentration process was a concern. This was addressed by comparing the composition of two powder replicate samples analyzed by INAA, one of which underwent heavy mineral concentration and one that did not (TSO-022 in Table 28 and TSO-005 in Table 27, respectively). The log-ratio values of most elements present in these samples are nearly identical, especially for the elements used for discriminant function analysis (Table 2). This demonstrates that contamination by the hematite concentration procedure is not significant, and samples are comparable whether or not they have undergone the procedure.

Table 2. Comparison of replicate sample log-ratios before and after heavy mineral concentration.

| Sample | lrSc | lrTi | lrV | lrCr | lrMn | lrCo | lrSb | lrNi |
|---|---|---|---|---|---|---|---|---|
| MHO005 | 4.736 | 1.277 | 2.738 | 4.333 | 2.638 | 3.874 | 5.628 | 3.631 |
| MHO022 | 4.742 | 1.254 | 2.722 | 4.330 | 2.625 | 3.873 | 5.627 | - |
| Mean | 4.739 | 1.266 | 2.730 | 4.332 | 2.631 | 3.873 | 5.627 | - |
| Std. Dev. | 0.005 | 0.016 | 0.011 | 0.002 | 0.009 | 0.001 | 0.001 | - |
| CoV* | 0.001 | 0.013 | 0.004 | 0.000 | 0.003 | 0.000 | 0.000 | - |
| Sample | lrZn | lrAl | lrLa | lrSm | lrEu | lrTh | lrHf | lrNa |
| MHO005 | 3.914 | 2.078 | 5.935 | 6.429 | 6.933 | 6.015 | 6.217 | 3.559 |
| MHO022 | 3.834 | 2.130 | 5.972 | 6.535 | - | 6.357 | 6.356 | 3.602 |
| Mean | 3.874 | 2.104 | 5.954 | 6.482 | - | 6.186 | 6.287 | 3.581 |
| Std. Dev. | 0.056 | 0.037 | 0.027 | 0.075 | - | 0.242 | 0.098 | 0.031 |
| CoV* | 0.014 | 0.018 | 0.004 | 0.012 | - | 0.039 | 0.016 | 0.009 |

* CoV is Coefficient of Variation

INAA was conducted at the Missouri University Research Reactor (MURR). Samples of approximately 50 – 100 mg were subjected to long and short irradiations using the same methodology applied to pottery and other materials with appropriate reference standards (Glascock et al., 2004). Table 3 lists the detection limits for each of the 33 elements in an iron-rich matrix as determined at MURR measured in 172 samples (Glascock, pers. comm.; Glascock, 2004; Popelka-Filcoff, 2006).

Table 3. Minimum detection limits of selected elements for INAA (Popelka-Filcoff, 2006).

| **Element** | **Fe** | **Sc** | **Ti** | **V** | **Cr** | **Mn** | **Co** | **Sb** | **Ni** | **Zn** | **Al** |
|---|---|---|---|---|---|---|---|---|---|---|---|
| Detection Limit (ppm) | 500 | 0.02 | 700 | 2 | 2 | 5 | 0.1 | 0.1 | 150 | 5 | 2000 |
| **Element** | **As** | **La** | **Ce** | **Nd** | **Sm** | **Eu** | **Tb** | **Dy** | **Yb** | **Th** | **U** |
| Detection Limit (ppm) | 2 | 0.1 | 2 | 5 | 0.02 | 0.02 | 0.2 | 0.2 | 0.2 | 0.2 | 1 |
| **Element** | **Lu** | **Ta** | **Rb** | **Cs** | **Zr** | **Hf** | **Ca** | **Sr** | **Ba** | **Na** | **K** |
| Detection Limit (ppm) | 0.04 | 0.1 | 10 | 0.3 | 50 | 0.2 | 500 | 100 | 100 | 20 | 2000 |

It is important to note that the heavy mineral concentration process only removes the majority of the light minerals but not all of them. Also, any heavy minerals other than hematite will remain in the sample. The main goal of the concentration process was simply to concentrate the heavy minerals, especially hematite, and remove the light minerals so that the tailings samples more closely approximated the specularite-rich archaeological samples. Most first-row

transition metal cations substitute into the hematite crystal structure and are immobile during most chemical weathering (Cornell and Schwertmann, 2003). Other geochemical studies of red ochre have also shown these elements to be the most significant for source determination as well, despite hematite content ranging from <10 wt% to >70 wt% (Popelka-Filcoff, 2006), which suggests that minerals besides hematite contribute little to the concentrations of those elements. Thus, it is assumed that the contribution of the light minerals to the geochemical signature is negligible, especially after the data preparation methods outlined in the next section.

### *3.2 DATA ANALYSIS*

Preliminary analysis of the data eventually led to the methodology of fingerprinting presented here. The large volume of geochemical data was collected in stages, and initial analysis was conducted using some samples from the Tsodilo Hills and all samples from Sebilong and Dikgatlampi. Several statistical methods were tested through repetition and refinement using varying parameters including:

- Correlation and covariance analyses to identify patterns among the elements
- Plotting elemental concentrations and ratios against each other
- K-means cluster analysis
- Simple methods of zero replacement
- Discriminant function analysis (DFA) using different sets of source groups and elements, including Transition Metals (TMs) and Rare Earth Elements (REEs), and methods of DFA such as stepwise versus simultaneous entering of variables.

Results of these first studies were reasonably successful and have been published in Kiehn et al., (2007). Subsequent studies using additional sample data and published information (Bau and Dulski, 1996; Cornell and Schwertmann, 2003; Erlandson et al., 1999; Popelka-Filcoff et al.,

2007) helped refine the methodology outlined in Kiehn et al. (2007). The following were important in shaping the methodology presented here and applied in this study:

1) Discriminant function analysis (DFA) was found to be the most accurate method for classifying geologic samples with the correct mines.
2) To satisfy assumptions of normality, remove effects of scale, and to normalize samples with varying hematite content, it was necessary to us a log transform of the elemental ratios to iron for each sample for multivariate statistics instead of raw compositions.
3) Problems with missing values limit which elements can be log-transformed and used for DFA.
4) Missing values or values below the detection limits of INAA are not randomly distributed among mine groups in many important elements such as Ti. These mines with missing elements are important and useful data, but cannot be considered by DFA, following observation (3) without more data preparation.
5) Simple replacement of missing values with a single value at or below the detection limit allows for these elements and samples to be used in DFA, but can alter the variance and true signals present in the specularite. Thus, simple zero replacement was eschewed in favor of omission of samples with zeroes.
6) Transition metals are the most important elements for discriminating between mines. REEs also help in some cases, but their overall contribution to model accuracy is insignificant, so it is best to focus only on the TMs for complicated multivariate analyses such as DFA.

7) A deductive method of limiting the number of mines included as possible sources for DFA is necessary. This led to the development of graphical elemental limit series (ELS) analysis.

The resulting data analysis methods can be broken down into two stages: (1) elemental limit series analysis which uses the presence/absence of elements to deductively limit potential sources, and (2) discriminant function analysis. After stage 1, some data preparation was necessary for the data to meet the assumptions and requirements of the more statistically advanced DFA procedures. The ELS method uses the differences in presence or absence of individual elements at detectable levels between sources to form a graphic series similar in appearance and application to DNA fingerprints formed by gel electrophoresis. Group ELSs are compared to those of the samples being classified, and the set of possible sources is reduced deductively. The sources remaining after ELS analysis are used as the training set for DFA. Multivariate DFA was then used to compare the geochemical signature of the randomly chosen validation samples to those of the training groups, ideally resulting in a logical and accurate classification.

ELS analysis serves two purposes. First, as stated previously, it reduces the set of possible sources to include in DFA, which classifies samples more accurately when there are fewer groups. Secondly, it prevents fatal errors in the statistical program. The ELS analysis chooses the sources that are the best matches for the validation sample. The validation or archaeological sample(s) determine which elements are used for DFA; samples with missing values are omitted from DFA by default, so only the elements present in the validation sample can be used.

Without the ELS, all mines would be included in the classification functions, but some groups may turn out to be "empty", or have most or all of its samples omitted, because one or more elements are missing from most or all of the samples in the mine, even though they are present in the sample(s) being classified. If the group is completely empty the statistical program will have a fatal error and stop the DFA process. If the majority of the samples in a group are omitted, the accuracy of the DFA is impacted because the number of samples will not be robust or representative of the overall group signature. Neither of these situations is desirable, and ELS helps to prevent them occurring. However, the implementation of ELS can still have the last-mentioned problem as discussed in Chapter 4.3.2 during Archaeological DFA Trial 3a. The details and implementation of ELS analysis are discussed in Chapter 3.2.4.

### *3.2.1 DATA PREPARATION*

The raw compositional data from INAA do not meet the mathematical requirements for the advanced statistical methods to be used later and must be modified to improve statistical validity and usefulness. Previous work using subcompositions (selected groups of elements rather than the total composition of the rock) in geochemical data analysis suggests that raw compositional data are not suitable for multivariate methods such as discriminant function analysis (DFA) (Aitchison, 1986). This is because DFA assumes that the variables are continuous scale unconstrained variabless that are normally distributed between groups.

Several transformations have been suggested in the geochemical statistical literature, and for the purpose of this study, a modification of the additive log-ratio transform (ALR) was used to transform the bounded subcompositional data to meet the assumptions of DFA. ALR was suggested by Aitchison (1986) and serves to unconstrain the data while preserving the elemental ratios regardless of the subcomposition or denominator chosen.

The ALR transformation process consists of forming ratios between each element in the subcomposition and another arbitrarily chosen element that is present in but variable across all samples, these ratios are then converted to logarithms. The mathematical form of the transformation used in this study is:

$$\mathbf{lrX_{sample} = Log_{10}\,(\,Fe_{sample} / X_{sample}\,)}$$

where X is the raw concentration of an element for the sample; Fe is the raw concentration of iron in that sample; and lrX is the ALR transformed log-ratio of X.

The raw concentration of iron was chosen for the denominator because this essentially normalizes the data for relative hematite content. Additionally, the small degree of analytical error associated with most INAA analyses does not significantly affect the log-ratios in this study because most elements in the subcomposition occur at levels several orders of magnitude lower than Fe. In the following sections, ALR transformed data have "lr" prepended to the atomic symbol while raw data are simply denoted by the atomic symbol.

One drawback to this transformation is that a log-ratio cannot be taken for elements not present or below detection limits. Sophisticated multiple imputation techniques, simple replacement, and variable omission are strategies for dealing with these zeroes (Aitchison, 1986). Simpler strategies of replacement with a single value for each missing element allow all data to be transformed and included in DFA, but can artificially change the variance of samples for a mine with harmful effects on the DFA.

The more sophisticated techniques replace the missing values by simulating the distribution of the real population, and maintain the source variance. However, these reliable techniques are much more complicated and impractical for implementation in this beginning study due to time and computing constraints. So, elements not present in all samples were simply

omitted from the DFA. As a result, the ELS technique was developed to use omitted elemental data to help improve DFA accuracy, and to mitigate the apparent loss of relevant data caused by omitting elements with zero or below detection values from the DFA.

### *3.2.2 SAMPLE SELECTION*

Samples with <225,000 ppm Fe, or approximately one-third hematite after heavy mineral concentration, were excluded from the analyses to avoid violating the Specularite Signature assumption. In any case, samples with extremely low specularite content are unlikely to be useful in describing archaeological samples. Eleven samples were excluded, one from Blinkklipkop and ten from Tsodilo Hills (Table 26 in Appendix). The low hematite of these samples may reflect difficulty at some mines to obtain samples rich in specularite as these had been removed by the miners leaving deposits less rich in the mineral.

Replicate powder samples were also excluded to avoid artificially increasing confidence in the DFA. Replicate samples were analyzed to check sample homogeneity and reproducibility of INAA. Only one sample from each set of replicates was included in the ELS analysis, so a total of eight samples were excluded: four from Dikgatlampi, three from Sebilong, and one from Tsodilo (Table 27 in Appendix).

The remaining geologic samples were split into training and validation sets to test whether a validation sample from one of the 5 sources can be confidently associated with the correct region using first ELS and then DFA. This was done to evaluate the methods without sacrificing valuable archaeological samples. Only training samples were used for ELS and to develop the classification functions in DFA. The validation samples were treated as archaeological samples of unknown provenance and classified using the results of analyses on the training set.

Validation samples were about 10 % of the total data set (15/152) and were selected proportionally rather than completely randomly to ensure that Dikgatlampi and the other sources with fewer samples were left with enough training samples for statistical robustness during DFA. Blinkklipkop, Matsiloje, and Sebilong provided two validation samples each, whereas Dikgatlampi provided one and Tsodilo eight (Table 4).

Table 4. Training and Validation sample distribution among specularite sources.

| Source | Total Samples | Training Samples | Validation Samples |
|---|---|---|---|
| Blinkklipkop | 26 | 24 | 2 |
| Dikgatlampi | 11 | 10 | 1 |
| Matsiloje | 21 | 19 | 2 |
| Sebilong | 23 | 21 | 2 |
| Tsodilo | 71 | 63 | 8 |
| Total | 152 | 137 | 15 |

### *3.2.3 SELECTION OF VARIABLES*

Steps were taken to ensure that conclusions and inferences would meet the Specularite Signature assumption and to avoid contamination during preparation of the samples for INAA. Published information on the geochemistry of hematite and other iron oxides (Harding, 2004; Singh and Gilkes, 1992; Singh et al., 2000; Wernicke and Lippolt, 1994) and preliminary analyses in this study suggest that the most likely and reliable elements for fingerprinting specularite sources are ion species that can easily substitute into the hematite crystal lattice for $Fe^{3+}$, such as the transition metals. Therefore, the elements selected for use in this study have ionic radii or charge to radius ratios similar (within about 10%) to that of $Fe^{3+}$ (0.65 Å) in crystalline phases . They include: $Sc^{3+}$ (0.75 Å), $Ti^{4+}$ (0.61 Å), $V^{4+}$ (0.54 Å), $Cr^{3+}$ (0.62 Å), $Mn^{3+}$ (0.65 Å), $Co^{3+}$ (0.74 Å), $Ni^{2+}$ (0.69 Å), $Al^{3+}$ (0.54 Å), and $Sb^{5+}$ (0.76 Å) (Shannon, 1976).

If these transition metal elements are primarily present in hematite, their ratios to iron should be relatively consistent, even among samples with varying hematite content. This is

shown to be the case by five replicate samples from Dikgatlampi, which were split from a single heavy mineral concentrate sample. Table 5 shows that the raw compositions, but not the ratio of elements to iron, of the replicate samples differ markedly despite attempts to homogenize the samples by grinding; this is most likely because the small sample sizes used for INAA can find heterogeneity even in samples that are homogeneous at larger scales, or the inclusion of a small amount of impurity that would be overshadowed in a larger bulk sample. This anomalous variability is also known as the 'nugget effect'.

The nugget effect is illustrated most clearly by the anomalously high Co value in DIK-066 compared to the other replicate samples. In some cases, a very small inclusion of a different heavy mineral phase could change the geochemical signature, but a large data set and use of multiple transition metals should dampen the negative effects of this extraneous variation. If these precautions do not work as presumed, then the multivariate analyses would ultimately fail. However, success of these methods will show that the assumptions do hold and that the nugget effect is not a major problem in this case.

Table 6 shows that the log-transformed values have very low coefficients of variation (CV) for a set of replicate samples. CVs of log-ratios for the hematite substituents are 0.01 or lower, except for lrCo. CVs of log-ratios for the rare-earth elements are 0.01-0.02, but CVs of log-ratios for the other elements suspected to be primarily present in the non-hematite minerals are higher, mostly between 0.04 and 0.18.

Low variation in the transformed values of the transition metals between these replicate samples demonstrates that normalizing the compositions for iron content is an effective solution for the variable hematite content problem. Additionally, it shows that this treatment of the data

is robust against the slight variations introduced by the small sample sizes used for INAA, despite a relatively homogenized sample.

Table 5. Raw compositions and summary statistics for five replicate heavy mineral concentrate samples from Dikgatlampi Mine, Botswana as determined by INAA.

| Sample ID | Fe[a] | Sc | Ti | V | Cr | Mn | Co | Sb | Ni | Zn | Al |
|---|---|---|---|---|---|---|---|---|---|---|---|
| DIK-066 | 529025 | 24.96 | 5227 | 1009.2 | 321.3 | 202.5 | 106.5 | 30.8 | 0 | 176.5 | 14396 |
| DIK-067 | 471677 | 20.64 | 4837 | 1111.7 | 280.0 | 213.7 | 4.4 | 30.9 | 65.9 | 236.1 | 27446 |
| DIK-068 | 443017 | 18.09 | 4333 | 968.4 | 255.0 | 177.8 | 4.0 | 29.8 | 119.3 | 106.7 | 33696 |
| DIK-069 | 400726 | 16.64 | 3809 | 887.7 | 234.0 | 168.8 | 4.0 | 27.7 | 0 | 32.2 | 41582 |
| DIK-070 | 539791 | 21.64 | 5415 | 1227.5 | 308.0 | 221.8 | 4.7 | 35.2 | 0 | 47.0 | 29668 |
| Mean | 476847 | 20.40 | 4724 | 1040.9 | 279.6 | 196.9 | 24.7 | 30.9 | 37.0 | 119.7 | 29358 |
| S.D. [b] | 58417 | 3.23 | 658 | 131.9 | 36.2 | 22.8 | 45.7 | 2.7 | 54.1 | 86.4 | 9948 |
| C. of V. [c] | 0.12 | 0.16 | 0.14 | 0.13 | 0.13 | 0.12 | 1.85 | 0.09 | 1.46 | 0.72 | 0.34 |
| Sample ID | As | La | Ce | Nd | Sm | Eu | Tb | Dy | Yb | Lu | Th |
| DIK-066 | 112.4 | 31.48 | 121.28 | 19.39 | 7.61 | 2.10 | 1.16 | 7.91 | 8.16 | 0.99 | 62.76 |
| DIK-067 | 87.9 | 24.40 | 94.63 | 17.97 | 5.81 | 1.43 | 0.94 | 7.23 | 5.91 | 0.94 | 22.34 |
| DIK-068 | 279.3 | 21.51 | 74.97 | 14.95 | 4.78 | 1.13 | 0.54 | 5.48 | 4.84 | 0.86 | 16.39 |
| DIK-069 | 571.2 | 23.69 | 86.71 | 17.80 | 4.85 | 1.18 | 0.80 | 5.36 | 4.19 | 0.55 | 14.96 |
| DIK-070 | 156.2 | 27.14 | 102.99 | 16.28 | 5.99 | 1.43 | 0.67 | 7.30 | 5.43 | 0.84 | 18.24 |
| Mean | 241.4 | 25.64 | 96.12 | 17.28 | 5.81 | 1.45 | 0.82 | 6.66 | 5.71 | 0.84 | 26.94 |
| S.D. | 198.6 | 3.83 | 17.45 | 1.70 | 1.15 | 0.39 | 0.24 | 1.16 | 1.52 | 0.17 | 20.22 |
| C. of V. | 0.82 | 0.15 | 0.18 | 0.10 | 0.20 | 0.27 | 0.29 | 0.17 | 0.27 | 0.20 | 0.75 |
| Sample ID | U | Ta | Zr | Hf | Ca | Sr | Ba | Na | K | Rb | Cs |
| DIK-066 | 37.65 | 42.08 | 1473 | 62.14 | 795 | 0 | 112 | 478 | 3445 | 0 | 0 |
| DIK-067 | 14.83 | 5.13 | 1175 | 49.33 | 783 | 0 | 71 | 481 | 3931 | 0 | 0 |
| DIK-068 | 12.04 | 3.30 | 1110 | 44.58 | 0 | 0 | 87 | 425 | 6909 | 23.6 | 0 |
| DIK-069 | 11.09 | 2.33 | 758 | 33.16 | 311 | 0 | 134 | 382 | 8200 | 29.5 | 0.4 |
| DIK-070 | 14.79 | 2.84 | 1143 | 49.18 | 0 | 0 | 0 | 264 | 2091 | 27.1 | 0 |
| Mean | 18.08 | 11.14 | 1132 | 47.68 | 378 | 0 | 81 | 406 | 4915 | 16.0 | 0.1 |
| S.D. | 11.06 | 17.33 | 254 | 10.42 | 396 | 0 | 51 | 89 | 2543 | 14.8 | 0.2 |
| C. of V. | 0.61 | 1.56 | 0.22 | 0.22 | 1.05 | 0.00 | 0.63 | 0.22 | 0.52 | 0.92 | 2.24 |

[a] All compositional data reported as parts-per-million (ppm). [b] Standard Deviation.
[c] Coefficient of Variation

Overall, the theoretical basis for a Specularite Signature based on the first-row transition metals is firm. It has been shown previously that the Transition Metal (TM) model is robust and successful in DFA on specularite sources and that the laboratory methods used here result in a consistent signature in replicate samples. Thus, DFA analyses focused on the TM model. Further

explanations in this section will delineate more reasons for the focus on TMs to the exclusion of other elemental variables.

Table 6. ALR transformed compositions and summary statistics for five replicate heavy mineral concentrate samples from Dikgatlampi Mine, Botswana.

| Sample ID | lrSc[a] | lrTi | lrV | lrCr | lrMn | lrCo | lrSb | lrZn | lrAl | lrAs | lrLa | lrCe | lrNd | lrSm |
|---|---|---|---|---|---|---|---|---|---|---|---|---|---|---|
| DIK-066 | 4.33 | 2.01 | 2.72 | 3.22 | 3.42 | 3.70 | 4.24 | 3.48 | 1.57 | 3.67 | 4.23 | 3.64 | 4.44 | 4.84 |
| DIK-067 | 4.36 | 1.99 | 2.63 | 3.23 | 3.34 | 5.03 | 4.18 | 3.30 | 1.24 | 3.73 | 4.29 | 3.70 | 4.42 | 4.91 |
| DIK-068 | 4.39 | 2.01 | 2.66 | 3.24 | 3.40 | 5.05 | 4.17 | 3.62 | 1.12 | 3.20 | 4.31 | 3.77 | 4.47 | 4.97 |
| DIK-069 | 4.38 | 2.02 | 2.65 | 3.23 | 3.38 | 5.00 | 4.16 | 4.10 | 0.98 | 2.85 | 4.23 | 3.66 | 4.35 | 4.92 |
| DIK-070 | 4.40 | 2.00 | 2.64 | 3.24 | 3.39 | 5.06 | 4.19 | 4.06 | 1.26 | 3.54 | 4.30 | 3.72 | 4.52 | 4.95 |
| Mean | 4.37 | 2.00 | 2.66 | 3.23 | 3.38 | 4.77 | 4.19 | 3.71 | 1.23 | 3.40 | 4.27 | 3.70 | 4.44 | 4.92 |
| S.D.[b] | 0.03 | 0.01 | 0.03 | 0.01 | 0.03 | 0.60 | 0.03 | 0.35 | 0.22 | 0.37 | 0.04 | 0.05 | 0.06 | 0.05 |
| C. of V.[c] | 0.01 | 0.01 | 0.01 | 0.00 | 0.01 | 0.13 | 0.01 | 0.10 | 0.18 | 0.11 | 0.01 | 0.01 | 0.01 | 0.01 |
| Sample ID | lrEu | lrTb | lrDy | lrYb | lrLu | lrTh | lrU | lrTa | lrZr | lrHf | lrBa | lrNa | lrK | lrRb |
| DIK-066 | 5.40 | 5.66 | 4.83 | 4.81 | 5.73 | 3.93 | 4.15 | 4.10 | 2.56 | 3.93 | 3.67 | 3.04 | 2.19 | -- |
| DIK-067 | 5.52 | 5.70 | 4.81 | 4.90 | 5.70 | 4.32 | 4.50 | 4.96 | 2.60 | 3.98 | 3.82 | 2.99 | 2.08 | -- |
| DIK-068 | 5.59 | 5.91 | 4.91 | 4.96 | 5.71 | 4.43 | 4.57 | 5.13 | 2.60 | 4.00 | 3.70 | 3.02 | 1.81 | 4.27 |
| DIK-069 | 5.53 | 5.70 | 4.87 | 4.98 | 5.86 | 4.43 | 4.56 | 5.24 | 2.72 | 4.08 | 3.48 | 3.02 | 1.69 | 4.13 |
| DIK-070 | 5.58 | 5.91 | 4.87 | 5.00 | 5.81 | 4.47 | 4.56 | 5.28 | 2.67 | 4.04 | -- | 3.31 | 2.41 | 4.30 |
| Mean | 5.52 | 5.78 | 4.86 | 4.93 | 5.76 | 4.32 | 4.47 | 4.94 | 2.63 | 4.01 | 3.67 | 3.08 | 2.03 | 4.24 |
| S.D. | 0.08 | 0.12 | 0.04 | 0.08 | 0.07 | 0.22 | 0.18 | 0.49 | 0.07 | 0.06 | 0.14 | 0.13 | 0.29 | 0.09 |
| C. of V. | 0.01 | 0.02 | 0.01 | 0.02 | 0.01 | 0.05 | 0.04 | 0.10 | 0.03 | 0.01 | 0.04 | 0.04 | 0.14 | 0.02 |

[a] lrNi, lrCa, lrSr, lrCs are omitted from this table due to missing values and space issues.
[b] Standard Deviation. [c] Coefficient of Variation.

Twenty of the 33 elements analyzed by INAA (As, Ba, Ca, Ce, Cs, Dy, Eu, Hf, K, Lu, Nd, Ni, Rb, Sr, Ta, Tb, U, Yb, Zn, Zr) were frequently missing from samples in most or all groups. This indicates that they are not very useful for fingerprinting because they do not reliably reflect the Specularite Signature, but may still be useful for simpler whole rock comparisons. Additionally, their inclusion in DFA would cause the omission of nearly all geologic samples. For these reasons, those 20 elements were excluded from the DFA and used only in the ELS analysis, where their minor significance could still be put to some use. Many of these elements were also excluded to avoid violating the Specularite Signature assumption.

Data preparation also excluded elements possibly contaminated by laboratory methods. The heavy mineral solution could have imparted excess sodium (Na) and so Na was left out of

the analysis. The mortar and pestle used could have contaminated the sample with aluminum (Al) and so Al was tracked with observations during sample preparation to identify samples with possible contamination, but not used for further statistical analyses. Based on the relative hardness of the material, contribution to the sample is likely not a significant problem. In both cases, the elements would also have been excluded because they are sufficiently common in non-hematite minerals to violate the Specularite Signature assumption.

Aluminum which is a major component of the concentrated samples has been found to substitute for iron in hematite at up to 23 mol % in soils (Singh and Gilkes, 1992). Some of the heavy mineral concentrates have higher Al:Fe ratios than this, so aluminum is present in large quantities outside of the hematite. Thus, the Al:Fe ratio of the concentrate is not representative of the hematite ratio and cannot be used in discriminant analysis, unlike the other transition metals.

Elements with ionic species commonly associated with quartz silicate and carbonate minerals were excluded from discriminant analysis because their geochemical signatures are not representative of hematite. For this reason, the following elements were excluded from discriminant analysis: Ba, Ca, K, Sr, Rb, and Zr.

The rare-earth elements (REE) appear to have consistent log-ratios and low variation among replicate samples. This elemental data set has been used previously for provenance of rock samples and formations (Bau and Dulski, 1996 and references therein; Luckenbach et al., 1975), including ochre provenance (Popelka-Filcoff, 2006; Popelka-Filcoff et al., 2007). The REE curves also have significant potential to make geologic interpretations on the genetic and metamorphic history of those rocks. However, the REE signature in hematite, which is important to maintain the Specularite Signature assumption, is not clearly understood. DFA using REEs

does not improve results significantly compared to a TM only model (Kiehn et al., 2007). For these reasons, REEs were not used in DFA in this study which focused on the TMs.

In summary, careful consideration of published research and preliminary data analyses led to a model for DFA that uses the log-ratio transformed values of the transition metals as the independent variables. These variables are significant because they will substitute and be associated with iron cations in hematite. The log-ratio transformation of the values allows the use of iron content in the samples as a proxy for hematite content. Aluminum was excluded from the model because of its ubiquity in minerals associated with quartz in these samples. Also, Zn was excluded due to its high variation among replicate samples and frequent absence in multiple mine sources. This leaves a final model that will attempt to classify the samples using the log-transformed values of Sc, Ti, V, Cr, Mn, Co, and Sb. Finally, any of the variables still included in the model will be excluded from the DFA on a trial-by-trial basis by ELS analysis if they are missing from a significant proportion of any group in the trial.

### *3.2.4 ELEMENTAL LIMIT SERIES ANALYSIS*

The initial fingerprinting technique used here is a graphical representation method of simple summary statistics that characterize the sources or the samples. It is a useful visual tool to quickly analyze and limit the number of potential sources for a sample of unknown provenance; it improves the accuracy of subsequent DFA by reducing the number of potential sources.

The ELS of an individual sample is an array of boxes, one for each included element, colored black if the element is present above the detection limit in the sample, and white if below the detection limit. The group arrays are arranged the same way, but a black box indicates that the element is present in at least 95 % of the group samples, white indicates presence in no more

than 5 % of group samples, and a gray or shaded box indicates a value somewhere between. The black and white boxes can be considered as absolute boxes while gray boxes are indeterminate.

The ELS of the validation or archaeological sample is then compared to the group ELS of each of the sources. Potential sources are removed from consideration when the ELS on the archaeological sample conflicts with one or more of the source's absolute boxes; i.e. an element present in the archaeological sample would eliminate any sources with 5 % presence or less of that element, and an element absent from the archaeological sample eliminates any sources with 95 % or greater presence. In other words, if an archaeological sample has a black box any groups with white boxes are rejected as possible sources, and vice versa, while the gray or indeterminate boxes do not exclude possible sources.

The ELS technique is rather simple and very useful. However, there are issues that need to be understood whenever it is implemented. First, samples analyzed using different techniques or even using the same techniques with different equipment may have different detection limits, and thus data need to be examined carefully before the ELS is developed. For instance, samples from a source with an average Ti concentration of 200 ppm could be marked as absent by INAA analysis with a detection limit of 700 ppm, but present by X-Ray Fluorescence with a detection limit of 5 ppm. This issue is easily addressed because the elemental limits are arbitrary to an extent and can be adjusted to any level at or above the highest detection limit of any of the techniques used to obtain the data. In this case values determined by the more sensitive techniques that fall below the limit are simply treated as missing because they presumably would have been missing if analyzed by the less sensitive technique. This approach would allow consistent cross-technique fingerprinting.

A second issue for the ELS technique is the arbitrary nature of the definitions of presence and absence for the collective group series. Five percent differences from the extremes were chosen to allow for the effect of outliers on the appearance of the ELS, and general statistical convention was the basis for choosing these levels. The group ELS can have a drastically different appearance if different presence/absence levels are used. The levels essentially act as a band-pass filter that can be adjusted to suit the investigators' needs. A wider band will mean relatively more gray boxes and thus fewer and more confident deductions of potential sources by the ELS. Conversely, using a narrower band, 10% and 90% instead of 5% and 95% for instance, will increase the number of absolute boxes, but also increase the chances of a Type II error by the ELS analysis.

### *3.2.5 DISCRIMINANT FUNCTION ANALYSIS*

The prepared INAA compositional data were subjected to discriminant function analysis (DFA). DFA attempts to discriminate groups from a population and then classify samples into groups based on multiple independent variables (Davis, 2002; McLachlan, 2004). In this study, the analysis will use the geologic data as a training set to develop linear classification functions of the independent variables to classify validation or archaeological samples. In order to do this, DFA attempts to maximize the ratio of between-group variance to within-groups variance.

After the discriminant functions are calculated, the Mahalanobis distance from the centroid of each group to each sample's discriminant score is calculated (Davis, 2002; McLachlan, 2004). Each observation is then classified based on its Mahalanobis distance to the group centroids with the nearest group centroid as the most probable candidate for group membership. The accuracy of a model can be evaluated by examining the percentage of misclassified observations in this, the initial classification.

As with any multivariate statistical technique, there are several assumptions that must be met. The most basic assumption is that the data are real, unbounded, continuous, and independent. These assumptions and the transformation of the compositional data to meet them were discussed previously in section 0. DFA also assumes multivariate normality, or normal distribution of each variable across groups (Davis, 2002; McLachlan, 2004). This assumption was tested using the Shapiro-Wilk *W*-test for each DFA trial and the assumption held for all. It also assumes that variables are not singular or collinear, which will cause an error and interruption of the process using these methods, which did not occur. Another important assumption is that of equal covariance across groups, which was checked using Box's M test and again found to hold for all trials.

After all of the multivariate data assumptions were found to be valid the actual analyses were conducted using the lda (linear discriminant analysis) function in the **R** 2.4.0 statistical package. In all trials, results were obtained by entering variables simultaneously with equal prior group probabilities.

# CHAPTER 4 RESULTS AND DISCUSSION

## *4.1 GEOLOGIC CHARACTERIZATION OF SOURCES*

The hand samples collected from the prehistoric mines were first described in the field, and later in more detail by adding data from petrography and X-Ray diffraction along with the INAA analyses. Representative samples were chosen from each mining region for analysis because more samples were collected than could be examined. Petrography was performed on thin section samples from each region, with the powder XRD performed on the crushed and milled off-cuts of those same thin-sectioned samples. The list of samples chosen for petrography and XRD as well as their mineralogy and relative abundances are summarized in Table 7.

XRD analysis was not performed on Blinkklipkop samples. A comparison of the petrography and XRD results of the other samples shows that XRD would have provided little additional information. The rock descriptions of the samples analyzed by petrography are summarized here to give a broad view of the rock types that were sampled for this study.

The XRD and petrographic analyses are valuable supplemental tools for this study, and in most cases provided more insight and detail in support of the initial field observations. However, the descriptions of mineralogy and texture provided by these methods have limited potential for determining provenance of specularite when used on their own, as has been shown in provenance studies conducted on similar materials such as ochre (Wilen, 2000). Yet, despite the lack of discriminating power when used alone, the importance of including these or similar methods is clearly better than relying on a single set of features for discriminating between sources.

Table 7. Brief summary of results of analyses performed on representative source samples.

| Thin Section Sample | Source | Mineralogy | |
|---|---|---|---|
| | | Petrography | XRD |
| TSO-95/4 | Tsodilo | Quartz (85%)<br>Hematite (15%)<br>Muscovite (5%) | Quartz (Major)<br>Hematite (Minor)<br>Muscovite (Minor) |
| TSO-95/7 | Tsodilo | Quartz (80%)<br>Hematite (20%)<br>Muscovite (Trace) | N/A |
| TSO-95/9 | Tsodilo | Hematite (80%)<br>Quartz (15%)<br>Muscovite (5%) | N/A |
| SEB-6A | Sebilong | Quartz (80%)<br>Hematite (10%)<br>Muscovite (10%) | Quartz (Major)<br>Hematite (Minor)<br>Muscovite (Minor) |
| DIK-1A | Dikgatlampi | Quartz (80%)<br>Hematite (20%) | Quartz (Major)<br>Hematite (Major) |
| DIK-5A | Dikgatlampi | Quartz (90%)<br>Hematite (10%) | Quartz (Major)<br>Hematite (Minor) |
| MAT-107 | Matsiloje | Quartz (50%)<br>Hematite (50%) | Quartz (Major)<br>Hematite (Major) |
| MAT-109 | Matsiloje | Quartz (70%)<br>Hematite (30%) | Quartz (Major)<br>Hematite (Major) |
| BKK-1A | Blinkklipkop | Quartz (95%)<br>Hematite (5%) | N/A |
| BKK-1B | Blinkklipkop | Quartz (90%)<br>Hematite (10%) | N/A |
| BKK-1C | Blinkklipkop | Quartz (95%)<br>Hematite (5%) | N/A |

### *4.1.1 PETROGRAPHY OF GEOLOGIC SAMPLES*

One of the advantages to petrographic analyses is the ability to identify important trace minerals. Mineralogy and fabric provide details and insights into the genetic and metamorphic history of the rock samples. Summarized here are the mineralogy and fabric of representative samples from each mine region.

Thin sections were cut to 30 micron thickness for examination on a Leica DM ED transmitted light petrographic microscope in the UGA Geology Department. Opaque minerals in transmitted light were identified as hematite by hand sample and 40x binocular microscope

examination, and by XRD analysis. The micaceous mineral visible in thin section and hand sample was identified as muscovite in subsequent XRD analysis discussed in the next section.

*The TsodiloHills*

The Tsodilo samples fall into two main types: 1) medium to fine grained hematite banded meta-quartzites or low-grade schists; 2) coarse grained hydrothermal vein deposits containing quartz and specularite and sometimes rimmed by kyanite that follow faults and fractures in the quartzite. In hand sample, all of the quartzite and schist samples primarily contain fine-medium grain quartz and smaller amounts of fine grained hematite; some also include minor amounts of mica. The vein deposits contain large amounts of specularite in some places, as well as pale orange kyanite blades up to 4 cm long.

TSO-95/4 is a garnet-kyanite-muscovite-hematite quartzite. In hand sample TSO-95/4 is a fine-grained and homogeneous quartzite with and some gray/purple banding on the 5-10 cm scale. It is mostly quartz with minor hematite and mica. Other hand samples collected from the area contain pale orange kyanite crystals up to 5 cm long in vein deposits that were not observed in this thin section.

Thin section TSO-95/4 has a granoblastic texture with complete recrystallization from the sandstone protolith. It contains roughly 90% quartz in euhedral grains 1-4 mm diameter. It is also roughly 5% anhedral opaque minerals, most likely hematite, 0.5-1 mm in diameter that are conterminous with the quartz grains. The remaining 5% of the sample consists of subhedral elongate muscovite and kyanite grains and a few anhedral garnet grains. The muscovite is pale brown in plane polarized light (PPL) with high order interference colors in cross polarized light (XPL) and colorless in hand sample. The muscovite is 0.2-1 mm wide and 0.5-5 mm long and cross cuts the quartz grains in some places suggesting that some of it may have crystallized after

the quartz. The trace amounts of kyanite are 0.2-0.5 mm wide and 0.5-1 mm long. The garnet crystals are up to 1 mm in diameter. During sample preparation, kyanite was present in only a few samples, and no garnet was identified by the naked eye or 45x binocular magnification.

Unsurprisingly, samples from TSO-95/7 are very similar to those from TSO-95/4. TSO-95/7 is a coarse grained specularite and macroquartz vein deposit. Other hand samples collected from the area include a fine-to-medium grained schist with some medium grained specularite concentrations between bands of fine-grained quartz and micas.

Thin section TSO-95/7 has a porphyritic texture with complete recrystallization and suturing of grain boundaries. It contains approximately 60% quartz in euhedral grains 1-4 mm diameter. It contains about 40% euhedral platy specularite crystals from 1-10 mm long and 0.1-5 mm wide with no preferred orientation. A minor amount (<5%) of anhedral elongate muscovite, 0.1-0.5 mm wide and 0.5-1 mm long is also present.

Other samples collected with TSO-95/9 include a muscovite-specularite-quartz schist. In hand sample TSO-95/9 is fine-grained and banded with 1-5 cm wide white quartz and 3-5 cm wide specularite bands. This sample is mostly quartz and hematite with trace amounts of mica. All samples in this group are of the same type.

Thin section TSO-95/9 shows a granoblastic texture with complete recrystallization from the sandstone protolith. It contains approximately 40% quartz in euhedral grains 1-4 mm diameter that are heavily fractured. It is approximately 55% euhedral opaque hematite crystals, 0.5-1 mm in diameter. The remaining 5% of the sample consists of subhedral elongate muscovite grains that are up to 0.5 mm long and generally found interstitially in the quartz bands or between quartz and hematite grains.

*Sebilong*

Sample SEB-6A is a purple fine-grained muscovite-hematite quartzite that has been cut by a quartz vein. Only one INAA sample, SEB-054, is associated with the same rock as thin section and XRD sample SEB-6A. In hand sample it has a homogeneously speckled aphanitic matrix that is cut by a coarse-to-medium-grained quartz and specularite vein. In thin section the matrix zone is about 70% subhedral rounded quartz grains 0.5-1.5 mm in diameter. The matrix is about 20% euhedral platy hematite crystals 0.1-0.3 mm long grouped in rosettes and bands with anhedral muscovite grains of the same size. All matrix grains have choppy irregular boundaries. The matrix may be metamorphosed sandstone with hematite and muscovite recrystallized from iron rich micas or other clay minerals.

The veins crosscut the matrix and are composed mostly of a core of euhedral prismatic quartz crystals 1-5 mm in diameter with smaller 0.5-2 mm subhedral quartz grains mixed in on the outer edges. There are a few (<5%) specularite crystals up to 1.5 mm long aggregated in outer zones of the veins. All grains have sharp polygonal boundaries in this zone with an overall granoblastic texture.

*Dikgatlampi*

The INAA and thin section samples come from different parts of the same rock type. In general, the rock is a fine-grained quartzite with coarse-grained quartz and specularite veins cutting through it. The hematite is found finely disseminated interstitially in the quartzite matrix, as fine concentrated masses on vein edges, as specular crystals in the hydrothermal veins, and as thin coatings on large quartz crystals. The samples are very weathered and porous in places.

Thin section DIK-1A is a banded hematite quartzite with granoblastic texture and fine concentrated hematite masses and coatings. Thin section DIK-1A is representative of INAA

samples DIK-059 and DIK-060. It is about 80% quartz overall, reaching 95% quartz in zones. The grains are subhedral to euhedral and 1-5 mm in diameter, many of which are fractured. Hematite makes up about 20% of the rock overall, and up to 90% in zones. The hematite grains are subhedral to euhedral platy aggregates 0.1-0.5 mm wide and 1-5 mm long. Quartz boundaries are polygonal triple junctions while hematite crystals are interstitial and extend into the quartz crystals in many places. Some areas also show fine hematite stains on quartz grain surfaces.

The thin section of DIK-5A shows a quartzite with finely disseminated hematite matrix. DIK-5A is associated with INAA sample DIK-073. It exhibits granoblastic texture with 90% euhedral to subhedral quartz grains 1-3 mm in diameter. Most quartz grain boundaries are polygonal. The thin section is about 10% hematite, mostly as fine coatings and stains on quartz grain surfaces and cracks. There are also a few interstitial euhedral platy hematite crystals 0.1-0.5 mm long.

*Matsiloje*

The Matsiloje samples are taken from variously metamorphosed Banded Iron Formation quartzites. In hand sample the rock is a banded quartzite with alternating fine purple quartz and specularite bands that is cut by hydrothermal veins up to 5 cm wide that generally follow mineral bands. In places the veins contain relatively unchanged inclusions of Banded Iron Formation up to 3 cm wide, while in other places the inclusions have recrystallized into specularite crystal aggregates.

The MAT-107 thin section (INAA sample also) is mostly banded quartzite, but has a small hydrothermal vein cutting through it. The fine grained quartzite consists of 5-10 mm wide bands of subhedral quartz grains 0.05 mm in diameter and 5-15 mm wide fine hematite masses. The core of the quartz vein is euhedral quartz crystals 0.25 mm in diameter with polygonal

boundaries. Toward the edge of the vein, quartz crystals are subhedral and elongated and up to 0.3 mm in length with irregularly sutured boundaries and undulose extinction and become smaller and bimodal closer to the edges. This zone also contains subhedral platy hematite crystals up to .05 mm long included in the zoned quartz crystals.

The MAT-109 thin section (INAA sample also) has a mineralogy and texture very similar to MAT-107, but the texture is closer to migmatitic. Visible in the thin section is a 5 cm quartzite inclusion in a larger quartz vein that has only begun to recrystallize in discontinuous zones. The thin section shows inclusions in the edge of the vein. The recrystallized textures found in MAT-107 are present again, but as zones in discontinuous lenses a about 1 mm wide rather than in a continuous vein.

*Blinkklipkop*

The Blinkklipkop samples are also metamorphosed Banded Iron Formation. In hand sample, the thin section off-cuts are aphanitic microbanded red and white hematitic quartzites. These samples represent portions of BIF breccia fragments 5-10 cm long included in hydrothermal quartz veins up to 10 cm wide in the field. The thin section samples show only the smaller scale metamorphism inside the fragments.

Thin section BKK-1A shows a microbanded very fine-grained hematitic quartzite with granoblastic texture. The sample is upwards of 90% fine-grained or microcrystalline quartz. Some of the microbands of quartz have recrystallized into subhedral quartz grains up to 0.1 mm in diameter. Approximately 5% of the sample is fine anhedral masses of opaque hematite in microbands with a few 0.1-0.3 mm long blades perpendicular to banding. There is also a 0.5 mm wide hematite vein cutting across banding with some angular quartz crystals entrained.

Thin section BKK-1B reveals a very fine-grained hematitic quartzite with aphanitic and brecciated texture. The sample is upwards of 90% cryptocrystalline quartz that is heavily fractured and brecciated with fine hematite coatings and subhedral quartz grains up to 0.1 mm in diameter filling the fractures. Approximately 5% of the sample is fine anhedral masses of opaque hematite. Some recrystallized quartz grains show offset by fractures and the sample is nearly 5% void space.

Thin section BKK-1C shows a microbanded hematitic quartzite largely devoid of the alteration observed in the other two BKK thin sections. The hematite content gives the appearance of jasper, which is the likely protolith. This sample is well over 90% quartz with grain sizes ranging from microcrystalline up to 0.05 mm in diameter with the microbands separated by grain size and hematite content. The hematite is mostly present as staining and coating on grain surfaces, but also as fine anhedral masses in microbands. There some small 0.1 mm wide fractures perpendicular to banding and filled with hematite stains. The hematite microbands also show some minor shearing.

*Summary*

Overall, the petrography of samples analyzed shows the diversity of genetic and diagenetic processes among these sources on the small scale. Micro-textures include brecciation and fracturing in Blinkklipkop samples and hydrothermal veins common to all of the sources. The mineralogy shows that hematite and quartz are ubiquitous to all five sources, but also that muscovite is only present in some of the Sebilong and Tsodilo samples. Kyanite and garnet are also to some of the Tsodilo samples. These descriptive measures could be very useful in cases where more in-depth qualitative methods are inconclusive or impractical.

### *4.1.2 X-RAY DIFFRACTION*

As a general rule, the XRD settings used here only allowed the identification of minerals present in the samples at a minimum level of about 5 percent by weight. This means that petrography can identify much less abundant minerals, but XRD can help confirm the identity of particular mineral phases that may be problematic to identify with petrography alone.

The petrographic analysis showed only two or three minerals likely to be abundant enough for identification using XRD; hematite and quartz should be apparent in all samples, and a mica mineral may be present in the Tsodilo and Sebilong samples. The diffractogram shows the counts-per-second versus the angle of the detector (2-theta). The detector angle is related to the d-spacing of the unit cells of the mineral phases by Bragg's Law, which was used to label the significant peaks with the associated d-spacings.

The XRD analyses were performed using the University of Georgia Geology Department's Scintag XDS 2000. This machine uses a cobalt radiation source with a K-alpha wavelength of 1.790 Å. All samples were run using a detector step of 0.01º, counting time of 0.2 seconds from 2º to 60º for a scan rate of 3º per minute.

The diffraction patterns were matched to ICDD cards from the Powder Diffraction File using simple peak matching. Figure 4 shows an overlay of the diffraction patterns for all six samples with significant peaks annotated with pink lines and labeled with the corresponding d-spacings. All samples showed the major hematite (ICDD card 77-2234) peaks in the 2º-60º range, and all major and minor quartz (ICDD card 79-1906) peaks. Samples TSO-95/4 and SEB-6A also had major peaks at 9.94, 4.976, and 3.203 nm, which indicate that the mica found in these samples by petrography is muscovite (ICDD card 80-0742). There is some shifting in the muscovite peaks that is likely due to iron substitution for aluminum in the crystal structure.

Overall, the XRD analysis served its purpose by helping to identify the mica mineral as muscovite despite its unusual appearance in the petrographic analyses. The XRD results showed that hematite is the dominant opaque mineral as assumed. This analysis can be very helpful if samples of unknown provenance are too fine-grained for in-depth petrographic study and also help confirm uncertain mineralogical interpretations. Thus, XRD seems to be a good tool for specularite provenance, but in most cases it could be substituted with more in-depth transmitted or reflected light petrography.

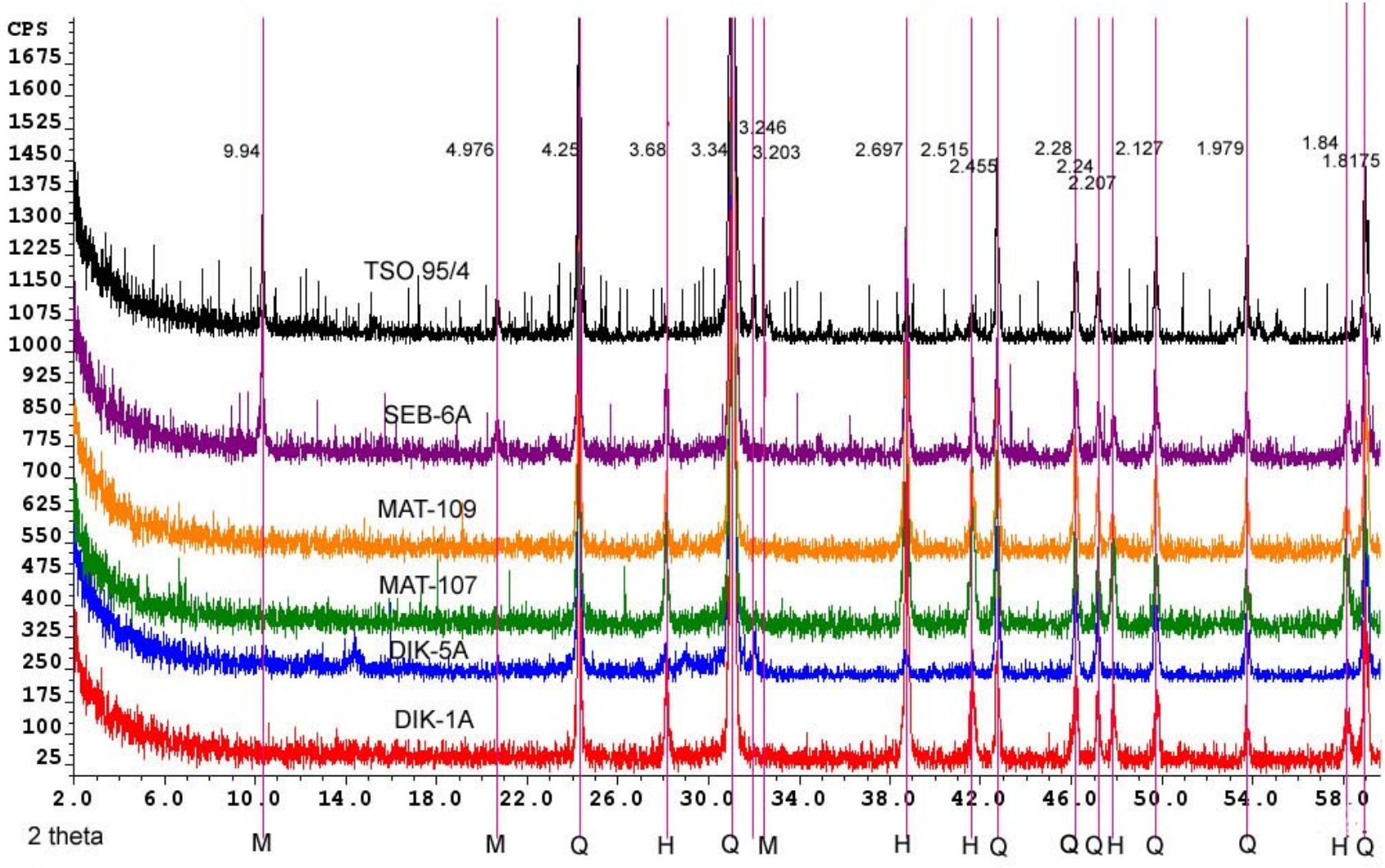


Figure 4. Annotated XRD diffractogram of representative geologic source samples. Peaks marked in pink; labels above peaks denote d-spacing in Å; bottom labels denote mineral association (Q=quartz, H=Hematite, M=Muscovite)..The X-axis is marked by degrees 2-theta for a Co radiation source with K-alpha wavelength of 1.790 Å.

## *4.2 GEOLOGIC SAMPLES - REGIONAL SOURCES*

### *4.2.1 ELEMENTAL LIMIT SERIES ANALYSIS*

The ELS for the individual validation samples were compared to the group arrays developed from the training samples and conflicts between the two were used to deductively choose the groups of sources used in the DFA. When reading individual sample ELS array, a black square indicates detectable levels of the element in that sample, while white indicates an absence. For group arrays, black indicates presence of that element at detectable levels for 95% or more of the samples in the group. A white square indicates presence of that element in 5% or fewer of the samples in the group, while a gray square indicates detectable levels of the element in between 95% and 5% of the samples. Conflicting black and white boxes for the group and individual array, and vice versa, for the same element eliminate that source group from further DFA analysis for the individual sample.

Figure 5 shows the group ELS arrays for the sources based only on the training samples. A quick visual inspection is enough to show that the most distinct differences are between Dikgatlampi, which has no missing elements at significant levels, and Blinkklipkop, which has nearly half of the elements missing. It also shows that it is difficult to separate Tsodilo, Sebilong, and Dikgatlampi based only on the ELS arrays, so DFA will be utilized in these cases.

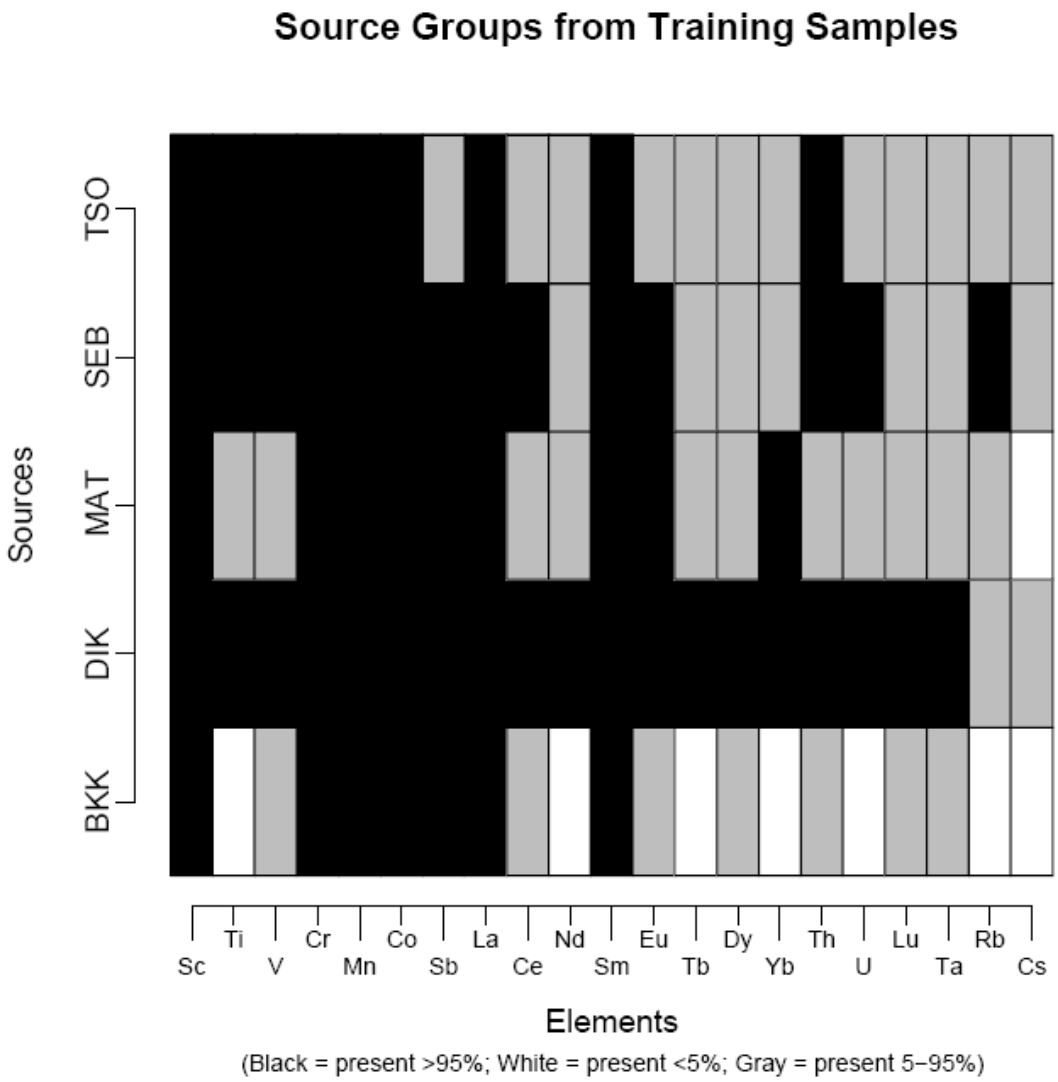


Figure 5. Source group ELS arrays based on geologic training sample set.

One of three subsequent actions for DFA may follow depending on the ELS results: 1) *All groups are excluded by ELS.* At this point, all sampled sources may be used for DFA. Sources may be entered with equal prior probabilities, or with weighted based on archaeological or geographic context, i.e. the closer sources are more likely. Alternatively, analysis could be stopped and the null hypothesis, that the true source is not among the choices, accepted.

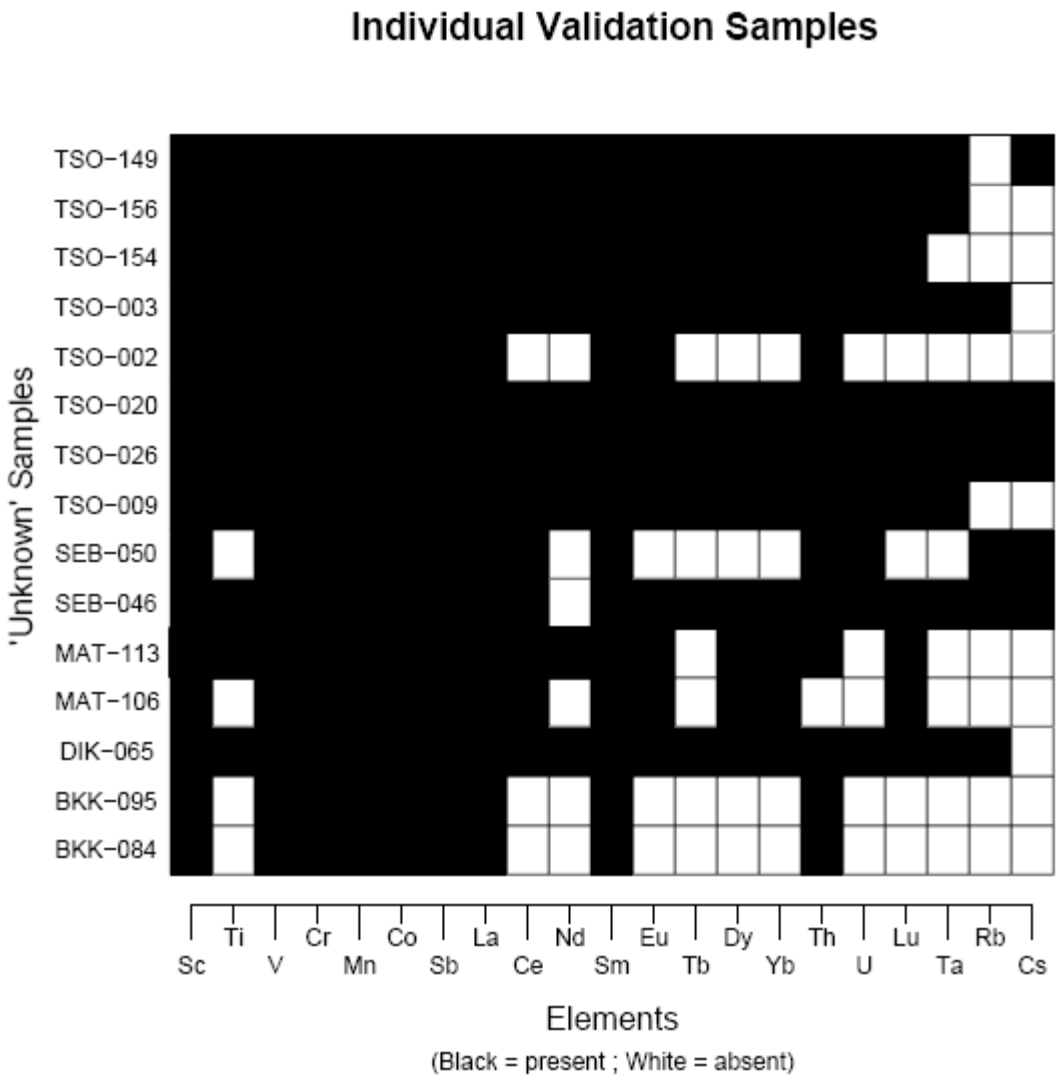


Figure 6. Individual ELS arrays from geologic validation sample set.

2) *All but one group is excluded.* If the remaining source seems to make sense, no further DFA may be needed. If, however, more confidence in the result is required or the source seems unlikely for other reasons, all sources may be used for DFA as in the first case.

3) *Two or more sources remain after ELS analysis.* This result is straightforward; the remaining sources will be used for DFA which will choose the closest match.

Table 8 summarizes the results of the ELS analysis for each validation sample. Notably only one, SEB-050, was clearly in error with no matching sources identified. All four cases that were limited to a single source had the correct mining region identified. Also, all cases with multiple possible sources remaining for DFA still had the correct source in contention. At this stage the ELS analysis appeared to be effective in limiting possible sources.

Table 8. Summary of ELS analysis and resulting parameters for DFA trials.

| DFA Trial | Groups (n) | Sources for DFA | Validation' Samples | Elements[a] |
|---|---|---|---|---|
| 4a | 4 | TSO, DIK, SEB, MAT | TSO-003, DIK-065 | |
| 3a | 3 | TSO, DIK, SEB | TSO-020, TSO-026 | Ti |
| 3b | 3 | TSO, DIK, MAT | TSO-009, TSO-156 | |
| 2a | 2 | TSO, SEB | SEB-046 | Ti |
| 2b | 2 | TSO, MAT | MAT-113, TSO-154 | |
| 2c | 2 | TSO, DIK | TSO-149 | Ti |
| 5a | 1 | TSO | TSO-002 | |
| 5a | 1 | MAT | MAT-106 | |
| 5a | 1 | BKK | BKK-084, BKK-095 | |
| 5a | 0 | | SEB-050 | |

[a] Sc, V, Cr, Mn, Co, Sb can be included as variables in all trials except 5a.

In the following section, DFA analysis of the six trial cases with multiple possible sources after ELS analysis is described. All of these cases used the same geologic training sample sets as the ELS analysis to develop the discriminant functions. These trials all used the log-ratio values of Sc, V, Cr, Mn, Co, and Sb as variables in the analysis, and Trials 3a, 2a, and 2c also included Ti. However, Ti was precluded from inclusion as a variable in any of the other DFA Trials because it is not present at Blinkklipkop and Matsiloje.

### *4.2.2 DISCRIMINANT FUNCTION ANALYSIS*

*TRIAL 5a*

Logically, the most complicated DFA trials, by numbers of potential sources and validation samples, would have the most cases misclassified. In this study, Trial 5a is by far the most complicated with two validation samples from differing sources being classified into four possible source areas. The discriminant functions were built using 132 samples from all five mining regions. Fifteen samples (11.4%) of the original training set were misclassified by the discriminant functions. Of the misclassified cases, Tsodilo samples were mistakenly classified with Sebilong and Dikgatlampi; Matsiloje samples were misclassified with Blinkklipkop and Sebilong; and five Blinkklipkop samples were misclassified with Matsiloje. These results show that even with the large data set and fewer elemental variables, most sources were well separated, except for Blinkklipkop and Matsiloje

The somewhat disappointing classification results of the training sets for DFA Trial 5a were not repeated when the validation samples were classified. Figure 8 shows that only one validation sample, SEB-046, was misclassified. Also, while sample MAT-106 is very close to the Blinkklipkop group centroid on this two-dimensional plot, the actual classification uses the 4 dimensions shown in Table 10, so it is indeed classified correctly.

Overall, the most difficult Geologic DFA trial was mostly successful. The accuracy achieved in classifying the validation samples was excellent given the problems experienced in discriminating the training set. So, the training error rate of a DFA analysis should be used as an important guide when judging confidence in the classifications of archaeological samples.

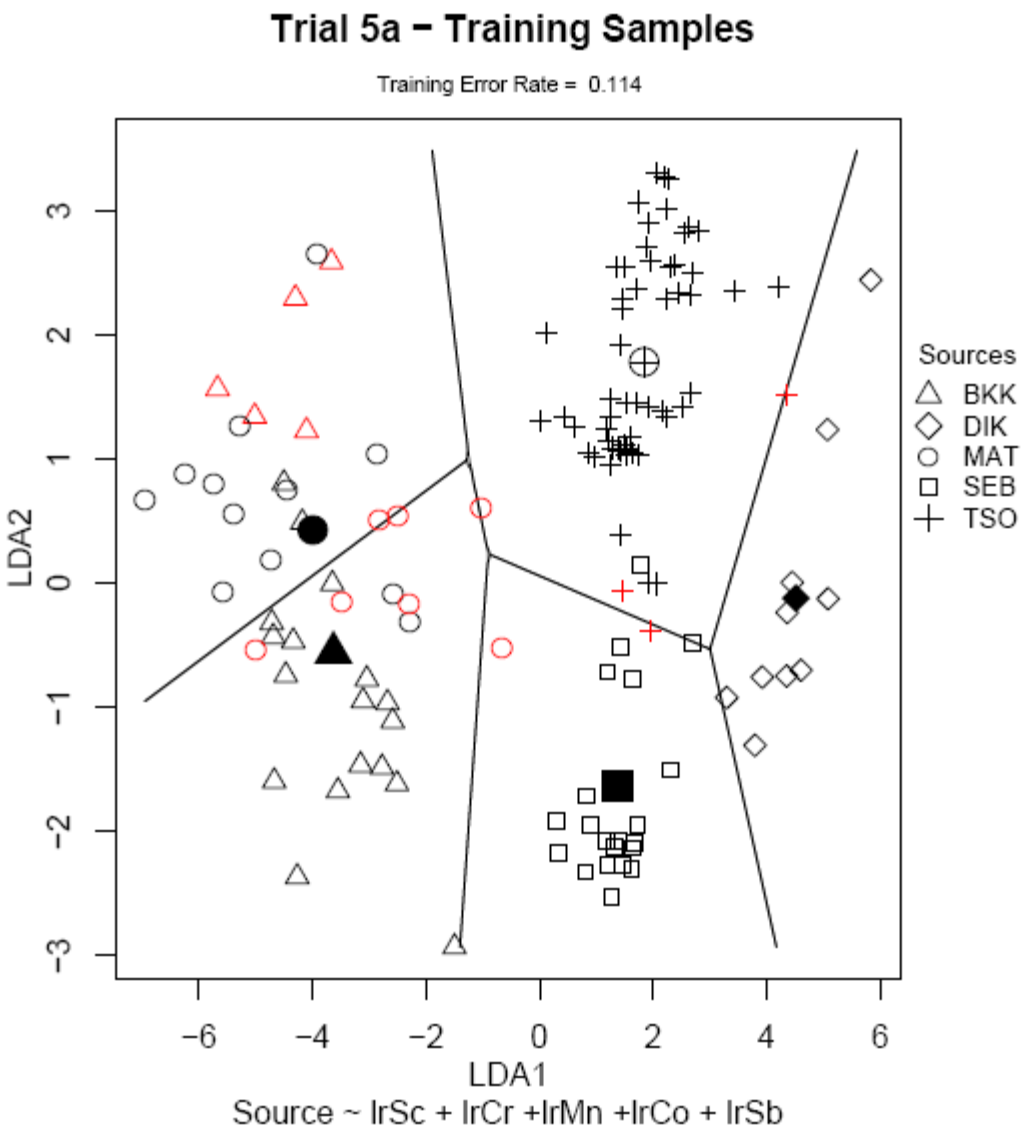


Figure 7. Geologic Trial 5a DFA plot showing the classification of training samples. Misclassified cases are shown in red.

Table 9. Geologic Trial 5a Training Sample DFA Classification matrix.

| Source | Predicted | | | | |
|---|---|---|---|---|---|
| | BKK | DIK | MAT | SEB | TSO |
| BKK | 18 | 0 | 5 | 0 | 0 |
| DIK | 0 | 10 | 0 | 0 | 0 |
| MAT | 5 | 0 | 12 | 2 | 0 |
| SEB | 0 | 0 | 0 | 21 | 0 |
| TSO | 0 | 1 | 0 | 2 | 56 |

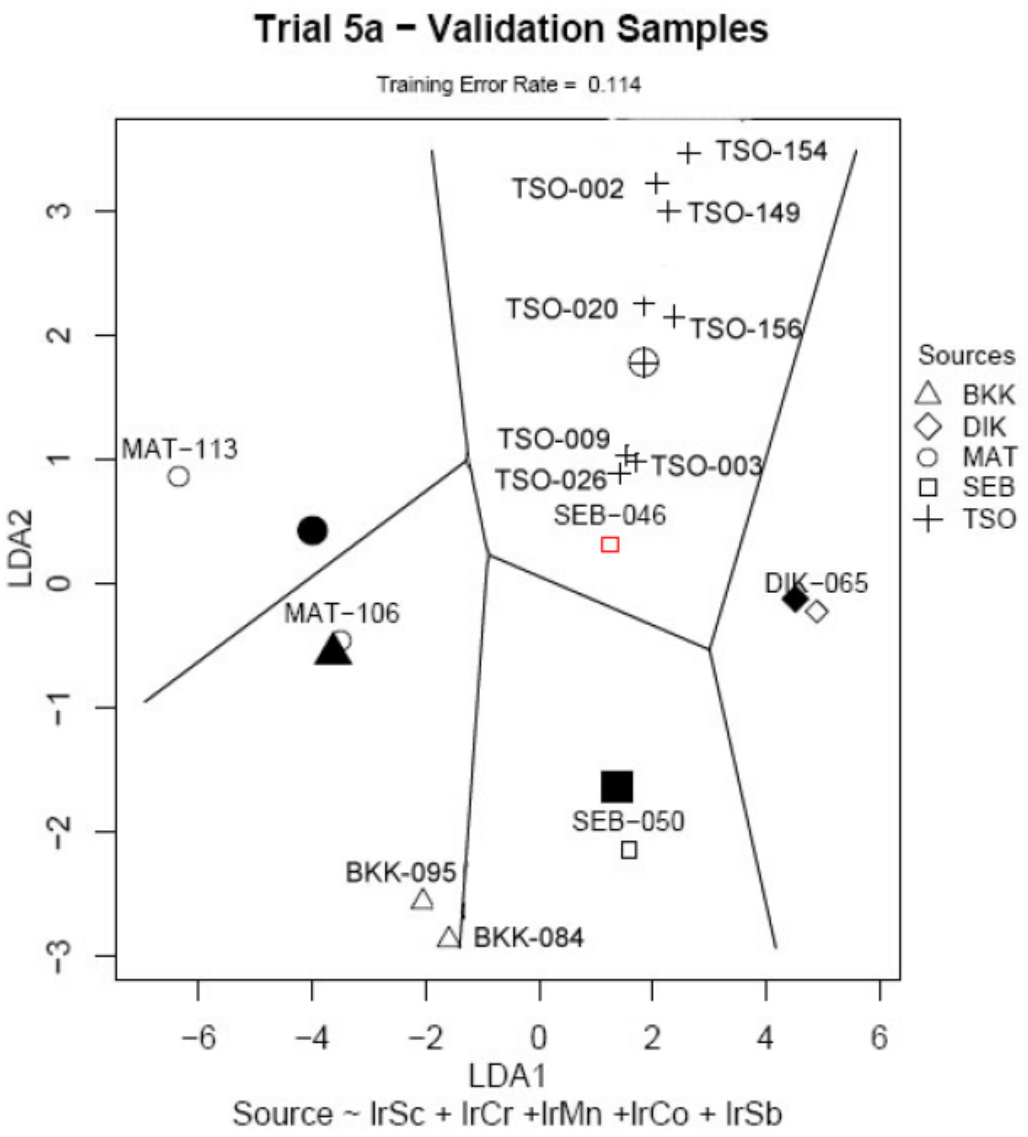


Figure 8. Geologic Trial 5a DFA plot showing the classification of the validation samples.

Table 10. Canonical discriminant function coefficients for Geologic Trial 5a.

| | LD1 | LD2 | LD3 | LD4 |
|---|---|---|---|---|
| lrSc | -5.5589 | -0.1581 | -1.5152 | 1.14016 |
| lrCr | 0.80605 | 0.5139 | 1.79362 | -0.6649 |
| lrMn | 2.2612 | -1.3924 | 0.09532 | -0.236 |
| lrCo | -0.5467 | -1.4221 | 0.48375 | 0.10937 |
| lrSb | 0.35843 | 0.47313 | -1.296 | -1.39 |

*TRIAL 4a*

Geologic Trial 4a used 106 samples from all mining regions except Blinkklipkop. Only four samples (3.8%) of the original training set were misclassified by the discriminant functions. Of the misclassified cases, two Tsodilo samples were grouped with Sebilong, one Tsodilo sample with Dikgatlampi, and one Sebilong sample with Tsodilo.

The success in classifying the training sets for DFA Trial 4a was repeated during validation. Figure 10 shows that both validation samples in this trial, TSO-003 and DIK-065, lie well within their correct group fields established by the training set.

Table 11. Geologic Trial 4a Training Sample DFA Classification matrix.

| Source | Predicted | | | |
|---|---|---|---|---|
| | DIK | MAT | SEB | TSO |
| DIK | 10 | 0 | 0 | 0 |
| MAT | 0 | 16 | 0 | 0 |
| SEB | 0 | 0 | 20 | 1 |
| TSO | 1 | 0 | 2 | 56 |

Table 12. Canonical discriminant function coefficients for Geologic Trial 4a.

| | LD1 | LD2 | LD3 |
|---|---|---|---|
| lrSc | 5.64563 | -1.0611 | -0.3431 |
| lrV | 0.25351 | -0.1137 | 1.23748 |
| lrCr | -1.1069 | 0.55108 | -1.2611 |
| lrMn | -3.5903 | -1.8157 | 0.73985 |
| lrCo | 0.47922 | -1.186 | -0.6328 |
| lrSb | 0.19192 | 0.88627 | 1.7721 |

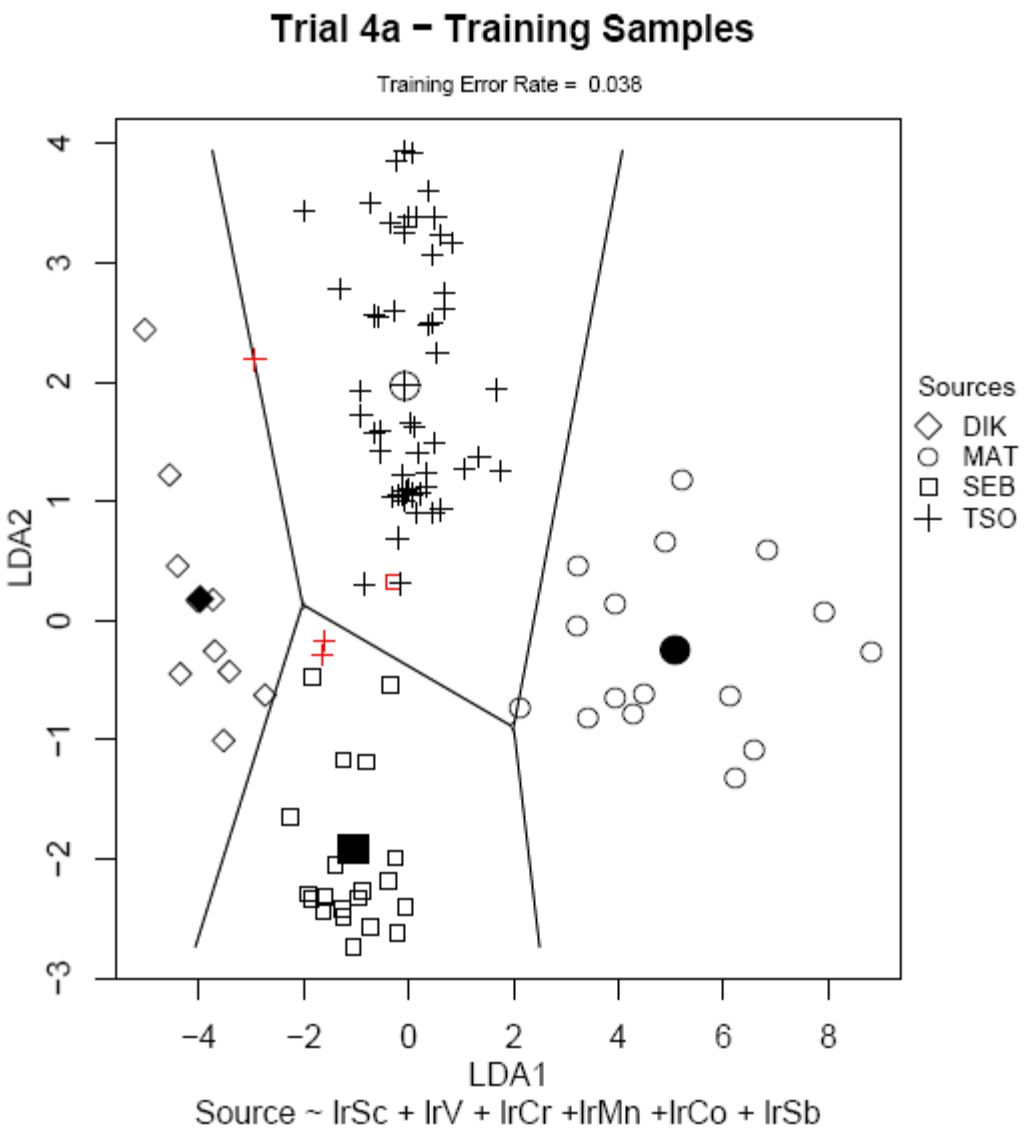


Figure 9. Geologic Trial 4a DFA plot showing the classification of training samples. Misclassified cases are shown in red.

*TRIAL 3a*

Trial 3a used the 89 training samples from Tsodilo, Dikgatlampi, and Sebilong. The training set was classified very successfully by the DFA procedure. Three samples from Tsodilo were classified as Sebilong but there were no other errors resulting in an overall 3.4 % error rate (Table 14).

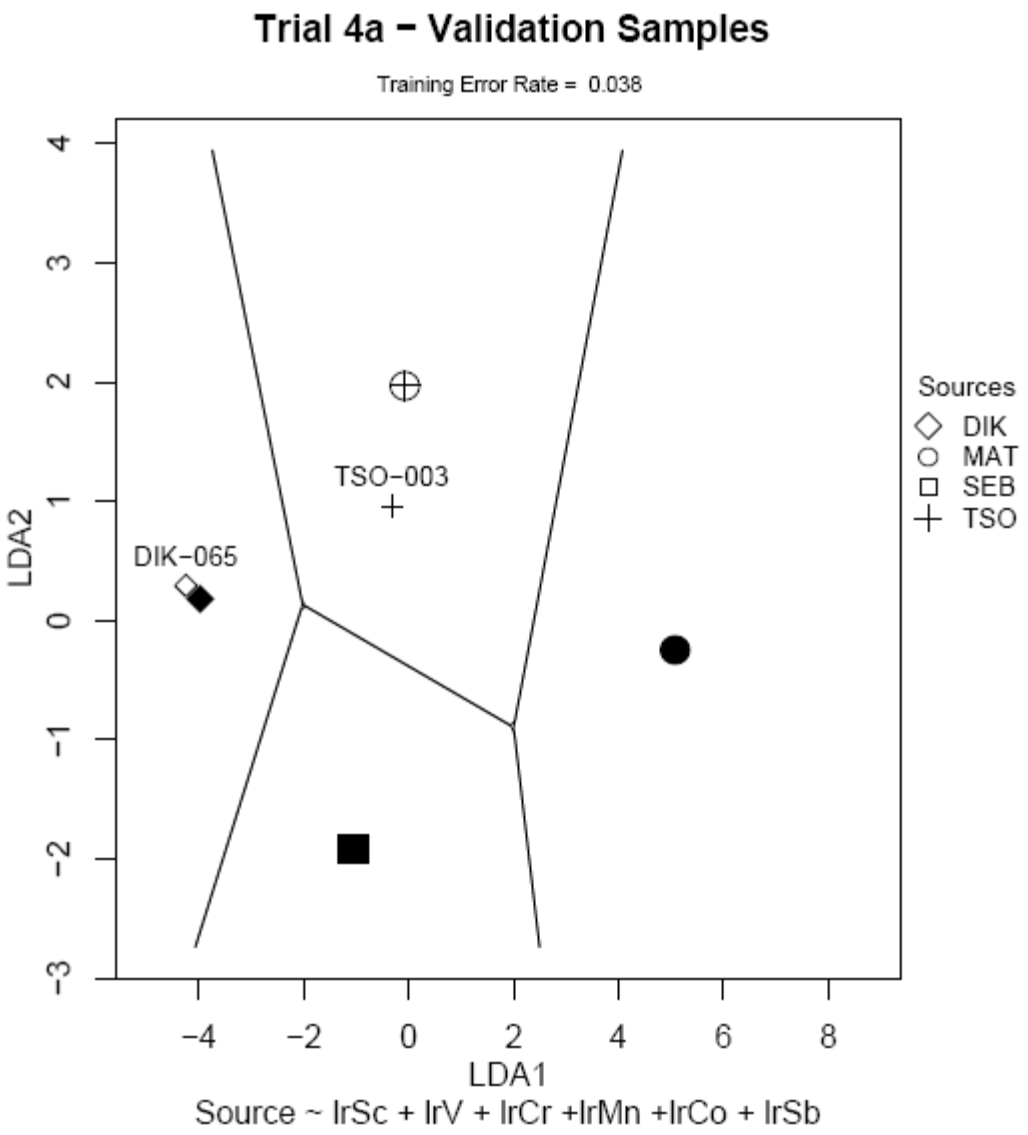


Figure 10. Geologic Trial 4a DFA plot showing the classification of the validation samples.

Overall, the Dikgatlampi samples appear more distinct than the other groups because of the wider separation of that cluster of samples, while some samples from Sebilong and Tsodilo are more similar to each other than to samples from the rest of their respective regions. The classification of the validation samples was successful once again. Both TSO-020 and TSO-026 were well within the Tsodilo field as seen in Figure 12.

Table 13. Canonical discriminant function coefficients for Geologic Trial 3a.

| | LD1 | LD2 |
|---|---|---|
| lrSc | 5.74154 | -2.0602 |
| lrTi | -2.2531 | -0.0772 |
| lrV | 1.63285 | -0.4343 |
| lrCr | -0.1238 | 1.26077 |
| lrMn | -2.4885 | -0.634 |
| lrCo | -0.2271 | -1.333 |
| lrSb | 1.25028 | 0.28996 |

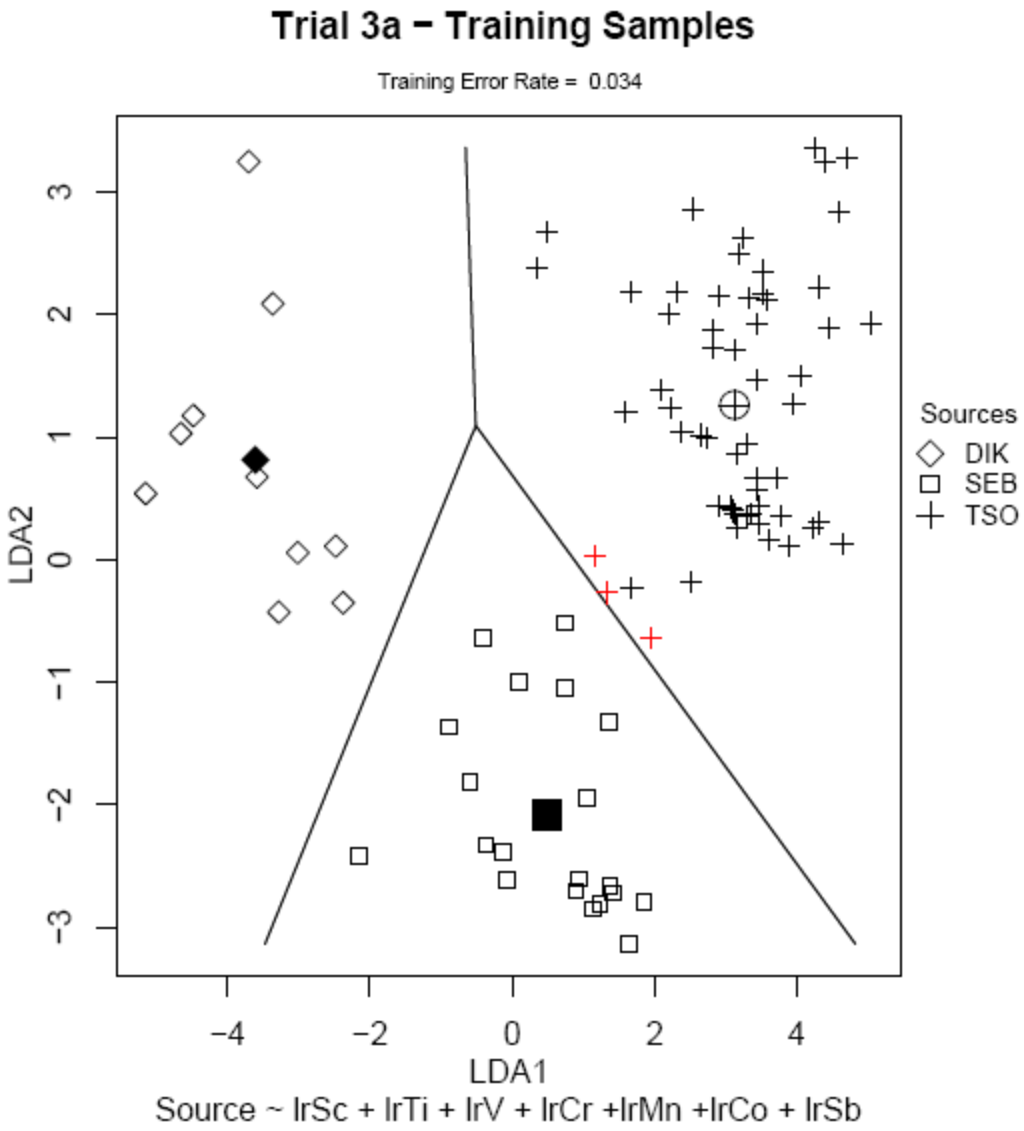


Figure 11. Geologic Trial 3a DFA plot showing the classification of training samples. Misclassified cases are shown in red.

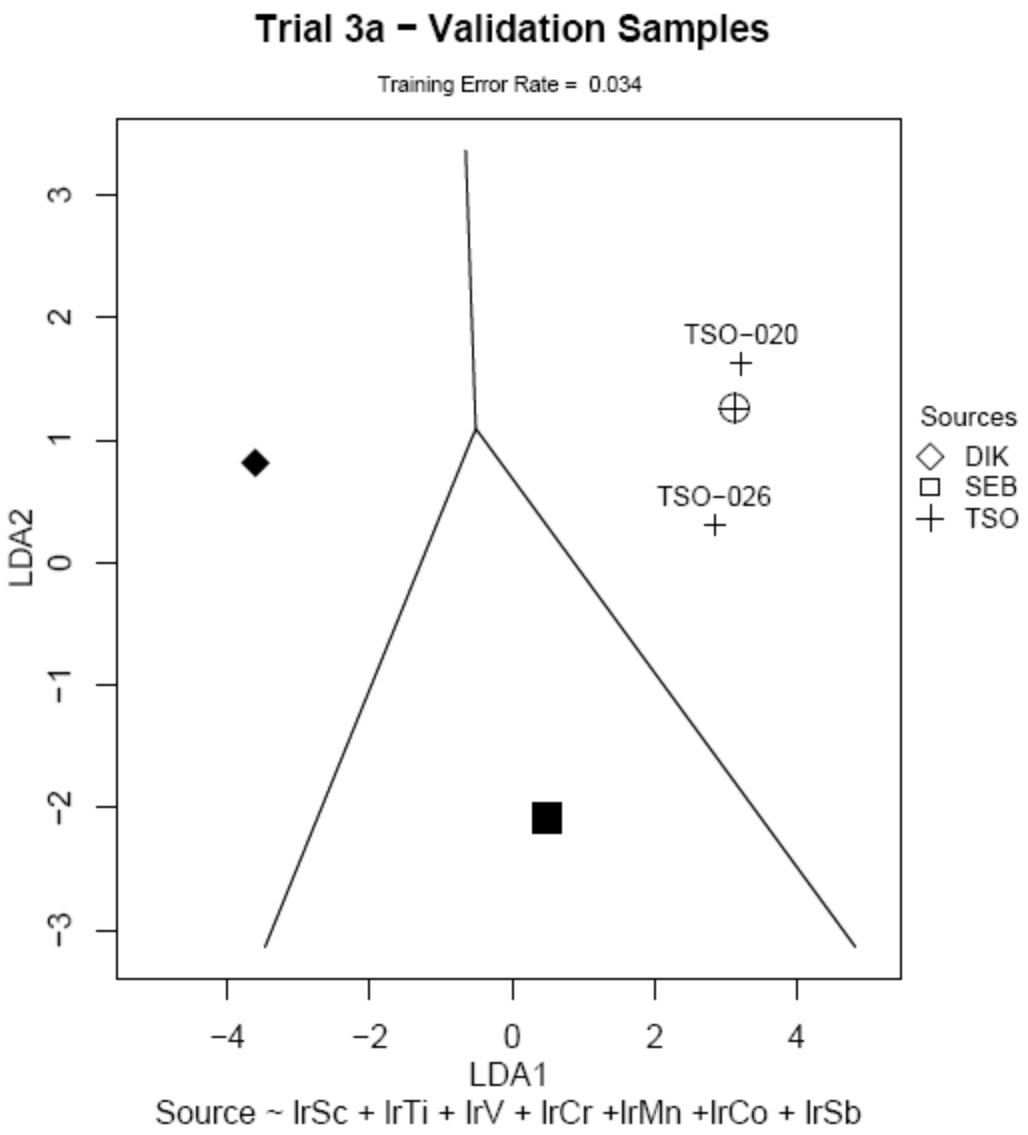


Figure 12. Geologic Trial 3a DFA plot showing the classification of the validation samples.

Table 14. Geologic Trial 3a Training Sample DFA Classification matrix.

| Source | Predicted | | |
|---|---|---|---|
| | DIK | SEB | TSO |
| DIK | 10 | 0 | 0 |
| SEB | 0 | 20 | 0 |
| TSO | 0 | 3 | 56 |

*TRIAL 3b*

Trial 3b used the 85 sample training set from Dikgatlampi, Matsiloje, and Tsodilo. The error rate in classification was 3.5% (Table 15). All three misclassified cases were samples from Tsodilo classified with Dikgatlampi.

Figure 13 shows that the misclassified samples fall near the border between regions, as are do two samples from Matsiloje that were correctly classified. Other than these "near misses", the results are promising because of the otherwise tight clustering of samples and clear separation of groups. Both validation samples from Tsodilo were correctly classified as they were well within the Tsodilo group boundaries.

Table 15. Geologic Trial 3b Training Sample DFA Classification matrix.

| Source | Predicted | | |
|---|---|---|---|
| | DIK | MAT | TSO |
| DIK | 10 | 0 | 0 |
| MAT | 0 | 16 | 0 |
| TSO | 3 | 0 | 56 |

Table 16. Canonical discriminant function coefficients for Geologic Trial 3b.

| | LD1 | LD2 |
|---|---|---|
| lrSc | 5.47818 | -0.5257 |
| lrV | 0.20433 | 0.30852 |
| lrCr | -1.3025 | -0.5505 |
| lrMn | -3.3467 | -1.3616 |
| lrCo | 0.43246 | -1.2848 |
| lrSb | 0.27248 | 1.65365 |

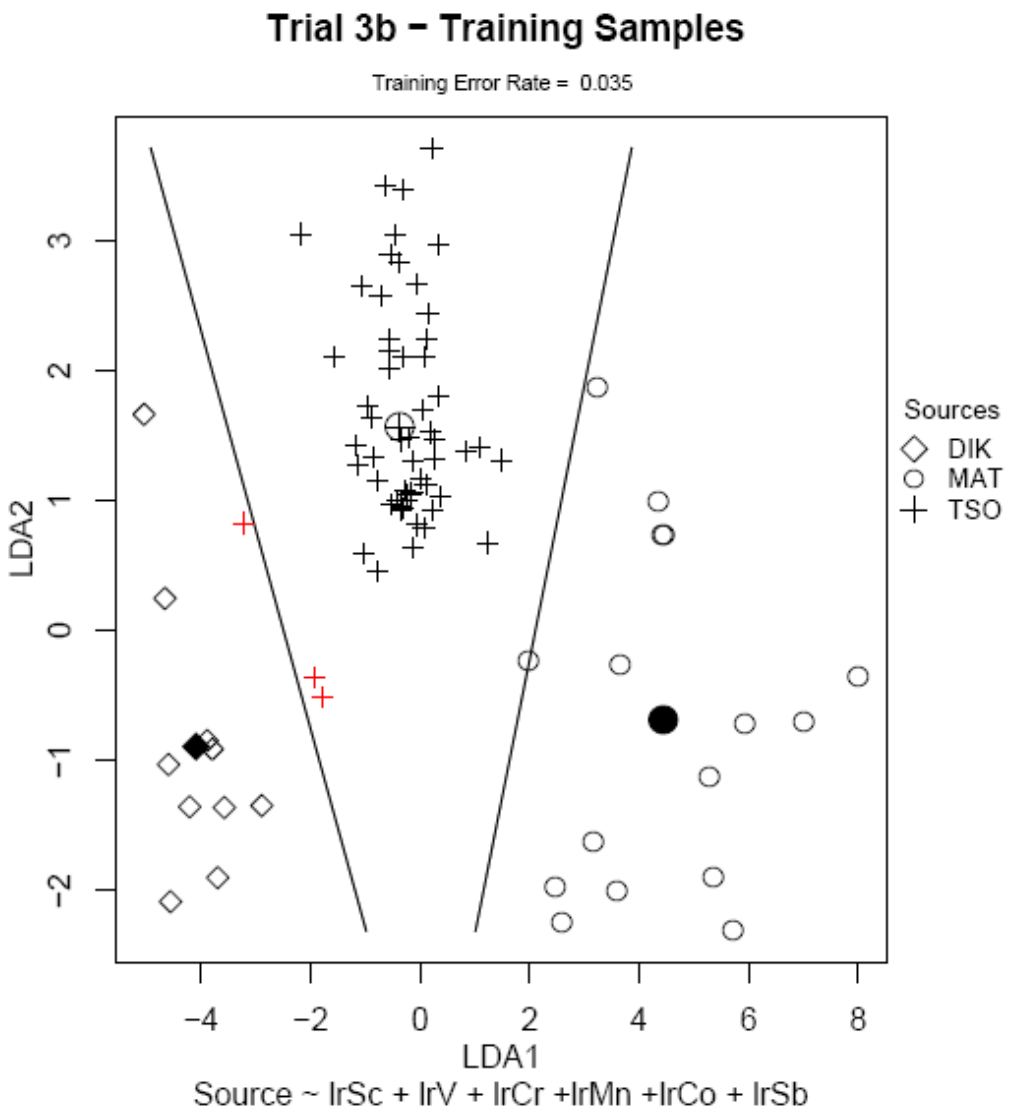


Figure 13. Geologic Trial 3b DFA plot showing the classification of training samples. Misclassified cases are shown in red.

*TRIAL 2a*

Trials 2a, 2b, and 2c were conducted to classify one or two validation samples between only 2 groups per trial. These trials are the simplest to illustrate graphically because there is only one discriminant score calculated for classifying the samples. Thus the plots are also uni-dimensional. This dimensionality also makes classifying the samples much simpler; essentially a line is drawn at the midpoint between the two group centers and the samples are classified with the group to whose midpoint they are nearest.

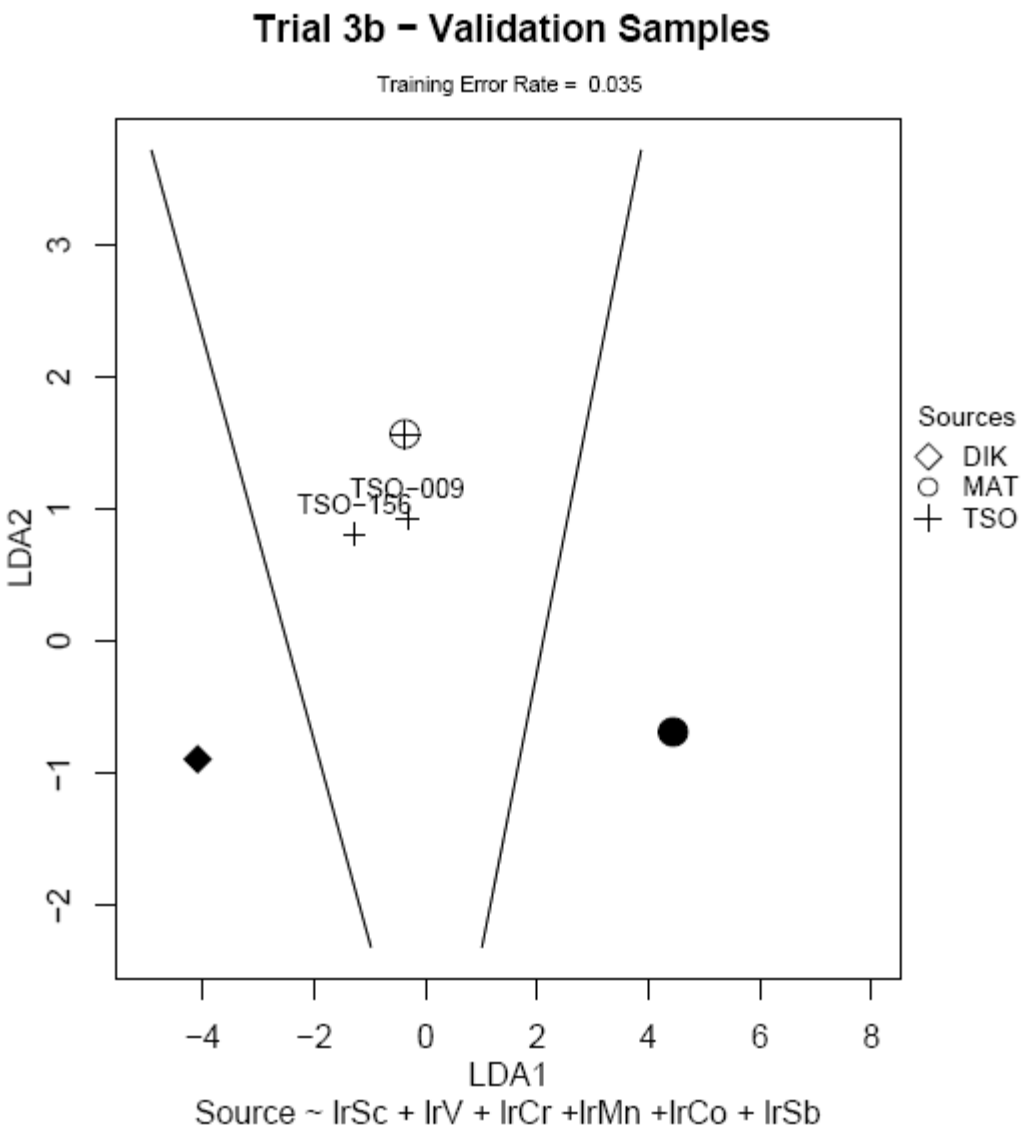


Figure 14. Geologic Trial 3b DFA plot showing the classification of the validation samples.

Trial 2a was conducted with a training set of 79 total samples, 59 from Tsodilo and 20 from Sebilong, and the resulting discriminant functions were applied to the validation sample of SEB-046. The only errors in classification of training samples were that two Tsodilo samples were classified to Sebilong resulting in a 2.5% error rate.

Figure 15 also shows that Trial 2a correctly classified the validation, sample SEB-046. It fell well within the Sebilong range of discriminant score and much closer to the correct group center. Overall it appears the LDA discriminated well between Sebilong and Tsodilo in this trial.

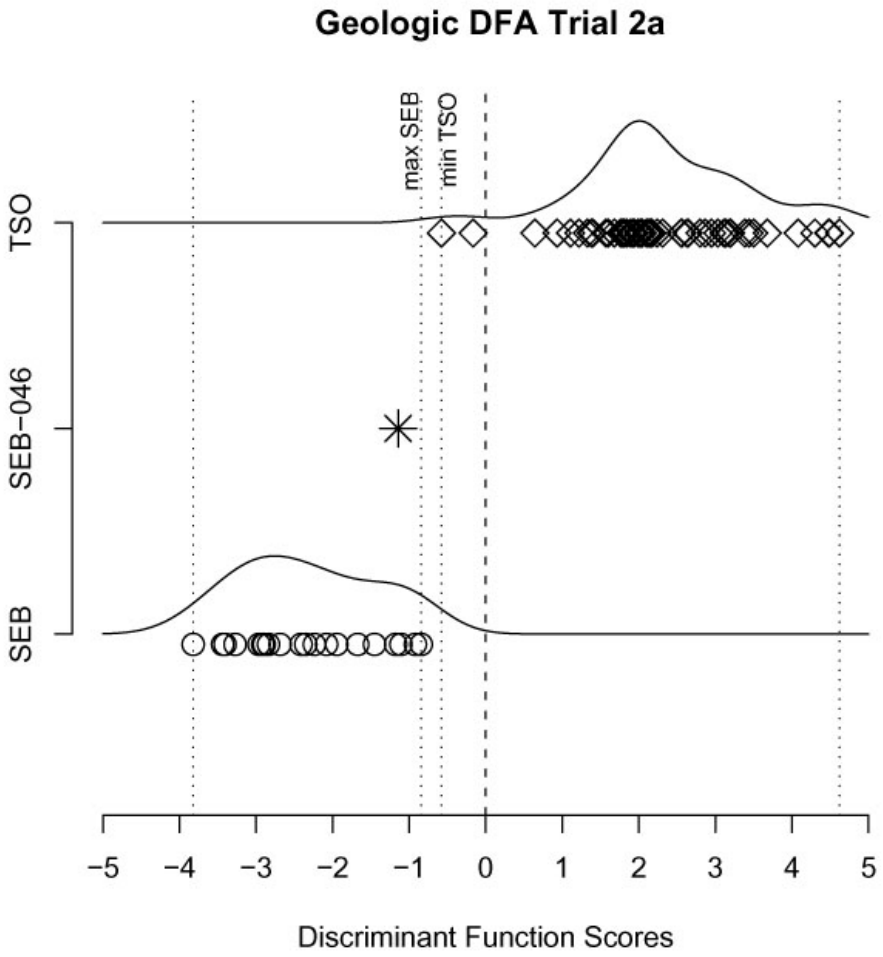


Figure 15. Geologic Trial 2a DFA plot showing the classification of the validation sample.

Table 17. Canonical discriminant function coefficients for Geologic Trial 2a.

| | LD1 |
|---|---|
| lrSc | 1.16277 |
| lrTi | -0.4127 |
| lrV | 0.97221 |
| lrCr | 1.06695 |
| lrMn | 0.77828 |
| lrCo | -4.2448 |
| lrSb | 0.67356 |

*TRIAL 2b*

Trial 2b classified two validation samples, MAT-113 and TSO-154, into the Tsodilo or Matsiloje source groups. The classification functions were developed using a total of 77 training samples; 17 from Matsiloje and 60 from Tsodilo. There were no errors in the reclassification of training samples.

Figure 16 shows the successful classification of the validation samples by DFA. There is no overlap between classification fields, and both validation samples are within their correct fields. The discriminant analysis worked well in this trial, not surprisingly because of the simplicity of the trial and the contrasting rock types of the sources.

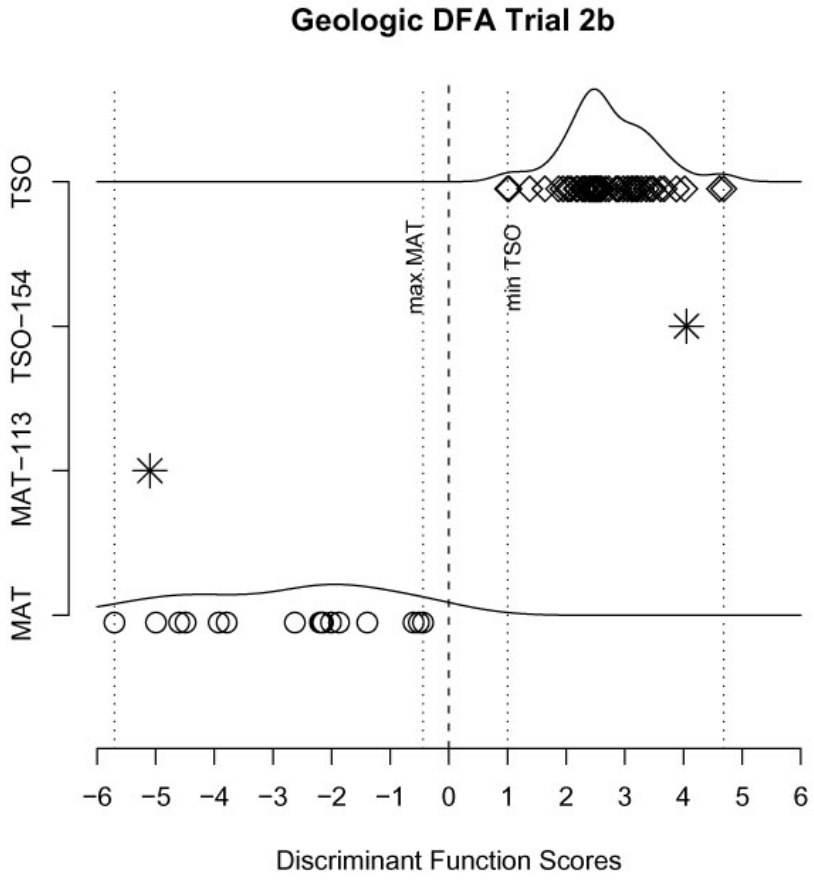


Figure 16. Geologic Trial 2b plot showing the classification of the validation samples.

*TRIAL 2c*

Trial 2c attempted to classify one validation sample TSO-149, between the Tsodilo or Dikgatlampi sources. The classification functions were developed using a total of 70 training samples; 10 from Dikgatlampi and 60 from Tsodilo. There were no errors in the classification of training samples.

Figure 17 shows the successful classification of the validation samples by DFA. There is no overlap between classification fields, and TSO-149 is well within the Tsodilo field. Overall, this trial was completely successful, although the relatively small sample size from Dikgatlampi may have contributed to the accuracy.

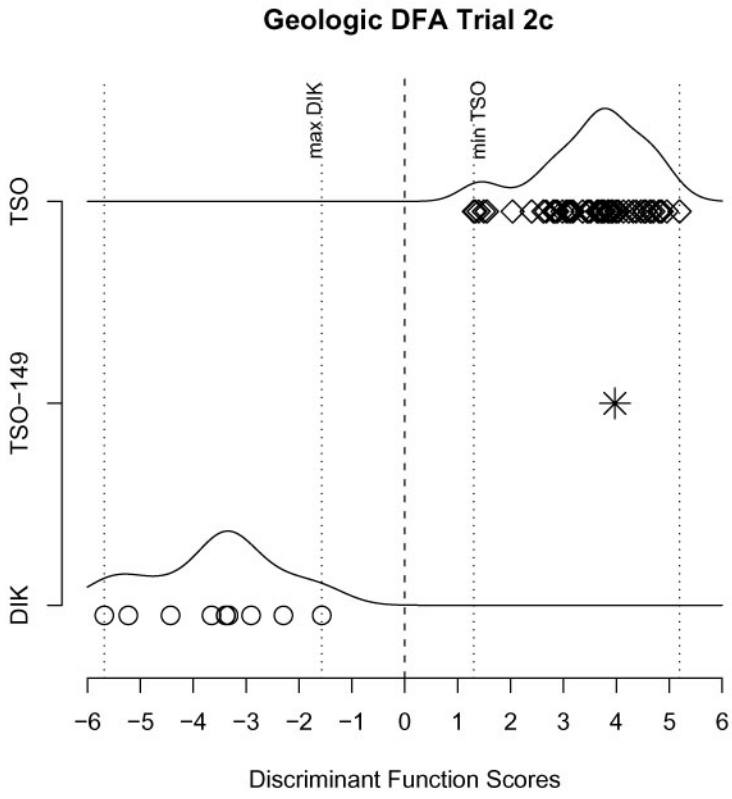


Figure 17. Geologic Trial 2c plot showing the classification of the validation sample.

Table 18. Canonical discriminant function coefficients for Geologic Trial 2b.

| | LD1 |
|---|---|
| lrSc | -4.7052 |
| lrV | -0.1057 |
| lrCr | 1.02071 |
| lrMn | 2.82388 |
| lrCo | -1.7945 |
| lrSb | 0.36369 |

Table 19. Canonical discriminant function coefficients for Geologic Trial 2c.

| | LD1 |
|---|---|
| lrSc | 4.35703 |
| lrTi | -3.5693 |
| lrV | 1.83557 |
| lrCr | -0.4945 |
| lrMn | -1.4795 |
| lrCo | -0.2469 |
| lrSb | 2.07784 |

*SUMMARY*

ELS and DFA were shown to be successful in classifying validation samples, both when used as separate procedures, but especially when used in combination. ELS only misclassified one of the validation samples, eliminating all of the possible sources including the correct one, for sample SEB-050. ELS also correctly identified an individual source for four of the fifteen validation samples. The remaining ten samples were limited to a set of two-to-four sources per sample, all of which included the correct source for each validation sample.

DFA also misclassified only one validation sample, and this was in Geologic Trial 5a which essentially was run without implementing ELS beforehand. Interestingly, the sample misclassified by DFA was not the same one misclassified by ELS, although both were from the Sebilong mine. This indicates that heterogeneity may be greater among the Sebilong samples than the other sources, which would cause more problems for any classification procedures.

The combination of ELS and DFA was very successful, and improved upon the overall model accuracy from DFA alone. All ten validation samples in the six Geologic Trials preceded by ELS were correctly classified. Also, the error rate of the training sets in those six trials ranged from zero to 3.8%. Meanwhile, the training error rate for Trial 5a was 11.4% which shows the ELS made a marked improvement by limiting the potential number of sources and raising the number of discriminating log-ratios that could be included in the DFA trials.

Overall, the combined ELS and DFA procedures showed great success in classifying the validation samples chosen from the geological specularite sample set. This achieved one of the main goals of this study by demonstrating that provenance could reliably be determined for samples simulating artifacts from archaeological contexts with truly unknown provenance. The

procedures developed thus far could now be applied to archaeological samples because significant information can be learned by sacrificing only a small amount of archaeological material.

## *4.3 ARCHAEOLOGICAL SAMPLES*

### *4.3.1 ELEMENTAL LIMIT SERIES ANALYSIS*

The ELS process used on the mine samples was repeated on the archaeological samples with minor changes. The utility and efficacy of the ELS and DFA process has already been shown, so the complete data sets were used for each source region, not just the geologic training set. Obviously, the more complete the starting data sets are, the more trustworthy the results. Also, the same INAA analysis methods were used on all samples, so no changes were necessary to the minimum detection levels used to determine presence of an element for the samples.

Once again, the ELS arrays of the archaeological samples, shown in Figure 19, were compared to the group arrays of each geologic source region, shown in Figure 18, to determine groups and elements to be used for the DFA.

Table 20. Summary of Archaeological ELS analysis results.

| **Arch. Sample** | **Matching Sources** | **DFA Trial** | **Complete Elements** | **Partial Elements** |
|---|---|---|---|---|
| TSRC-02 | DIK, MAT, TSO | 3a | Sc, Cr, Mn, Co | Ti, V, Sb |
| TSRC-01 | TSO | | | |
| TOTG-01 | TSO, DIK | 2a | Sc, Cr, Mn, Co, Ti, V | Sb |
| NQOM-01 | TSO | | | |
| MACG-01 | BKK | | | |
| AK47-02 | BKK | | | |
| AK47-01 | TSO, SEB | 2b | Sc, Cr, Mn, Co, V | Ti, Sb |

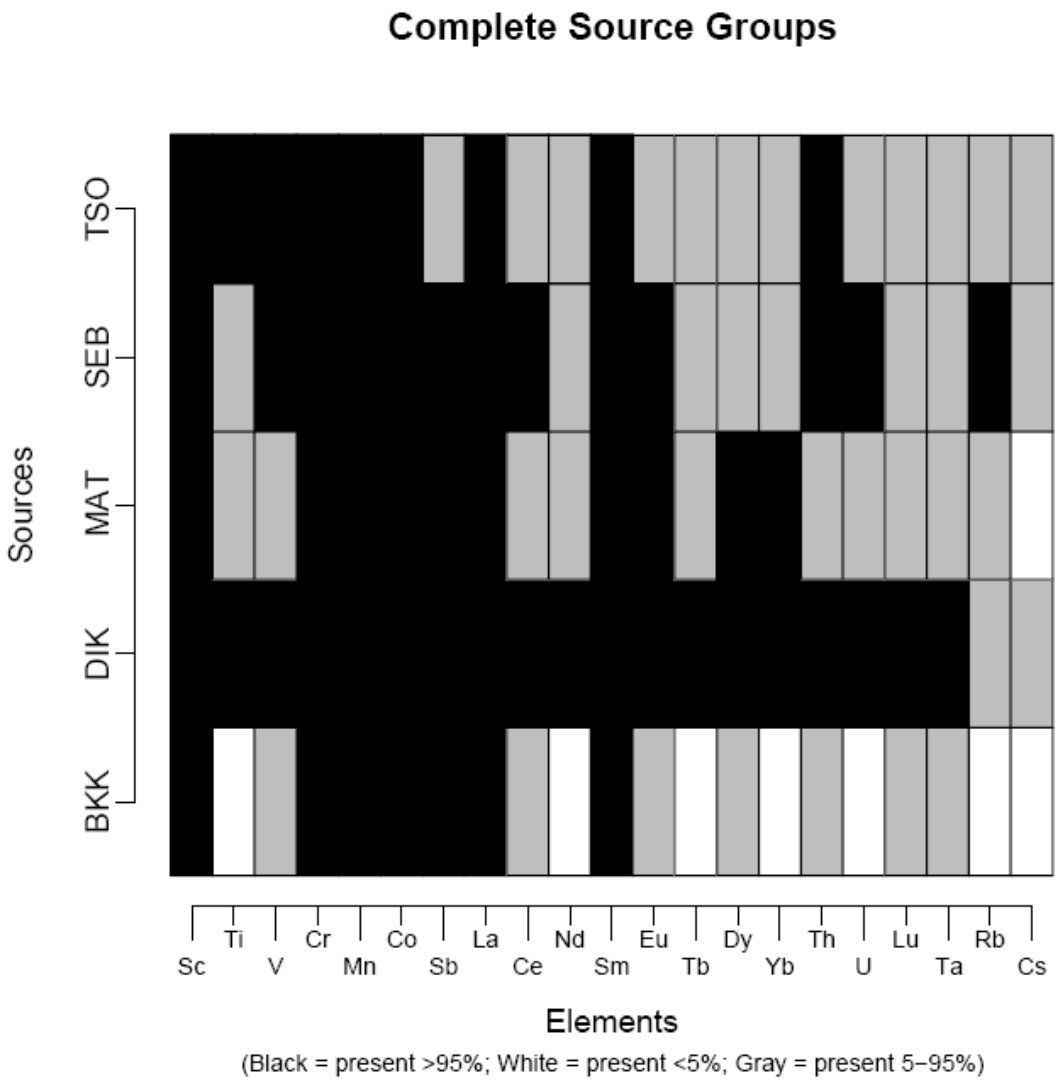


Figure 18. Complete ELS arrays for the geologic sources used for Archaeological DFA trials.

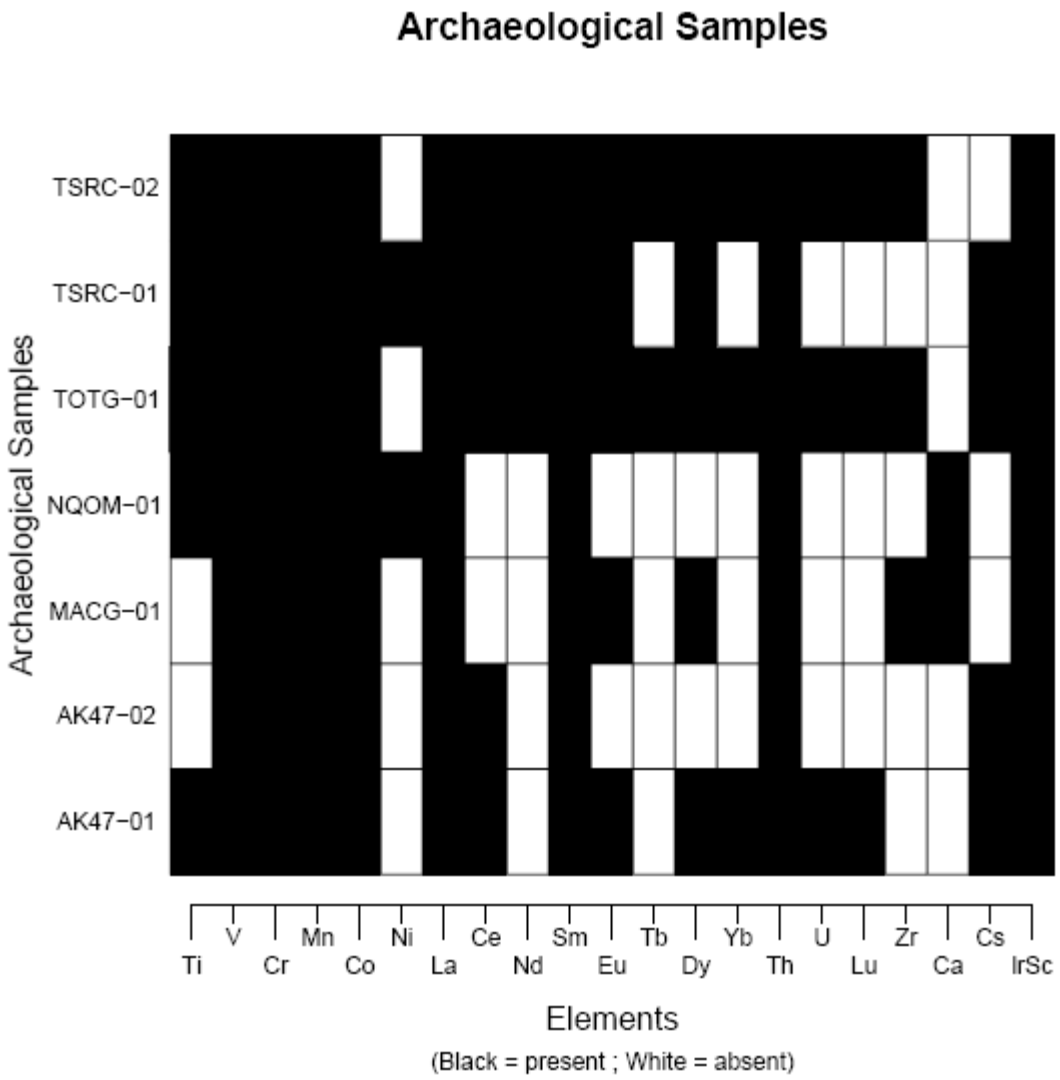


Figure 19. Individual ELS arrays of the seven archaeological samples.

### *4.3.2 DISCRIMINANT FUNCTION ANALYSIS*

*TRIAL 5a*

Trial 5a was run with all seven archaeological samples including those that were assigned to only one group by ELS analysis to determine how the DFA results may differ if ELS is not used, especially for the four cases for which ELS analysis identified a single source. All 5 geologic sources were used as the training set primarily to assign samples AK47-02, MACG-01,

NQOM-01, and TSRC-01 to potential sources. In this trial 151 geologic samples were used for the training set. There were 17 misclassification errors giving an error rate of 11.2%. Distribution of samples and errors among groups are shown in Table 21.

Figure 21 shows the seemingly poor results of the classification of the archaeological samples using all five geologic sources as the training set. Archaeological samples TSRC-01, TSRC-02, and NQOM-01 all come from archaeological contexts within the Tsodilo Hills, which makes difficult to believe that only one of these samples, TSRC-02, came from the local Tsodilo sources located within a kilometer. Obviously, the classification accuracy of Trial 5a is very suspect because of the high training error rate and the seemingly erroneous archaeological classifications. This illustrates the utility of a more limited training set provided by logical source exclusion processes such as ELS.

Table 21. Archaeological DFA Trial 5a Training Sample Classification matrix.

| | **Predicted** | | | | |
|---|---|---|---|---|---|
| **Source** | BKK | DIK | MAT | SEB | TSO |
| BKK | 20 | 0 | 5 | 0 | 0 |
| DIK | 0 | 11 | 0 | 0 | 0 |
| MAT | 6 | 0 | 14 | 1 | 0 |
| SEB | 0 | 0 | 0 | 23 | 0 |
| TSO | 0 | 2 | 0 | 3 | 66 |

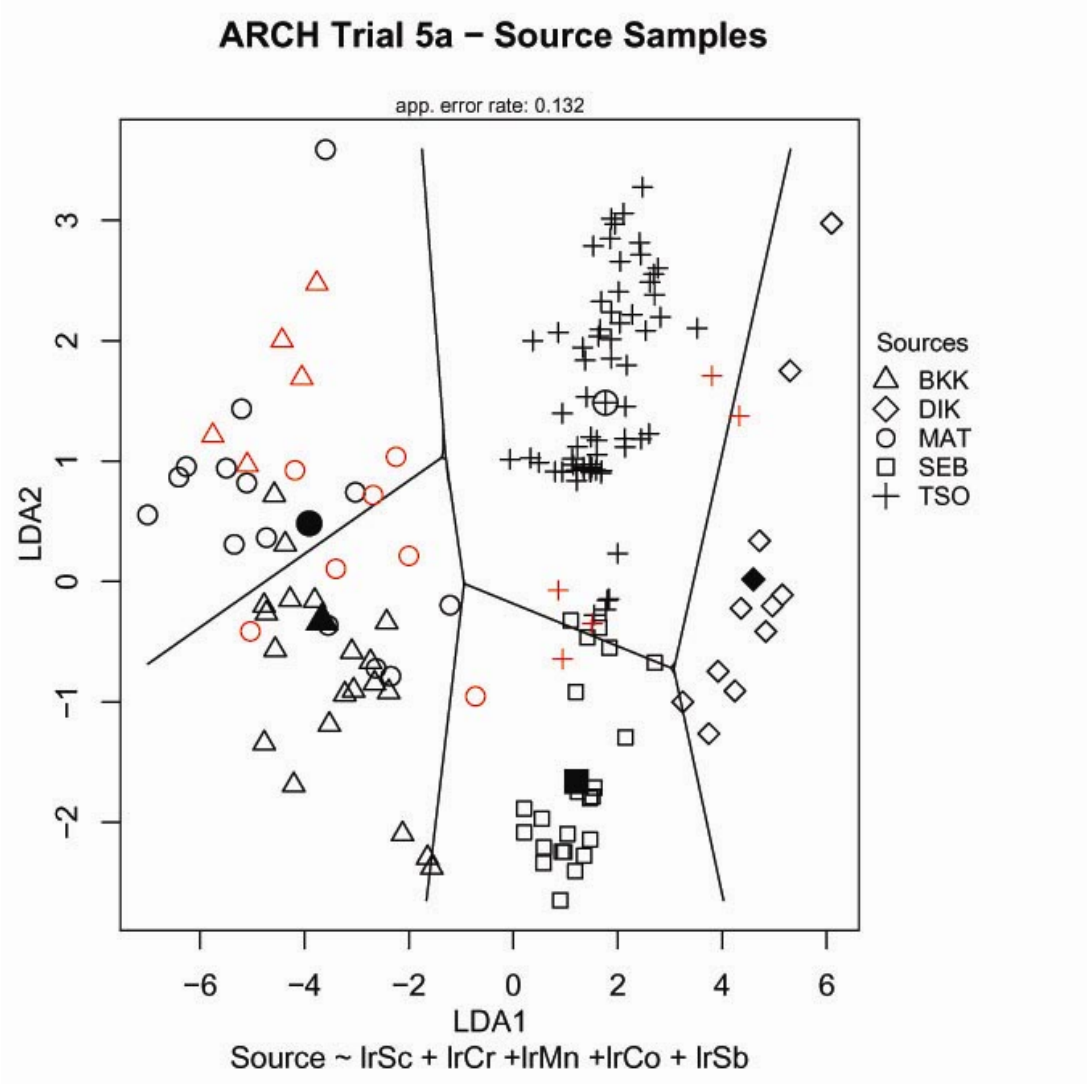


Figure 20. Archaeological Trial 5a DFA plot showing classification of geologic source samples with training set errors in red.

Table 22. Canonical discriminant function coefficients for Archaeological Trial 5a.

| | LD1 | LD2 | LD3 | LD4 |
|---|---|---|---|---|
| lrSc | -5.4608 | -0.0554 | -2.0819 | -0.6131 |
| lrCr | 0.95096 | 0.90633 | 1.52709 | -0.7358 |
| lrMn | 2.34655 | -0.7896 | -0.4958 | -2.3932 |
| lrCo | -0.665 | -1.7162 | 1.05893 | 2.15461 |

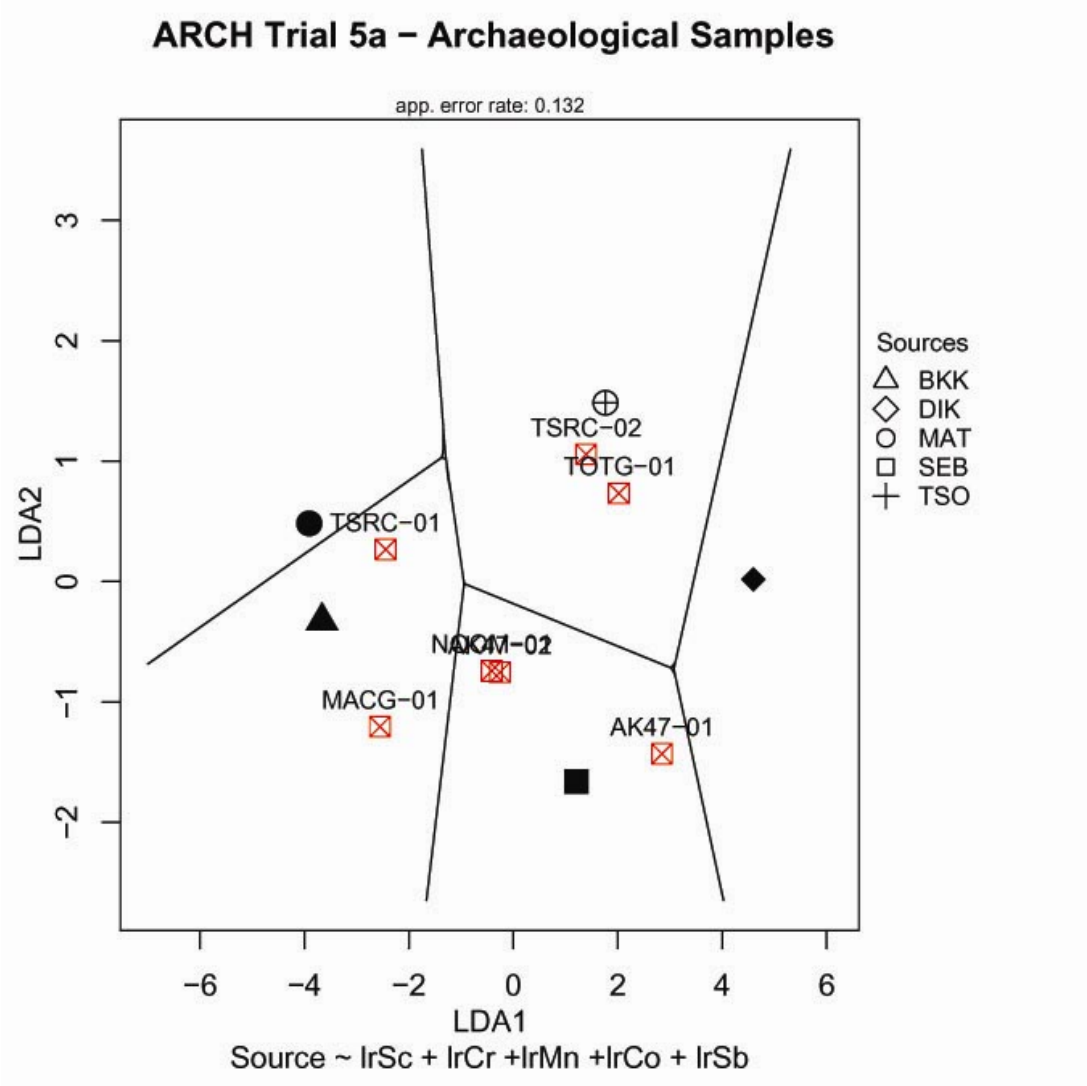


Figure 21. Archaeological Trial 5a DFA plot showing classification archaeological samples.

*TRIAL 3a*

Trial 3a was run using Dikgatlampi, Matsiloje, and Tsodilo as the potential sources for archaeological sample TSRC-02. The clear expectation for this sample, as well as for TSRC-01, is that it was mined at one of the Tsodilo Hills mines near the cave where it was found.

The training set for this trial consisted of 11 samples from Dikgatlampi, 67 from Tsodilo, but only 4 from Matsiloje (see Figure 22). The reclassification of the training set resulted in no errors. Figure 23 shows that archaeological sample TSRC-02 was classified very strongly with

the Tsodilo source region as was hoped for. After calculating the discriminant functions, there were no errors in classifying the training data set.

The small sample set used in the DFA for the Matsiloje source group exposed a problem with the ELS method as implemented for the archaeological trials. The problem is easily corrected and will be in future implementations of these methods, but was kept in this trial to illustrate and discuss this important issue. The decision was made to include log-ratios present in less than 95% of samples at each potential source as variables in the DFA trials. As usual, samples that were missing one or more of the elements selected for the DFA by ELS were excluded from the training set by default. In Trial 3a lrTi was used and only four samples (14%) from Matsiloje contained measurable amounts of Ti. In the other trials this was not a problem because most of the variables included, despite some missing values, are still present in about 80%-90% of the samples for any source group. In retrospect, lrTi should not be included in this trial, and in general, the inclusion of any variable that would cause omission of a significant portion of a source group's samples should be avoided.

Table 23. Canonical discriminant function coefficients for Archaeological Trial 3a.

| | LD1 | LD2 |
|---|---|---|
| lrSc | 5.72611 | 4.31335 |
| lrTi | 3.74546 | -3.851 |
| lrV | -0.8579 | 2.06266 |
| lrCr | -2.0306 | -0.0498 |
| lrMn | -4.9178 | -0.9235 |
| lrCo | 0.29538 | -0.3785 |
| lrSb | -0.841 | 1.83256 |

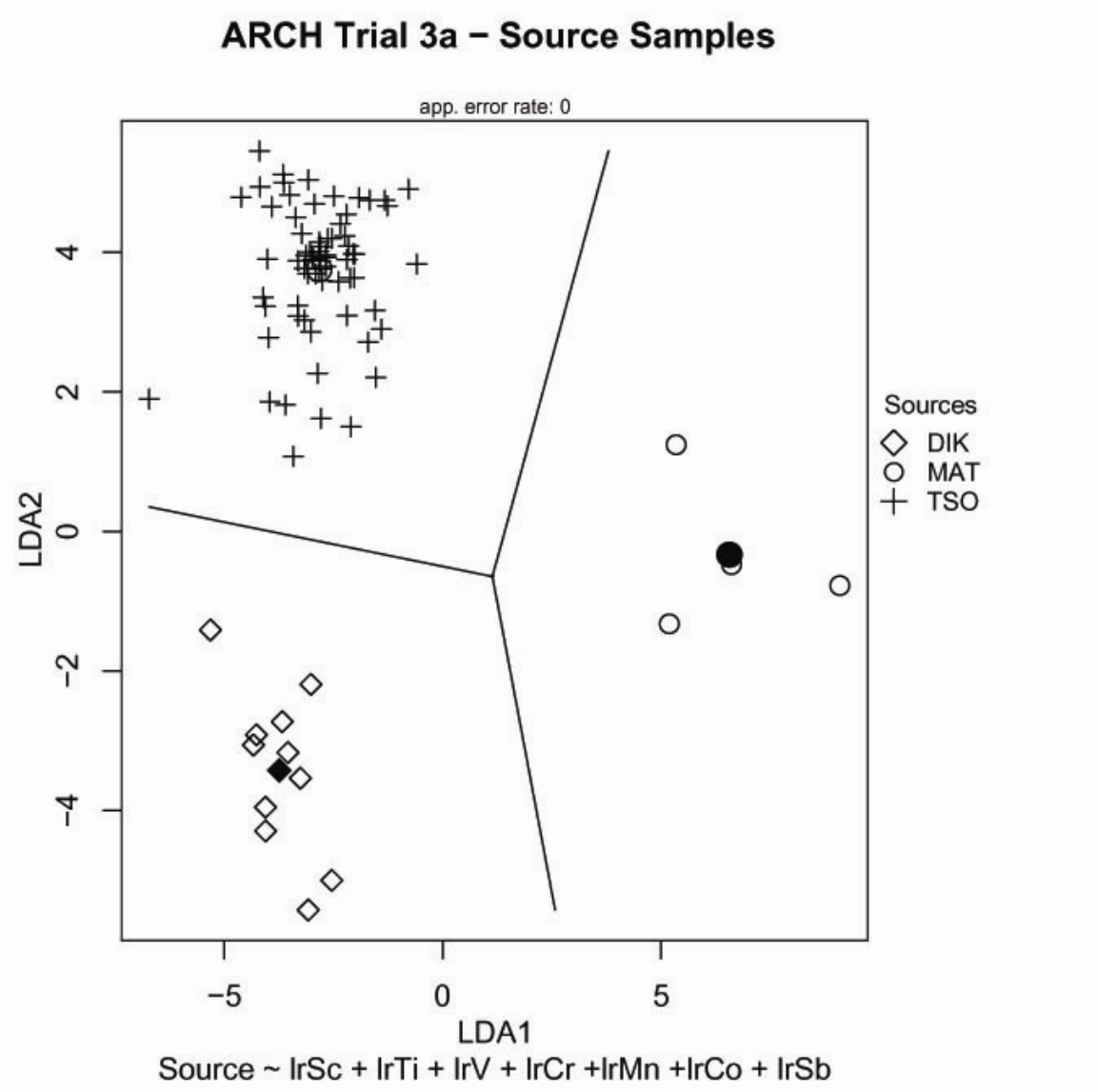


Figure 22. Archaeological Trial 3a DFA plot showing classification of geologic training samples.

The simplest solution to this problem is to remove any log-ratios missing from a significant portion of any group from the DFA. Although this is completely valid theoretically, it does potentially remove variance between groups that could improve the classification accuracy of the DFA. In extreme cases, this could lead to linearity or a singularity in the covariance

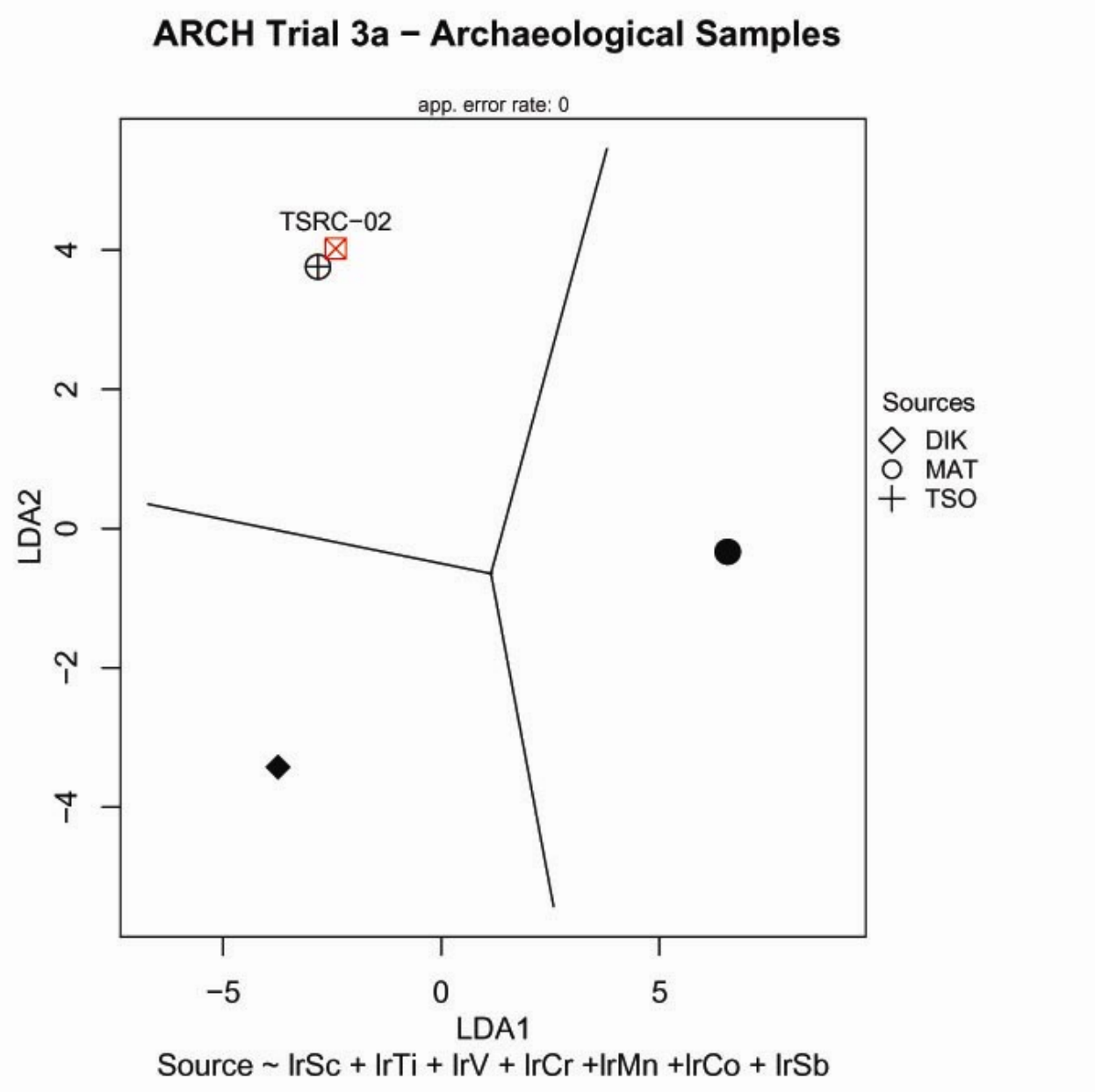


Figure 23. Archaeological Trial 3a DFA plot showing classification of sample TSRC-02.

matrix, resulting in a complete failure of the DFA routine. Another more robust but more complicated strategy is to use one of the zero replacement strategies such as bootstrap estimation or others discussed by Aitchison (1986).

After the ELS process, any missing values in the data set would be replaced with values below the detection limit, thus allowing the cases with missing log-ratios to be included in the

DFA. These more complicated strategies can potentially lead to much more powerful discriminating functions, but some assumptions must be made about group variances and could potentially introduce more or less variance in the source groups than is actually present.

This problem will be remedied in future studies by using a data set for DFA with the missing data appropriately replaced while still using the non-replaced data for ELS analysis. This process would likely yield valid results but is beyond the scope of this study.

*TRIAL 2a*

Trial 2a used Dikgatlampi and Tsodilo as the potential sources for archaeological sample TOTG-01. This sample is geographically much closer to the Tsodilo Hills, so a result indicating Dikgatlampi as the source would be surprising.

The training set for this trial included only 11 samples from Dikgatlampi and 67 from Tsodilo. There was no overlap or misclassification errors on the original training set with the discriminant functions. The log-ratios of Sc, Ti, V, Cr, Mn, Co, and Sb were used to generate the discriminant function scores for this trial.

Table 24. Canonical discriminant function coefficients of Archaeological Trial 2a.

| | LD1 |
|---|---|
| lrSc | 4.78184 |
| lrTi | -3.422 |
| lrV | 1.7903 |
| lrCr | -0.5995 |
| lrMn | -1.5395 |
| lrCo | -0.4084 |
| lrSb | 1.93284 |

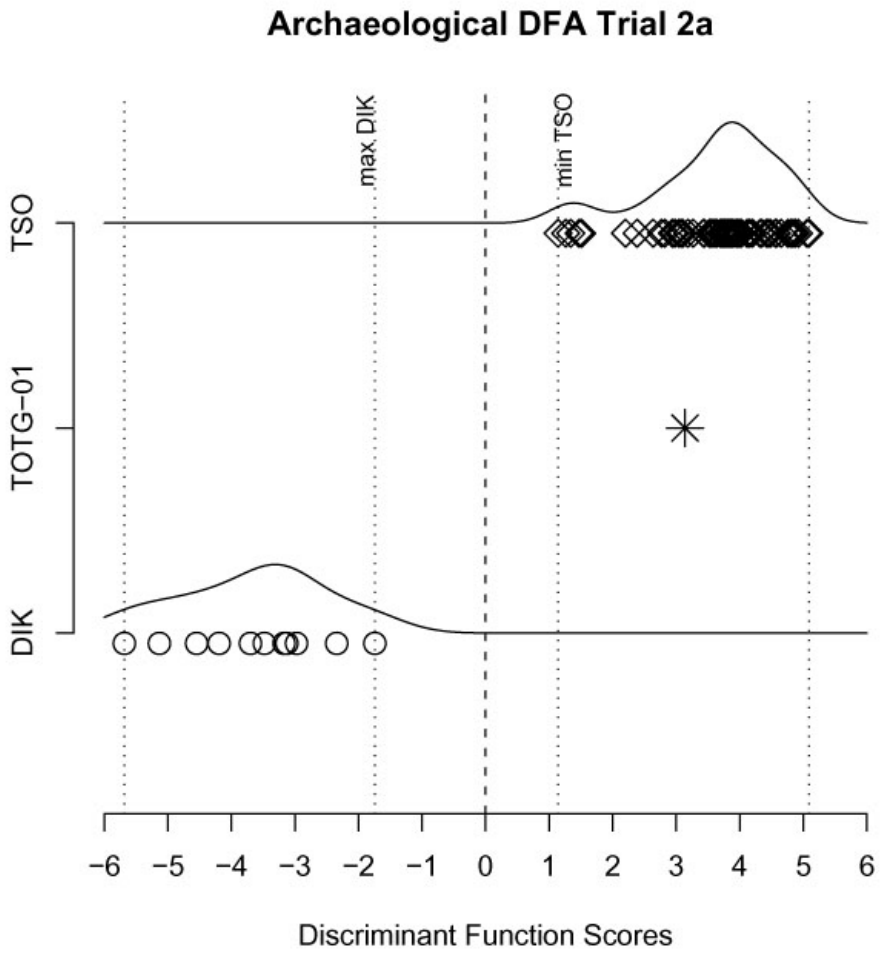


Figure 24. Archaeological DFA Trial 2a plot showing the classification of sample TOTG-01.

*TRIAL 2b*

Trial 2b used Sebilong and Tsodilo as the potential source regions for AK47-01. Once again, this archaeological sample is geographically much closer to one of the DFA source groups, Sebilong. It was also found relatively near the Dikgatlampi mine, but that source was eliminated by ELS analysis.

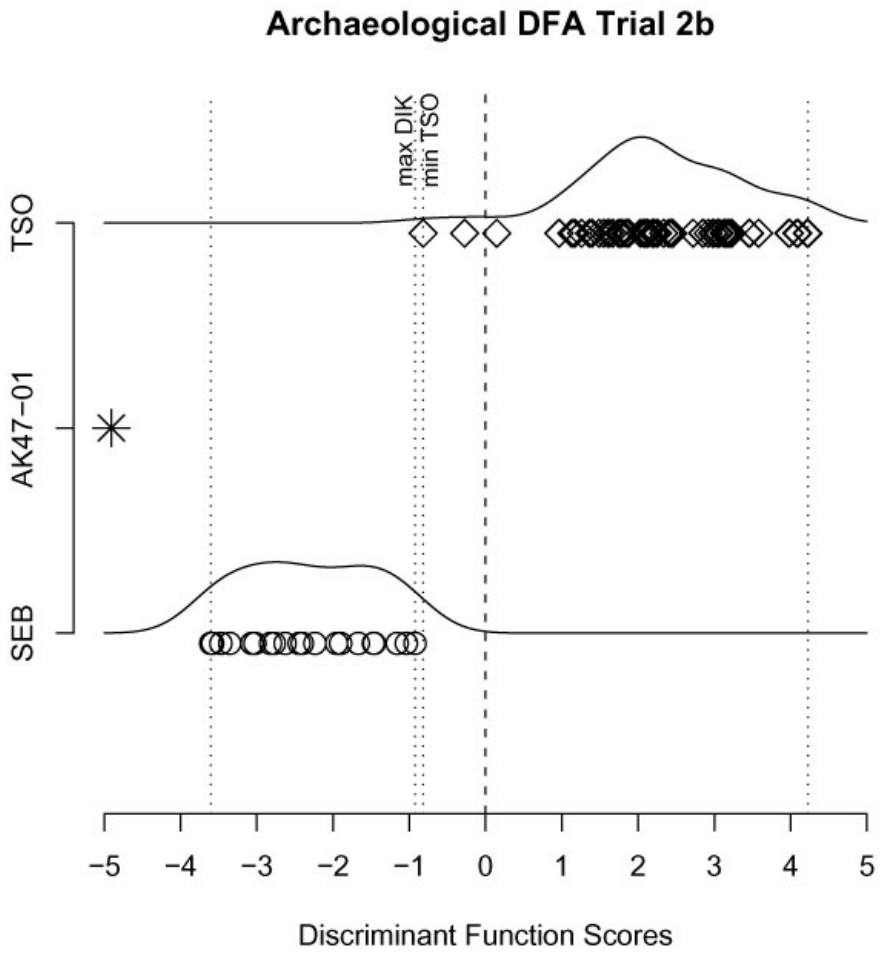


Figure 25. Archaeological DFA Trial 2b plot showing the classification of sample AK47-01.

Table 25. Canonical discriminant function coefficients of Archaeological Trial 2b.

| | LD1 |
|---|---|
| lrSc | 1.12704 |
| lrV | 1.2944 |
| lrCr | 1.0158 |
| lrMn | 1.35424 |
| lrCo | -4.8809 |
| lrSb | 0.52503 |

The training set consisted of 21 samples from Sebilong and 67 from Tsodilo (Table 25). Two of the Tsodilo samples grouped closer to the Sebilong group centroid for an error rate of

2.2%, however there was still no overlap between groups (Figure 25). The log-ratios of Sc, V, Cr, Mn, Co, and Sb were used to generate the discriminant function scores for this trial.

*SUMMARY*

Overall, six out of seven archaeological samples were classified as expected, with the geographically closest mine. The only ELS case that seems in error is AK47-02 which was associated with Blinkklipkop. However, in Archaeological Trial 5a, it was classified with the Sebilong group. This makes more sense from a geographic standpoint because it was recovered only ten kilometers from Sebilong. Otherwise, the ELS analysis did not have any obvious flaws.

The subsequent DFA trials worked well also. AK47-01 was associated with Sebilong rather than Tsodilo by Trial 2b, which again makes sense from the geography. Sample TSRC-02 was classified with Tsodilo instead of Dikgatlampi or Matsiloje by Trial 3a as expected. Perhaps most interesting was Trial 2a which classified sample TOTG-01, distant from all possible source mines, with Tsodilo rather than Dikgatlampi. This is the most logical and probable source for the sample because it is the closest and could be reached easily by the Okavango delta system (Robbins et al., 1998a).

Archaeological Trial 5a also showed how limiting the potential number of sources by ELS analysis can affect the outcome of DFA classification. In this trial where all 5 sources were included, only 4 of the 7 samples were sourced to the closest mine. Likely errors include TSRC-01 and NQOM-01 which were almost certainly mined in the Tsodilo Hills where they were found. However, sample AK47-02 was classified with Sebilong rather than Blinkklipkop as suggested by ELS alone, so the results of this more complicated trial were somewhat mixed.

## CHAPTER 5 CONCLUSIONS

Overall, this study has shown that the concept of specularite provenance is viable and has helped to reach several conclusions and a few starting points for future research. The transition metal compositions of specularite can successfully discriminate between groups and are relatively homogeneous among replicate samples and sources. Elemental Limit Series analysis is a very useful and often essential tool for limiting the number of possible source groups included in subsequent discriminant function analyses and a good way of incorporating the below-detection-limit values that are excluded and unused by DFA. Despite the ELS analysis method's simplicity, care must be taken with larger data sets to ensure that comparable detection limits and classification thresholds are used when producing the ELS arrays.

The five source groups sampled appear discrete and six of seven archaeological samples were classified to the closest mine. Compositional variation in the Tsodilo Hills group indicated that these methods may be successful at the local source scale as well. Finally, the source database needs to be enlarged, and as it grows hopefully our ability to identify provenance of archaeological specularite will too, but success with a more populated database will hinge on the ability to limit those potential sources using ELS and other comparative and exclusive methods that can incorporate zero values and the absence of elements and minerals along with their presence and concentrations.

The geologic and archaeological DFA trials show that these methods have been very successful at classifying samples between sources at the regional scale. Some important trends were apparent throughout the trials. One is that DFA is more successful at developing functions when there are fewer groups, which reduces the training error rate and should also increase the accuracy of the predictive classification of archaeological samples.

The first-row transition metals proved to be very useful as a data set for differentiating the mine regions. All of the elemental log-ratios contributed to the power of the functions, but Sc, Mn, and Ti were usually the most important discriminators in the first discriminant dimension. The other transition metals were also very important on a case-by-case basis depending on which set of sources were being contrasted.

Another trend that is slightly less obvious and intuitive is the variation present at the local scale. Although all of the DFA trials presented here were run at the regional scale, the Tsodilo Hills groups continually showed the most variation among the groups. This is most likely due to the greater number of separate mines and deposits sampled at Tsodilo than the other regions. It may also be a simple artifact of sample sizes as more than twice as many samples from Tsodilo were included than from any of the other sources. This is illustrated in the figures that show some slight clustering among Tsodilo samples, and the fact that most of the misclassified cases in the trials involved the Tsodilo group.

This apparent variation among the Tsodilo mines indicates three things. First, it hints that the same methods applied at the regional scale in this study should be successful at the local scale as well because the variation that caused the clustering and misclassification errors at the regional scale can be used to differentiate individual mines. This conclusion is corroborated by previous work using parts of the same data set used here that was reasonably successful at classifying geologic samples from Tsodilo using much of the same methodology (Kiehn et al., 2007).

Secondly, the amount of variation needed to determine provenance at the local scale may be excessive and cause problems at the regional scale. The results from Archaeological Trial 5a show that trials on specularite with more than 3 or 4 potential source groups may be much less

accurate than those with fewer groups. At regional scale, some variation is good, but it is often likely be too much unless the number of potential sources can be limited by sound reasoning. So, comparisons among sources using mineralogy, petrography, or ELS analysis are essential to exclusively limit potential source regions for an artifact before the DFA is carried out.

Thirdly, the need for ELS and other deductive processes is something to keep in mind when future specularite provenance studies are carried out using these or other methods. This study sampled only 5 potential sources and had very good success. However, other methods of provenance on other materials, such as REE signatures of soapstone artifacts, have started out this same way before problems with their accuracy became apparent as the source database grew and the true nature of the variation was shown (Luckenbach et al., 1975; Moffat and Buttler, 1986). In all likelihood, as the specularite source database grows and these methods are applied, sample populations that appear discrete and separable now will become more of a continuum, limiting the success of future studies. However, it is also possible that the picture may stay as clear or even improve with an expansion of this specularite source study.

Application of these methods to ochre study should be approached with optimism and caution. The mineralogical similarities between fine-grained ochre and coarse-grained specularite indicate that geochemical fingerprinting of ochre sources may be possible, as indicated by the more plentiful ochre studies (Erlandson et al., 1999; Popelka-Filcoff, 2006; Smith et al., 1998). However, it should also be kept in mind that sedimentary ochre source tend to be more widespread and less localized, which has caused problems for studies that attempted to source another sedimentary mineral, chert(Cackler et al., 1999). Testing ochres sources that are localized and discrete, possibly formed from the weathering of coarse-grained igneous or

metamorphic hematite, would yield the highest likelihood of success for the procedures outlined in this study.

As usual, the answers to the original questions of this study only raise more in-depth questions and possibilities for further research are plentiful and promising. Tsodilo Hills has almost two dozen known mines only few kilometers apart. Samples collected from 14 of these mines can be used to test whether specularite can be sourced to individual mines at the local scale. These mines can also be used to examine the relative importance of geographic separation versus geologic character of the specularite deposits to the geochemical signatures being used to determine provenance. In addition, four of the archaeological samples used in this study are likely from this region, so future studies will examine if these samples can be linked to a group of mines, or even an individual mine in the Tsodilo Hills. This in turn holds great promise if successful, as trade networks and relationships can be examined through specularite movement.

Future specularite provenance studies should continue to include petrographic analysis and ELS analysis, but should use sophisticated zero-replacement strategies to prepare the data set for DFA as well. Archaeological Trial 3a illustrated the serious problems that occur if a simple strategy of omission is followed. Another strategy of excluding elemental variables that are only partially present would also be valid, but this strategy unnecessarily reduces the discriminating power of the functions and could potentially cripple otherwise useful data sets. When used correctly, advanced zero replacement techniques, such as bootstrap estimation, can validly simulate a population that is partially below the analytical detection limit without introducing false groupings or collinearity.

**BIBLIOGRAPHY**

Aitchison, J., 1986, The statistical analysis of compositional data: London ; New York, Chapman and Hall, xv, 416 p.

Aldiss, D.T., Tombale, A.R., Mapeo, R.M.B., and Chiepe, M., 1989, The Geology of the Kanye Area, Bulletin Series: Gaborone, Geological Survey Department, Republic of Botswana, p. 170.

Bau, M., and Dulski, P., 1996, Distribution of yttrium and rare-earth elements in the Penge and Kuruman iron-formations, Transvaal Supergroup, South Africa: Precambrian Research, v. 79, p. 37-55.

Beaumont, P.B., 1973, The Ancient Pigment Mines of Southern Africa: South African Journal of Science, v. 69, p. 140-146.

Beaumont, P.B., and Boshier, A.K., 1974, Report on test excavations in a prehistoric pigment mine near Postmasburg, Northern Cape: South African Archaeological Bulletin, v. 29, p. 41-59.

Burchell, W.J., 1822, Travels in the interior of southern Africa: Cape Town,, C. Struik.

Cackler, P.R., Glascock, M.D., Neff, H., Iceland, H., Pyburn, K.A., Hudler, D., Hester, T.R., and Chiarulli, B.M., 1999, Chipped Stone Artefacts, Source Areas, and Provenance Studies of the Northern Belize Chert-bearing Zone: Journal of Archaeological Science, v. 26, p. 389-397.

Campbell, A.C., Denbow, J.R., and Wilmsen, E.N., 1994, Painting like engravings: Rock art at Tsodilo, *in* Dowson, T.A., and Williams, D.L., eds., Contested Images: Diversity in Southern African Rock Art Research: Johannesburg, Witwatersrand University Press, p. 131-158.

Campbell, A.C., and Main, M., 2003, Guide to Greater Gaborone: Gaborone, Botswana Society, 292 p.

Clarke, J., 1976, Two Aboriginal Rock Art Pigments from Western Australia: Their properties, use, and durability: Studies in Conservation, v. 21, p. 134-142.

Cohen, G., 1977, The Ancient Workings at Gakgale: Botswana Notes and Records, v. 9, p. 17-19.

Cornell, R.M., and Schwertmann, U., 2003, The iron oxides : structure, properties, reactions, occurrences and uses: Weinheim, Wiley-VCH, xxxix, 664 p. p.

Davis, J.C., 2002, Statistics and data analysis in geology: New York Chichester, Wiley, xvi, 638 p.

Denbow, J.R., and Wilmsen, E.N., 1986, Advent and course of pastoralism in the Kalahari: Science, v. 234, p. 1509-1515.

Erlandson, J.M., Robertson, J.D., and Descantes, C., 1999, Geochemical analysis of eight red ochres from western North America: American Antiquity, v. 64, p. 517-526.

Glascock, M.D., 2002, Obsidian Provenance Research in the Americas: Accounts of Chemical Research, v. 35, p. 611-617.

Glascock, M.D., 2004, Tables for Neutron Activation Analysis: Columbia, Missouri, Research Reactor Center, University of Missouri-Columbia, 150 p.

Glascock, M.D., and Neff, H., 2003, Neutron activation analysis and provenance research in archaeology: Measurement Science and Technology, v. 14, p. 1516-1526.

Glascock, M.D., Neff, H., Stryker, K.S., and Johnson, T.N., 1994, Sourcing archaeological obsidian by an abbreviated NAA procedure: Journal of Radioanalytical and Nuclear Chemistry, v. 180, p. 29-35.

Glascock, M.D., Neff, H., and Vaughn, K.J., 2004, Instrumental Neutron Activation Analysis and Multivariate Statistics for Pottery Provenance: Hyperfine Interactions, v. 154, p. 95-105.

Harding, C.J., 2004, Origin of the Zeekoebaart and Nauga East High-Grade Iron Ore Deposits, Northern Cape Province, South Africa: Johannesburg, South Africa, Rand Afrikaans University.

Humphreys, A.J.B., 1974, The Occurrence of Ostrich Egg Shells Filled with Specularite in the Northern Cape: South African Journal of Science, v. 70, p. 48.

Jacobson, L., 1977, A pottery cache from the Bethanie district, South West Africa: Cimbebasia, v. 2, p. 228-233.

Jercher, M., Pring, A., Jones, P.G., and Raven, M.D., 1998, Rietveld X-Ray Diffraction and X-Ray Flourescence Analysis of Australian Aboriginal Ochres: Archaeometry, v. 40, p. 383-401.

Key, R.M., 1976, The geology of the area around Francistown and Phikwe, Northeast and Central Districts, Botswana, District Memoirs: Gaborone, Geological Survey of Botswana.

Kiehn, A.V., Brook, G.A., Glascock, M.D., Dake, J.Z., Robbins, L.H., Campbell, A.C., and Murphy, M.L., 2007, Fingerprinting Specular Hematite from Mines in Botswana, Southern Africa, *in* Glascock, M., Speakman, R.J., and Popelka-Filcoff, R.S., eds., Archaeological chemistry : analytical techniques and archaeological interpretation: ACS symposium series: Washington, DC, American Chemical Society : Distributed by Oxford University Press, p. 460-479.

Luckenbach, A.H., Holland, R.O., and Allen, C.G., 1975, Soapstone Artifacts: Tracing Prehistoric Trade Patterns in Virginia: Science, v. 187, p. 157-158.

McLachlan, G.J., 2004, Discriminant analysis and statistical pattern recognition: Hoboken, N.J., Wiley & Sons, xv, 526 p.

Miller, D.E., and van der Merwe, N.J., 1994, Early Iron Age Metal Working at the Tsodilo Hills, Northwestern Botswana: Journal of Archaeological Science, v. 21, p. 101-115.

Moffat, D., and Buttler, S.J., 1986, Rare Earth Element Distribution Patterns in Shetland Steatite - Consequences for Artifact Provenancing Studies: Archaeometry, v. 28, p. 101-115.

Mooney, S.D., Geiss, C., and Smith, M.A., 2002, The Use of mineral magnetic parameters to characterize archaeological ochres: Journal of Archaeological Science, v. 29, p. 1-13.

Morris, D., and Beaumont, P.B., 2004, Archaeology in the Northern Cape: Some key sites, *in* Maggs, T., van Ryneveld, K., Voight, E., and Richardt, F., eds., Southern African Association of Archaeologists Post-Conference Excursion Guide: Kimberley, McGregor Museum.

Murphy, M.L., Murphy, L., Campbell, A.C., and Robbins, L.H., 1994, Prehistoric mining of mica schist at the Tsodilo Hills, Botswana: Journal of the South African Institute of Mining and Metallurgy, v. 94, p. 87-92.

Neff, H., 2000, Neutron activation analysis for provenance determination in Archaeology, *in* Ciliberto, E., and Spoto, G., eds., Modern Analytical Methods in Art and Archaeology, Volume 155: Chemical Analysis, A Series of monographs on Analytical Chemistry and Its Applications: New York, John Wiley and Sons, p. 81-134.

Phaladi, S.G.G., 1991, Hunter-gatherers and non-hunter-gatherers: A lithic analysis from N!oma, Tsodilo Hills, Botswana: East Lansing, Michigan, Michigan State University.

Popelka-Filcoff, R.S., 2006, Application of Elemental Analysis for Archaeometric Studies: Analytical and Statistical Methods for Understanding Geochemical Trends in Ceramics, Ochre, and Obsidian: Columbia, University of Missouri.

Popelka-Filcoff, R.S., Craig, N., Glascock, M.D., Robertson, J.D., Aldenderfer, M., and Speakman, R.J., 2007, Instrumental Neutron Activation Analysis of Ochre Artifacts from Jiskairumoko, Peru, *in* Glascock, M., Speakman, R.J., and Popelka-Filcoff, R.S., eds., Archaeological chemistry : analytical techniques and archaeological interpretation: ACS symposium series: Washington, DC, American Chemical Society : Distributed by Oxford University Press, p. 480-505.

Popelka-Filcoff, R.S., Robertson, J.D., Glascock, M.D., and Descantes, C., 2005, Sourcing red ochres by instrumental trace analysis: SAS Bulletin, v. 28, p. 9-11.

Robbins, L.H., 1990, The Depression Site: a Stone Age Sequence in the Northwest Kalahari Desert, Botswana: National Geographic Research, v. 6, p. 329-338.

Robbins, L.H., Murphy, M.L., Brook, G.A., Ivester, A.H., Campbell, A.C., Klein, R.G., Milo, R.G., Stewart, K.M., Downey, W.S., and Stevens, N.J., 2000, Archaeology, Palaeoenvironment, and Chronology of the Tsodilo Hills White Paintings Rock Shelter, Northwest Kalahari Desert, Botswana: Journal of Archaeological Science, v. 27, p. 1085-1113.

Robbins, L.H., Murphy, M.L., Brook, G.A., Reid, D.M., Haberyan, K.A., and Downey, W.S., 1998a, Test excavations and reconnaissance palaeoenvironmental work at Toteng, Botswana: South African Archaeological Bulletin, v. 53, p. 125-132.

Robbins, L.H., Murphy, M.L., Campbell, A.C., and Brook, G.A., 1996, Excavations at the Tsodilo Hills Rhino Cave: Botswana Notes and Records, v. 28, p. 23-45.

Robbins, L.H., Murphy, M.L., Campbell, A.C., and Brook, G.A., 1998b, Intensive mining of specular hematite in the Kalahari ca. A.D. 800-1000: Current Anthropology, v. 39, p. 144-150.

Robbins, L.H., Murphy, M.L., Stewart, K.M., Campbell, A.C., and Brook, G.A., 1994, Barbed bone points, paleoenvironment, and the antiquity of fish exploitation in the Kalahari Desert, Botswana: Journal of Field Archaeology, v. 21, p. 257-264.

Shannon, R.D., 1976, Revised effective ionic radii and systematic studies of interatomic distances in halides and chalcogenides: Acta Crystallographica Section A, v. 32, p. 751-767.

Singh, B., and Gilkes, R.J., 1992, Properties and distribution of iron oxides and their association with minor elements in the soils of south-western Australia: Journal of Soil Science, v. 43, p. 77-98.

Singh, B., Sherman, D.M., Gilkes, R.J., Wells, M., and Mosselmans, J.F.W., 2000, Structural chemistry of Fe, Mn, and Ni in synthetic hematites as determined by extended X-ray absorption fine structure spectroscopy: Clays and Clay Minerals, v. 48, p. 521-527.

Smith, M.A., and Fankhauser, B., 1996, An archaeological perspective on the geochemistry of Australian red ochre deposits: Prospects for fingerprinting major ore sources., Report to the Australian Institute of Aboriginal and Torres Strait Islander Studies: Canberra.

Smith, M.A., Fankhauser, B., and Jercher, M., 1998, The changing provenance of red ochre at Puritjarra rock shelter, Central Australia: Late Pleistocene to present: Proceedings of the Prehistoric Society, v. 64, p. 275-292.

Smith, M.A., and Pell, S., 1997, Oxygen-Isotope ratios in quartz as indicators of the provenance of archaeological ochres: Journal of Archaeological Science, v. 24, p. 773-778.

Tankersley, K.B., Tankersley, K.O., Shaffer, N.R., Hess, M.D., Benz, J.S., Turner, F.R., Stafford, M.D., Zeimens, G.M., and Frison, G.C., 1995, They have a rock that bleeds: Sunrise Red Ochre and its early Paleoindian occurrence at the Hell Gap Site, Wyoming: Plains Anthropologist, v. 40, p. 185-194.

Thackeray, A.I., Thackeray, J.F., and Beaumont, P.B., 1983, Excavations at the Blinkklipkop specularite mine near Postmasburg, northern Cape: South African Archaeological Bulletin, v. 38, p. 17-25.

Tobey, M.H., 1986, Trace Element Investigations of Maya Chert from Belize: San Antonio, Center for Archaeological Research, University of Texas, 79 p.

Trendall, A.F., Compstone, W., Williams, I.S., Amstrong, R.A., Arndt, N.T., McNaughton, N.J., Nelson, D.R., Barley, M.E., Beukes, N.J., Laeter, J.R., de Retief, E.A., and Thome, A.M., 1990, Precise Zirkon U-Pb chronological comparison of the volcano-sedimentary sequences of the Kaapval and Pilbara cratons beteween about 3.1 and 2.4 Ga, Proceedings of the 3rd International Archean Symposium: Perth, p. 81-83.

Tykot, R., H, 2002, Chemical Fingerprinting and Source Tracing of Obsidian: The Central Mediterranean Trade in Black Gold: Accounts of Chemical Research, v. 35, p. 618-627.

von Plehwe-Leisen, E., and Klemm, D.D., 1995, Geology and ore genesis of the manganese ore deposits of the Postmasburg manganese-field, South Africa: Mineralium Deposita, v. 30, p. 257-267.

Wagner, P.A., 1928, The iron deposits of South West Africa: Pretoria.

Weigand, P., Harbottle, G., and Sayre, E.V., 1977, *in* Earle, T.K., and Ericsion, J.E., eds., Exchange Systems in Prehistory: New York, Academic Press, p. 15.

Weinstein-Evron, M., and Ilani, S., 1994, Provenance of ochre in the Natufian layers of el-Wad Cave, Mount Carmel, Israel: Journal of Archaeological Science, v. 21, p. 461-467.

Wernicke, R.S., and Lippolt, H.J., 1994, Dating of vein specularite using internal (U+Th)/$^{4}$He isochrons: Geophysical Research Letters, v. 21, p. 345-347.

Wilen, J.E., Jr., 2000, Mineralogical analysis of red ochre samples from four sites in Knight's Valley, California; XRD and its potential for preliminary identification and sourcing of hematitic deposits: Abstracts with Programs, v. 32, p. 275.

Yong, L., Songlin, F., Xiangqian, F., Dongyu, F., Qing, X., Yin, S., Lin, C., Zhifang, C., Jie, J., Zhenxi, Z., Songlin, Z., and Yongmin, L., 2005, Study on the compositional differences of Tang Sancai from different kilns by INAA: Journal of Archaeological Science, v. 32, p. 183-191.

## APPENDIX – RAW COMPOSITIONS OF SPECULARITE SAMPLES

Table 26. Raw compositions for samples excluded from analyses due to low iron content as determined by INAA.

| Sample ID | Fe | Sc | Ti | V | Cr | Mn | Co | Sb | Ni | Zn | Al | As | La | Ce | Nd | Sm | Eu |
|---|---|---|---|---|---|---|---|---|---|---|---|---|---|---|---|---|---|
| BKK-075 | 13936 | 0.18 | 0 | 0 | 3.6 | 10727.6 | 3.4 | 0.2 | 9.2 | 14.8 | 0 | 4.6 | 1.12 | 2.64 | 0 | 0.26 | 0.07 |
| TSO-014 | 7071 | 1.13 | 0 | 9 | 16.5 | 12.5 | 0.4 | 0.2 | 0 | 4.5 | 22480 | 1.7 | 13.78 | 27.71 | 9.89 | 1.39 | 0.17 |
| TSO-015 | 17011 | 3.11 | 2052 | 31.2 | 31.2 | 27.7 | 2 | 0.9 | 0 | 8 | 64177 | 4.5 | 26.04 | 54.56 | 20.61 | 3.49 | 0.55 |
| TSO-031 | 75816 | 4.63 | 7090 | 93.4 | 95.5 | 102.5 | 7.8 | 3.1 | 0 | 18.7 | 238414 | 22.6 | 61.9 | 127.2 | 53.31 | 8.61 | 1.36 |
| TSO-011 | 149703 | 12.58 | 21738 | 81.5 | 272.7 | 518.6 | 33.4 | 17.2 | 0 | 59.4 | 27650 | 13.2 | 54.82 | 121.45 | 44.13 | 7.87 | 1.22 |
| TSO-006 | 201870 | 12.24 | 13573 | 375.6 | 57.3 | 467 | 29 | 4.1 | 0 | 23.5 | 35220 | 0 | 33.93 | 71.15 | 19.15 | 3.16 | 0.64 |
| TSO-007 | 70348 | 29.88 | 17744 | 168.2 | 152.8 | 88.7 | 5.9 | 16.6 | 0 | 0 | 109734 | 5.2 | 58.42 | 128.71 | 31.47 | 6.13 | 1.4 |
| TSO-146 | 162437 | 10.54 | 17652 | 41.1 | 163.6 | 1555.3 | 31.2 | 16.7 | 92.5 | 40.7 | 178342 | 53.6 | 64.78 | 128.42 | 61.22 | 13.62 | 2.43 |
| TSO-150 | 164830 | 12.92 | 19071 | 40.3 | 160.4 | 1740.4 | 30.1 | 19 | 79.2 | 43.4 | 164512 | 58.4 | 56.56 | 109.47 | 44.95 | 8.2 | 1.5 |
| TSO-151 | 141573 | 11.51 | 28269 | 26.8 | 130.1 | 2530.9 | 27.6 | 14.6 | 0 | 40.7 | 102942 | 40.7 | 39.8 | 76.05 | 24.14 | 4.77 | 0.85 |
| TSO-152 | 100267 | 18.73 | 18697 | 49.3 | 141.9 | 1547.4 | 22.7 | 14 | 0 | 44.8 | 178427 | 78.9 | 109.19 | 189.91 | 75.47 | 11.65 | 2.15 |

| Sample ID | Tb | Dy | Yb | Th | U | Lu | Ta | Zr | Hf | Ca | Sr | Ba | Na | K | Rb | Cs |
|---|---|---|---|---|---|---|---|---|---|---|---|---|---|---|---|---|
| BKK-075 | 0 | 0 | 0.07 | 0.13 | 0 | 0 | 0.04 | 0 | 0.04 | 0 | 68 | 0 | 150 | 0 | 4.8 | 0.1 |
| TSO-014 | 0.1 | 0.31 | 0.34 | 4.12 | 0.47 | 0.05 | 0.18 | 52 | 1.84 | 0 | 0 | 26 | 247 | 2215 | 11.4 | 0.2 |
| TSO-015 | 0.18 | 0.56 | 0.72 | 10.82 | 0.68 | 0.11 | 1.02 | 120 | 4.87 | 0 | 49 | 34 | 357 | 5235 | 22.6 | 0.4 |
| TSO-031 | 0.54 | 2.87 | 2.35 | 25.32 | 3.24 | 0.35 | 2.88 | 360 | 14.8 | 566 | 54 | 0 | 326 | 0 | 0 | 0 |
| TSO-011 | 0.71 | 4.35 | 2.14 | 13 | 11.88 | 0.44 | 4.28 | 270 | 9.74 | 335 | 0 | 115 | 828 | 10299 | 63 | 3.4 |
| TSO-006 | 0.52 | 2.14 | 0.95 | 11.33 | 1.69 | 0.15 | 1.27 | 153 | 5.15 | 0 | 0 | 108 | 481 | 6520 | 25.5 | 0.4 |
| TSO-007 | 1.1 | 7.45 | 4.94 | 39.11 | 6.32 | 0.73 | 4.49 | 374 | 16.9 | 0 | 0 | 673 | 1418 | 31307 | 121.3 | 2 |
| TSO-146 | 1.72 | 18.86 | 5.25 | 38.63 | 3.65 | 0.69 | 3.54 | 253 | 9.38 | 0 | 0 | 0 | 261 | 0 | 0 | 0 |
| TSO-150 | 1.17 | 7.67 | 4.49 | 19.15 | 3.84 | 0.61 | 5.02 | 271 | 10.1 | 0 | 0 | 0 | 273 | 0 | 0 | 0 |
| TSO-151 | 0.62 | 9.14 | 3.06 | 11.43 | 3.29 | 0.42 | 3.35 | 457 | 15.1 | 0 | 0 | 0 | 216 | 0 | 0 | 0 |
| TSO-152 | 1.61 | 16.85 | 7.08 | 33.38 | 2.61 | 0.89 | 3.77 | 462 | 19.9 | 0 | 0 | 0 | 239 | 0 | 0 | 0 |

*All values in parts-per-million

Table 27. Raw compositions for replicate samples excluded from analyses.

| Replicate Excluded | Sample Included | Fe | Sc | Ti | V | Cr | Mn | Co | Sb | Ni | Zn | Al | As | La | Ce | Nd | Sm | |
|---|---|---|---|---|---|---|---|---|---|---|---|---|---|---|---|---|---|---|
| DIK-067 | DIK-066 | 471677 | 20.64 | 4837 | 1111.7 | 280.0 | 213.7 | 4.4 | 30.9 | 65.9 | 236.1 | 27446 | 87.9 | 24.40 | 94.63 | 17.97 | 5.81 | |
| DIK-068 | DIK-066 | 443017 | 18.09 | 4333 | 968.4 | 255.0 | 177.8 | 4.0 | 29.8 | 119.3 | 106.7 | 33696 | 279.3 | 21.51 | 74.97 | 14.95 | 4.78 | |
| DIK-069 | DIK-066 | 400726 | 16.64 | 3809 | 887.7 | 234.0 | 168.8 | 4.0 | 27.7 | 0.0 | 32.2 | 41582 | 571.2 | 23.69 | 86.71 | 17.80 | 4.85 | |
| DIK-070 | DIK-066 | 539791 | 21.64 | 5415 | 1227.5 | 308.0 | 221.8 | 4.7 | 35.2 | 0.0 | 47.0 | 29668 | 156.2 | 27.14 | 102.99 | 16.28 | 5.99 | |
| SEB-034 | SEB-033 | 422223 | 3.02 | 1408 | 484.4 | 122.0 | 26.8 | 0.7 | 1.4 | 0.0 | 0.0 | 17376 | 0.0 | 2.87 | 4.07 | 0 | 0.57 | |
| SEB-057 | SEB-056 | 545354 | 5.65 | 4439 | 984.8 | 1037.8 | 50.4 | 2.1 | 3.8 | 0.0 | 70.0 | 7206 | 0.0 | 3.59 | 5.52 | 0 | 1.30 | |
| SEB-058 | SEB-056 | 551358 | 5.84 | 4947 | 1018.4 | 1062.4 | 51.8 | 2.1 | 3.8 | 0.0 | 71.1 | 7488 | 0.0 | 3.73 | 8.26 | 0 | 1.47 | |
| TSO-005 | TSO-022 | 626277 | 11.51 | 33072 | 1145.9 | 29.1 | 1442.6 | 83.8 | 1.5 | 146.5 | 76.4 | 5238 | 0.0 | 0.73 | 0 | 0 | 0.23 | |
| Sample ID | Mine | Eu | Tb | Dy | Yb | Lu | Th | U | Ta | Zr | Hf | Ca | Sr | Ba | Na | K | Rb | Cs |
| DIK-067 | DIK | 1.43 | 0.94 | 7.23 | 5.91 | 0.94 | 22.34 | 14.83 | 5.13 | 1175 | 49.33 | 783 | 0 | 71 | 481 | 3931 | 0.0 | 0.0 |
| DIK-068 | DIK | 1.13 | 0.54 | 5.48 | 4.84 | 0.86 | 16.39 | 12.04 | 3.30 | 1110 | 44.58 | 0 | 0 | 87 | 425 | 6909 | 23.6 | 0.0 |
| DIK-069 | DIK | 1.18 | 0.80 | 5.36 | 4.19 | 0.55 | 14.96 | 11.09 | 2.33 | 758 | 33.16 | 311 | 0 | 134 | 382 | 8200 | 29.5 | 0.4 |
| DIK-070 | DIK | 1.43 | 0.67 | 7.30 | 5.43 | 0.84 | 18.24 | 14.79 | 2.84 | 1143 | 49.18 | 0 | 0 | 0 | 264 | 2091 | 27.1 | 0.0 |
| SEB-034 | SEB | 0.10 | 0 | 0.28 | 0.42 | 0.06 | 4.20 | 1.28 | 0.33 | 197 | 7.35 | 356 | 0 | 0 | 304 | 4288 | 131.7 | 0.6 |
| SEB-057 | SEB | 0.26 | 0 | 1.36 | 1.60 | 0.36 | 10.23 | 3.58 | 0.81 | 694 | 34.32 | 0 | 0 | 35 | 171 | 2922 | 79.3 | 0.7 |
| SEB-058 | SEB | 0.25 | 0.22 | 1.32 | 2.51 | 0.52 | 11.59 | 5.32 | 1.01 | 848 | 39.72 | 0 | 0 | 24 | 154 | 2547 | 93.4 | 0.6 |
| TSO-005 | MH | 0.07 | 0 | 0 | 0 | 0 | 0.60 | 0 | 0 | 0 | 0.38 | 0 | 0 | 0 | 173 | 0 | 0.0 | 0.0 |

*All values in parts-per-million (ppm).

Table 28. Raw composition for geologic samples used in analyses as determined by INAA.

| Sample ID | Mine | Fe | Sc | Ti | V | Cr | Mn | Co | Sb | Ni | Zn | Al | As | La | Ce | Nd | Sm | Eu |
|---|---|---|---|---|---|---|---|---|---|---|---|---|---|---|---|---|---|---|
| BKK-074 | BKK | 628399 | 0.37 | 0 | 34.0 | 5.0 | 263.9 | 13.0 | 1.4 | 0.0 | 0.0 | 2702 | 3.4 | 0.51 | 1.91 | 0 | 0.12 | 0 |
| BKK-076 | BKK | 558954 | 0.56 | 0 | 34.3 | 6.0 | 538.4 | 1.4 | 0.8 | 0.0 | 148.4 | 2146 | 8.7 | 0.45 | 0.52 | 0 | 0.05 | 0 |
| BKK-077 | BKK | 545281 | 0.79 | 0 | 41.4 | 11.0 | 1808.2 | 10.6 | 1.2 | 0.0 | 24.6 | 0 | 8.0 | 0.79 | 0 | 0 | 0.13 | 0.05 |
| BKK-078 | BKK | 588588 | 0.85 | 0 | 38.8 | 7.7 | 1409.1 | 19.9 | 1.0 | 0.0 | 12.4 | 0 | 8.6 | 0.93 | 1.80 | 0 | 0.16 | 0 |
| BKK-079 | BKK | 658711 | 0.58 | 0 | 11.1 | 5.0 | 81.4 | 0.8 | 4.6 | 0.0 | 0.0 | 2033 | 6.7 | 0.53 | 0 | 0 | 0.17 | 0.05 |
| BKK-080 | BKK | 624799 | 0.51 | 0 | 10.2 | 5.2 | 90.7 | 0.7 | 4.1 | 0.0 | 0.0 | 2724 | 6.8 | 0.70 | 0 | 0 | 0.19 | 0.05 |
| BKK-081 | BKK | 672350 | 0.60 | 0 | 8.7 | 5.1 | 66.1 | 0.8 | 4.7 | 0.0 | 0.0 | 2639 | 9.5 | 0.48 | 1.24 | 0 | 0.18 | 0.09 |
| BKK-082 | BKK | 646603 | 0.54 | 0 | 7.3 | 4.4 | 71.1 | 1.5 | 4.4 | 0.0 | 0.0 | 2938 | 8.2 | 0.57 | 1.17 | 0 | 0.15 | 0 |
| BKK-083 | BKK | 539884 | 0.57 | 0 | 0.0 | 7.4 | 2450.8 | 2.6 | 2.1 | 0.0 | 0.0 | 1669 | 5.8 | 0.66 | 2.11 | 0 | 0.09 | 0.04 |
| BKK-084 | BKK | 679681 | 0.67 | 0 | 4.6 | 4.3 | 28.1 | 0.2 | 1.9 | 0.0 | 0.0 | 2878 | 0.0 | 0.25 | 0 | 0 | 0.06 | 0 |
| BKK-085 | BKK | 670551 | 0.70 | 0 | 2.6 | 5.6 | 25.9 | 0.2 | 2.0 | 0.0 | 0.0 | 2898 | 2.5 | 0.19 | 0 | 0 | 0.04 | 0 |
| BKK-086 | BKK | 518596 | 0.23 | 92 | 25.9 | 4.7 | 79.0 | 0.3 | 1.1 | 0.0 | 0.0 | 3268 | 0.0 | 0.21 | 0 | 0 | 0.05 | 0 |
| BKK-087 | BKK | 465627 | 0.51 | 0 | 0.0 | 1.6 | 120.7 | 0.3 | 1.2 | 0.0 | 0.0 | 1969 | 0.0 | 1.07 | 0 | 0 | 0.32 | 0.08 |
| BKK-088 | BKK | 654104 | 0.24 | 0 | 7.0 | 5.4 | 37.0 | 0.4 | 2.7 | 0.0 | 0.0 | 1623 | 7.6 | 0.46 | 0 | 0 | 0.07 | 0 |
| BKK-089 | BKK | 678138 | 0.86 | 0 | 0.0 | 5.3 | 67.6 | 0.0 | 3.2 | 0.0 | 0.0 | 2376 | 3.3 | 0.23 | 0 | 0 | 0.05 | 0 |
| BKK-090 | BKK | 632766 | 0.42 | 0 | 9.2 | 5.5 | 77.9 | 0.5 | 2.7 | 0.0 | 0.0 | 3107 | 5.5 | 0.46 | 0 | 0 | 0.09 | 0.02 |
| BKK-091 | BKK | 514348 | 0.68 | 0 | 5.5 | 10.7 | 394.8 | 1.1 | 1.3 | 0.0 | 0.0 | 14566 | 0.0 | 2.16 | 1.94 | 0 | 0.31 | 0.12 |
| BKK-092 | BKK | 563755 | 0.83 | 0 | 0.0 | 5.2 | 2907.7 | 1.5 | 2.6 | 0.0 | 0.0 | 3823 | 13.1 | 1.94 | 3.55 | 0 | 0.44 | 0.08 |
| BKK-093 | BKK | 627459 | 0.47 | 0 | 5.8 | 3.7 | 295.2 | 0.9 | 3.5 | 0.0 | 0.0 | 2791 | 11.1 | 1.60 | 1.38 | 0 | 0.38 | 0.10 |
| BKK-094 | BKK | 465772 | 0.63 | 0 | 5.2 | 6.5 | 187.9 | 0.4 | 1.6 | 0.0 | 0.0 | 7284 | 2.7 | 2.22 | 0.70 | 0 | 0.54 | 0.14 |
| BKK-095 | BKK | 587615 | 0.56 | 0 | 10.0 | 6.7 | 31.6 | 0.2 | 1.5 | 0.0 | 0.0 | 19801 | 0.0 | 0.31 | 0 | 0 | 0.06 | 0 |
| BKK-096 | BKK | 498983 | 0.32 | 0 | 26.4 | 3.9 | 225.4 | 0.7 | 1.5 | 0.0 | 0.0 | 2116 | 3.2 | 1.00 | 0 | 0 | 0.24 | 0.10 |
| BKK-097 | BKK | 501738 | 0.29 | 0 | 21.0 | 3.1 | 156.9 | 0.5 | 1.0 | 0.0 | 0.0 | 2636 | 0.0 | 0.47 | 0 | 0 | 0.09 | 0.04 |
| BKK-098 | BKK | 503559 | 0.59 | 0 | 25.9 | 4.2 | 174.6 | 0.5 | 1.8 | 0.0 | 0.0 | 1623 | 3.5 | 2.03 | 1.64 | 0 | 0.86 | 0.26 |
| BKK-099 | BKK | 507539 | 0.33 | 0 | 25.2 | 4.4 | 257.2 | 0.8 | 1.5 | 0.0 | 0.0 | 2544 | 2.6 | 6.39 | 3.74 | 0 | 0.49 | 0.13 |
| BKK-100 | BKK | 514776 | 0.53 | 0 | 20.6 | 4.3 | 768.5 | 1.6 | 1.5 | 0.0 | 0.0 | 1677 | 4.5 | 3.34 | 4.02 | 0 | 0.41 | 0.11 |

*All values in parts-per-million (ppm)

Table 28 continued

| Sample ID | Mine | Tb | Dy | Yb | Lu | Th | U | Ta | Zr | Hf | Ca | Sr | Ba | Na | K | Rb | Cs |
|---|---|---|---|---|---|---|---|---|---|---|---|---|---|---|---|---|---|
| BKK-074 | BKK | 0 | 0 | 0 | 0 | 0 | 0 | 5.34 | 0 | 0 | 0 | 0 | 0 | 208 | 0 | 0.0 | 0.0 |
| BKK-076 | BKK | 0 | 0 | 0 | 0 | 0 | 0 | 0.48 | 0 | 0 | 459 | 0 | 0 | 222 | 0 | 0.0 | 0.0 |
| BKK-077 | BKK | 0 | 0 | 0 | 0 | 0.43 | 0 | 0.41 | 0 | 0 | 1684 | 0 | 179 | 327 | 0 | 0.0 | 0.0 |
| BKK-078 | BKK | 0 | 0 | 0 | 0 | 0.40 | 0 | 0.16 | 0 | 0 | 2376 | 0 | 109 | 288 | 0 | 0.0 | 0.0 |
| BKK-079 | BKK | 0 | 0 | 0 | 0 | 0.27 | 0 | 0 | 0 | 0 | 0 | 0 | 33 | 238 | 830 | 0.0 | 0.0 |
| BKK-080 | BKK | 0 | 0 | 0 | 0 | 0.21 | 0 | 0 | 0 | 0 | 0 | 0 | 0 | 265 | 0 | 0.0 | 0.0 |
| BKK-081 | BKK | 0.20 | 0 | 0 | 0 | 0.33 | 0 | 0.08 | 0 | 0 | 0 | 0 | 28 | 297 | 0 | 24.7 | 0.0 |
| BKK-082 | BKK | 0 | 0 | 0 | 0 | 0.19 | 0 | 0 | 0 | 0 | 0 | 0 | 0 | 350 | 0 | 0.0 | 0.0 |
| BKK-083 | BKK | 0 | 0 | 0 | 0 | 0.14 | 0 | 0 | 0 | 0 | 37495 | 0 | 138 | 205 | 0 | 0.0 | 0.0 |
| BKK-084 | BKK | 0 | 0 | 0 | 0 | 0.21 | 0 | 0 | 0 | 0 | 0 | 0 | 0 | 151 | 0 | 0.0 | 0.0 |
| BKK-085 | BKK | 0 | 0 | 0 | 0 | 0 | 0 | 0 | 0 | 0 | 0 | 0 | 0 | 183 | 0 | 0.0 | 0.0 |
| BKK-086 | BKK | 0 | 0 | 0 | 0 | 0.08 | 0 | 0 | 0 | 0 | 50766 | 0 | 35 | 123 | 0 | 0.0 | 0.0 |
| BKK-087 | BKK | 0 | 0 | 0 | 0.04 | 0 | 0 | 0 | 0 | 0 | 101721 | 0 | 0 | 147 | 0 | 0.0 | 0.0 |
| BKK-088 | BKK | 0 | 0 | 0 | 0 | 0 | 1.04 | 0 | 0 | 0 | 0 | 0 | 0 | 177 | 0 | 0.0 | 0.0 |
| BKK-089 | BKK | 0 | 0 | 0 | 0 | 0 | 0 | 0 | 0 | 0 | 0 | 0 | 0 | 184 | 0 | 0.0 | 0.0 |
| BKK-090 | BKK | 0 | 0 | 0 | 0 | 0.26 | 0 | 0 | 0 | 0 | 6132 | 0 | 0 | 185 | 0 | 0.0 | 0.0 |
| BKK-091 | BKK | 0 | 0.14 | 0 | 0 | 0.49 | 0 | 0 | 0 | 0.71 | 32695 | 0 | 0 | 1057 | 0 | 0.0 | 0.0 |
| BKK-092 | BKK | 0 | 0 | 0 | 0.07 | 0.39 | 0 | 0 | 0 | 0.38 | 31869 | 0 | 0 | 156 | 0 | 0.0 | 0.0 |
| BKK-093 | BKK | 0 | 0.21 | 0 | 0.04 | 0 | 0 | 0 | 0 | 0 | 30316 | 0 | 55 | 178 | 0 | 0.0 | 0.0 |
| BKK-094 | BKK | 0 | 0.51 | 0 | 0 | 0.19 | 0 | 0 | 0 | 0 | 98426 | 0 | 0 | 187 | 0 | 0.0 | 0.0 |
| BKK-095 | BKK | 0 | 0 | 0 | 0 | 0.12 | 0 | 0 | 0 | 0.12 | 0 | 0 | 0 | 170 | 0 | 0.0 | 0.0 |
| BKK-096 | BKK | 0 | 0.17 | 0 | 0 | 0.44 | 0 | 0 | 0 | 0 | 100338 | 0 | 0 | 227 | 0 | 0.0 | 0.0 |
| BKK-097 | BKK | 0 | 0.13 | 0 | 0 | 0.29 | 0 | 0 | 0 | 0 | 89075 | 0 | 0 | 158 | 0 | 0.0 | 0.0 |
| BKK-098 | BKK | 0 | 0.42 | 0 | 0 | 0.35 | 0 | 0 | 0 | 0 | 94747 | 0 | 0 | 178 | 0 | 0.0 | 0.0 |
| BKK-099 | BKK | 0 | 0 | 0 | 0 | 0.35 | 0 | 0 | 0 | 0 | 94040 | 0 | 0 | 163 | 0 | 0.0 | 0.0 |
| BKK-100 | BKK | 0 | 0 | 0 | 0 | 0.50 | 0 | 0 | 0 | 0.51 | 80488 | 0 | 0 | 210 | 0 | 0.0 | 0.0 |

Table 28 continued

| Sample ID | Mine | Fe | Sc | Ti | V | Cr | Mn | Co | Sb | Ni | Zn | Al | As | La | Ce | Nd | Sm | Eu |
|---|---|---|---|---|---|---|---|---|---|---|---|---|---|---|---|---|---|---|
| DIK-059 | DIK | 480870 | 23.21 | 11622 | 1036.7 | 435.0 | 180.3 | 3.4 | 11.5 | 76.7 | 114.7 | 32738 | 0.0 | 17.07 | 47.96 | 9.31 | 6.44 | 1.70 |
| DIK-060 | DIK | 504170 | 15.12 | 3065 | 1091.4 | 195.3 | 118.2 | 1.8 | 12.3 | 0.0 | 65.1 | 41307 | 7.7 | 68.95 | 131.90 | 42.14 | 7.12 | 1.57 |
| DIK-061 | DIK | 359160 | 11.05 | 3828 | 809.4 | 266.3 | 129.0 | 2.1 | 10.5 | 0.0 | 50.5 | 76021 | 0.0 | 22.81 | 53.65 | 18.30 | 5.84 | 1.32 |
| DIK-062 | DIK | 392145 | 15.49 | 4285 | 827.6 | 248.1 | 147.5 | 2.9 | 15.1 | 161.6 | 71.6 | 85741 | 0.0 | 762.30 | 1282.06 | 514.43 | 63.21 | 13.76 |
| DIK-063 | DIK | 450938 | 21.30 | 3314 | 1046.7 | 252.4 | 205.3 | 5.7 | 15.1 | 91.0 | 83.0 | 64007 | 0.0 | 698.02 | 1655.94 | 427.29 | 56.57 | 13.79 |
| DIK-064 | DIK | 465508 | 37.44 | 5373 | 1217.9 | 263.8 | 328.5 | 5.5 | 32.1 | 0.0 | 0.0 | 48235 | 0.0 | 114.25 | 6079.35 | 51.73 | 15.46 | 3.49 |
| DIK-065 | DIK | 382762 | 27.94 | 4925 | 978.9 | 262.1 | 243.0 | 4.7 | 26.7 | 0.0 | 62.2 | 47573 | 6.4 | 206.27 | 3814.48 | 115.63 | 23.67 | 5.80 |
| DIK-066 | DIK | 529025 | 24.96 | 5227 | 1009.2 | 321.3 | 202.5 | 106.5 | 30.8 | 0.0 | 176.5 | 14396 | 112.4 | 31.48 | 121.28 | 19.39 | 7.61 | 2.10 |
| DIK-071 | DIK | 569009 | 35.25 | 4168 | 1355.9 | 340.7 | 275.9 | 5.5 | 102.3 | 0.0 | 0.0 | 14910 | 0.0 | 216.26 | 2427.06 | 129.67 | 27.82 | 6.05 |
| DIK-072 | DIK | 543620 | 32.12 | 4304 | 1337.4 | 418.1 | 323.5 | 15.1 | 101.0 | 99.9 | 0.0 | 15581 | 0.0 | 221.12 | 797.30 | 150.08 | 26.65 | 6.05 |
| DIK-073 | DIK | 495998 | 34.33 | 6084 | 1177.6 | 611.7 | 268.8 | 632.6 | 30.9 | 0.0 | 0.0 | 20817 | 0.0 | 431.45 | 4614.01 | 216.75 | 68.49 | 18.73 |
| MAT-101 | MAT | 547346 | 0.35 | 0 | 30.5 | 6.7 | 276.9 | 0.8 | 2.2 | 0.0 | 0.0 | 2411 | 0.0 | 2.54 | 3.46 | 0 | 0.40 | 0.34 |
| MAT-102 | MAT | 504765 | 0.36 | 0 | 21.1 | 7.2 | 315.1 | 2.0 | 2.2 | 0.0 | 0.0 | 1613 | 0.0 | 2.49 | 3.14 | 0 | 0.45 | 0.29 |
| MAT-103 | MAT | 425465 | 0.25 | 0 | 12.6 | 4.3 | 207.2 | 119.5 | 2.7 | 0.0 | 18.7 | 1715 | 0.0 | 0.82 | 0 | 0 | 0.18 | 0.17 |
| MAT-104 | MAT | 501802 | 0.22 | 0 | 82.0 | 5.6 | 584.6 | 2.9 | 1.7 | 0.0 | 9.3 | 0 | 1.6 | 1.28 | 0 | 0 | 0.22 | 0.18 |
| MAT-105 | MAT | 437060 | 1.08 | 0 | 37.2 | 88.1 | 496.4 | 8.5 | 1.7 | 0.0 | 48.6 | 2201 | 39.8 | 5.39 | 4.92 | 0 | 0.60 | 0.29 |
| MAT-106 | MAT | 392109 | 0.47 | 0 | 9.8 | 40.4 | 128.5 | 2.2 | 2.3 | 0.0 | 11.5 | 1485 | 17.9 | 2.75 | 3.28 | 0 | 0.28 | 0.16 |
| MAT-107 | MAT | 475227 | 0.31 | 0 | 128.3 | 9.8 | 378.6 | 1.9 | 10.1 | 0.0 | 7.0 | 0 | 3.6 | 2.16 | 2.80 | 0 | 0.30 | 0.25 |
| MAT-108 | MAT | 571883 | 0.23 | 0 | 66.8 | 24.0 | 672.8 | 3.9 | 2.1 | 0.0 | 0.0 | 0 | 0.0 | 1.66 | 2.47 | 0 | 0.23 | 0.22 |
| MAT-109 | MAT | 441013 | 0.89 | 0 | 700.9 | 6.6 | 337.1 | 3.9 | 9.7 | 0.0 | 0.0 | 3031 | 6.7 | 5.55 | 6.36 | 6.46 | 1.07 | 0.68 |
| MAT-110 | MAT | 401441 | 0.91 | 0 | 391.3 | 7.6 | 484.1 | 2.1 | 6.6 | 0.0 | 10.9 | 5451 | 4.5 | 5.05 | 7.25 | 4.40 | 0.75 | 0.48 |
| MAT-111 | MAT | 481619 | 0.35 | 0 | 238.4 | 5.1 | 702.9 | 4.6 | 2.7 | 0.0 | 0.0 | 0 | 0.0 | 4.25 | 4.78 | 0 | 0.64 | 0.41 |
| MAT-112 | MAT | 477353 | 0.63 | 0 | 603.0 | 13.2 | 262.5 | 2.0 | 5.3 | 0.0 | 0.0 | 5704 | 3.4 | 2.02 | 3.23 | 0 | 0.44 | 0.24 |
| MAT-113 | MAT | 596610 | 0.25 | 0 | 72.8 | 6.9 | 650.0 | 3.3 | 1.5 | 0.0 | 0.0 | 0 | 0.0 | 1.49 | 2.32 | 0 | 0.24 | 0.21 |
| MAT-114 | MAT | 571361 | 0.62 | 0 | 0.0 | 5.0 | 1513.5 | 1.6 | 21.7 | 0.0 | 0.0 | 0 | 7.4 | 7.23 | 8.61 | 5.96 | 1.05 | 0.68 |
| MAT-115 | MAT | 510227 | 0.52 | 0 | 0.0 | 4.1 | 1756.9 | 1.5 | 14.2 | 0.0 | 0.0 | 1469 | 4.5 | 2.67 | 3.53 | 0 | 0.56 | 0.44 |
| MAT-116 | MAT | 460537 | 1.50 | 140 | 14.6 | 14.6 | 482.0 | 1.7 | 30.1 | 0.0 | 0.0 | 2094 | 11.3 | 7.91 | 7.79 | 3.41 | 0.95 | 0.40 |
| MAT-117 | MAT | 522642 | 0.98 | 314 | 0.0 | 5.5 | 1903.2 | 1.6 | 24.5 | 0.0 | 0.0 | 0 | 10.1 | 1.26 | 0 | 0 | 0.34 | 0.28 |
| MAT-118 | MAT | 372810 | 5.22 | 3942 | 283.0 | 18618.9 | 644.6 | 29.4 | 13.2 | 216.9 | 55.7 | 31097 | 38.4 | 10.78 | 17.64 | 8.36 | 4.13 | 2.18 |
| MAT-119 | MAT | 437988 | 3.53 | 1438 | 386.9 | 31955.5 | 642.3 | 22.9 | 44.1 | 219.9 | 33.9 | 20179 | 40.6 | 6.42 | 9.97 | 11.74 | 2.80 | 1.23 |
| MAT-120 | MAT | 282819 | 3.29 | 843 | 186.1 | 2235.8 | 256.3 | 4.1 | 15.5 | 129.8 | 29.0 | 16993 | 10.2 | 38.50 | 73.79 | 22.72 | 4.35 | 1.51 |
| MAT-121 | MAT | 408322 | 2.46 | 0 | 208.9 | 1491.0 | 497.1 | 4.4 | 15.6 | 0.0 | 16.3 | 11233 | 13.1 | 57.58 | 95.68 | 38.07 | 6.95 | 2.03 |

Table 28 continued

| Sample ID | Mine | Tb | Dy | Yb | Lu | Th | U | Ta | Zr | Hf | Ca | Sr | Ba | Na | K | Rb | Cs |
|---|---|---|---|---|---|---|---|---|---|---|---|---|---|---|---|---|---|
| DIK-059 | DIK | 1.61 | 11.95 | 11.16 | 1.69 | 30.91 | 26.62 | 1.63 | 2860 | 110.92 | 0 | 0 | 0 | 500 | 618 | 0.0 | 0.2 |
| DIK-060 | DIK | 0.49 | 3.16 | 1.82 | 0.21 | 12.74 | 5.38 | 0.57 | 328 | 14.72 | 0 | 0 | 0 | 291 | 1004 | 0.0 | 0.0 |
| DIK-061 | DIK | 0.94 | 5.26 | 4.50 | 0.70 | 17.02 | 17.71 | 0.54 | 1547 | 61.45 | 0 | 0 | 71 | 465 | 0 | 0.0 | 0.0 |
| DIK-062 | DIK | 3.04 | 11.73 | 4.41 | 0.51 | 48.46 | 15.94 | 0.91 | 1071 | 33.97 | 0 | 0 | 31 | 477 | 2028 | 0.0 | 0.0 |
| DIK-063 | DIK | 4.57 | 17.00 | 4.90 | 0.40 | 34.89 | 9.29 | 0.44 | 734 | 21.55 | 0 | 0 | 98 | 705 | 826 | 0.0 | 0.0 |
| DIK-064 | DIK | 1.32 | 8.37 | 6.98 | 1.09 | 27.72 | 10.92 | 0.89 | 1395 | 59.21 | 0 | 0 | 111 | 334 | 0 | 0.0 | 0.0 |
| DIK-065 | DIK | 2.16 | 10.46 | 5.70 | 0.88 | 28.70 | 11.61 | 1.34 | 1303 | 50.75 | 0 | 0 | 121 | 443 | 2891 | 24.3 | 0.0 |
| DIK-066 | DIK | 1.16 | 7.91 | 8.16 | 0.99 | 62.76 | 37.65 | 42.08 | 1473 | 62.14 | 795 | 0 | 112 | 478 | 3445 | 0.0 | 0.0 |
| DIK-071 | DIK | 1.74 | 8.99 | 4.46 | 0.65 | 27.64 | 11.65 | 1.43 | 415 | 21.58 | 0 | 0 | 23 | 284 | 1269 | 36.5 | 0.2 |
| DIK-072 | DIK | 2.10 | 9.34 | 5.51 | 0.88 | 27.60 | 15.56 | 5.42 | 1079 | 43.98 | 0 | 0 | 0 | 273 | 0 | 0.0 | 0.0 |
| DIK-073 | DIK | 5.14 | 21.91 | 11.57 | 1.36 | 84.07 | 22.46 | 9.77 | 2344 | 78.99 | 0 | 0 | 77 | 309 | 0 | 0.0 | 0.0 |
| MAT-101 | MAT | 0 | 0.52 | 0.37 | 0.05 | 0 | 0 | 1.54 | 0 | 0 | 0 | 0 | 0 | 292 | 0 | 0.0 | 0.0 |
| MAT-102 | MAT | 0.20 | 0.52 | 0.33 | 0.07 | 0 | 0 | 0 | 0 | 0 | 0 | 0 | 0 | 137 | 0 | 0.0 | 0.0 |
| MAT-103 | MAT | 0 | 0.40 | 0.40 | 0 | 0 | 0 | 0 | 0 | 0 | 662 | 0 | 0 | 203 | 0 | 0.0 | 0.0 |
| MAT-104 | MAT | 0 | 0.20 | 0.38 | 0.04 | 0 | 0 | 0 | 0 | 0 | 0 | 0 | 0 | 190 | 0 | 0.0 | 0.0 |
| MAT-105 | MAT | 0.34 | 0.98 | 0.77 | 0.10 | 0.91 | 0 | 0 | 0 | 0.14 | 0 | 0 | 0 | 405 | 0 | 0.0 | 0.0 |
| MAT-106 | MAT | 0 | 0.25 | 0.34 | 0.06 | 0 | 0 | 0 | 0 | 0 | 0 | 0 | 0 | 311 | 0 | 0.0 | 0.0 |
| MAT-107 | MAT | 0 | 0.42 | 0.38 | 0.06 | 0 | 0 | 0 | 0 | 0 | 0 | 0 | 0 | 148 | 0 | 0.0 | 0.0 |
| MAT-108 | MAT | 0 | 0.26 | 0.30 | 0.04 | 0 | 0 | 0 | 0 | 0 | 0 | 0 | 0 | 199 | 0 | 10.4 | 0.0 |
| MAT-109 | MAT | 0.30 | 0.77 | 0.82 | 0.13 | 0 | 1.31 | 0 | 0 | 0 | 0 | 0 | 177 | 199 | 0 | 0.0 | 0.0 |
| MAT-110 | MAT | 0 | 0.59 | 0.81 | 0.13 | 0.24 | 0 | 0 | 0 | 0 | 0 | 0 | 0 | 314 | 0 | 0.0 | 0.0 |
| MAT-111 | MAT | 0 | 1.49 | 0.76 | 0.13 | 0 | 0 | 0 | 0 | 0 | 0 | 0 | 0 | 231 | 0 | 0.0 | 0.0 |
| MAT-112 | MAT | 0 | 0.50 | 0.38 | 0.05 | 0 | 0 | 0 | 0 | 0 | 0 | 0 | 0 | 180 | 0 | 0.0 | 0.0 |
| MAT-113 | MAT | 0 | 0.26 | 0.46 | 0.05 | 0.11 | 0 | 0 | 0 | 0 | 0 | 0 | 0 | 155 | 0 | 0.0 | 0.0 |
| MAT-114 | MAT | 0 | 0.92 | 0.99 | 0.16 | 0 | 0 | 0 | 0 | 0 | 0 | 0 | 0 | 149 | 0 | 0.0 | 0.0 |
| MAT-115 | MAT | 0 | 0.86 | 1.21 | 0.23 | 0 | 0 | 0 | 0 | 0 | 0 | 0 | 0 | 118 | 0 | 0.0 | 0.0 |
| MAT-116 | MAT | 0 | 0.42 | 0.48 | 0.07 | 0.30 | 0 | 0 | 0 | 0 | 0 | 0 | 20 | 158 | 0 | 0.0 | 0.0 |
| MAT-117 | MAT | 0 | 0 | 0.87 | 0.13 | 0 | 0 | 0.34 | 0 | 0 | 0 | 0 | 0 | 128 | 0 | 0.0 | 0.0 |
| MAT-118 | MAT | 1.35 | 10.83 | 6.18 | 0.81 | 2.23 | 5.53 | 0 | 0 | 2.10 | 1042 | 0 | 225 | 2248 | 4258 | 19.0 | 0.0 |
| MAT-119 | MAT | 0.56 | 2.18 | 1.56 | 0.18 | 0.55 | 4.89 | 0 | 0 | 0 | 627 | 0 | 47 | 1685 | 761 | 0.0 | 0.0 |
| MAT-120 | MAT | 0.51 | 2.57 | 1.12 | 0 | 1.65 | 3.15 | 0.34 | 31 | 0.85 | 417 | 143 | 0 | 2012 | 0 | 0.0 | 0.0 |
| MAT-121 | MAT | 0.74 | 3.14 | 0.90 | 0.12 | 1.66 | 1.03 | 0.13 | 0 | 0.27 | 1801 | 166 | 193 | 534 | 0 | 0.0 | 0.0 |

Table 28 continued

| Sample ID | Mine | Fe | Sc | Ti | V | Cr | Mn | Co | Sb | Ni | Zn | Al | As | La | Ce | Nd | Sm | Eu |
|---|---|---|---|---|---|---|---|---|---|---|---|---|---|---|---|---|---|---|
| SEB-033 | SEB | 472002 | 2.90 | 1296 | 521.7 | 107.6 | 27.3 | 0.6 | 1.5 | 0.0 | 0.0 | 10974 | 0.0 | 2.36 | 3.97 | 0 | 0.54 | 0.06 |
| SEB-035 | SEB | 519507 | 2.44 | 2017 | 353.4 | 252.4 | 42.4 | 1.2 | 4.4 | 0.0 | 0.0 | 12586 | 2.1 | 3.65 | 6.03 | 0 | 0.89 | 0.13 |
| SEB-036 | SEB | 520279 | 2.63 | 1615 | 125.2 | 165.5 | 24.6 | 0.6 | 0.9 | 0.0 | 0.0 | 19082 | 2.4 | 7.78 | 16.20 | 5.12 | 1.19 | 0.23 |
| SEB-037 | SEB | 506981 | 2.91 | 2154 | 124.9 | 218.5 | 31.0 | 1.0 | 1.1 | 0.0 | 0.0 | 29040 | 0.0 | 10.65 | 21.37 | 5.03 | 1.64 | 0.32 |
| SEB-038 | SEB | 607889 | 3.19 | 3005 | 664.3 | 212.1 | 44.5 | 0.9 | 2.8 | 0.0 | 0.0 | 4495 | 3.2 | 2.68 | 4.53 | 0 | 0.61 | 0.11 |
| SEB-039 | SEB | 525077 | 3.05 | 5774 | 563.8 | 750.6 | 55.3 | 2.4 | 7.6 | 0.0 | 0.0 | 5729 | 3.1 | 4.04 | 7.94 | 0 | 1.45 | 0.22 |
| SEB-040 | SEB | 620645 | 4.38 | 5311 | 572.8 | 1399.2 | 57.0 | 2.5 | 3.0 | 0.0 | 51.1 | 11105 | 0.0 | 6.60 | 15.22 | 0 | 1.62 | 0.34 |
| SEB-041 | SEB | 634535 | 4.83 | 7496 | 651.5 | 2124.4 | 69.4 | 4.0 | 4.2 | 0.0 | 75.8 | 9798 | 0.0 | 7.23 | 18.05 | 0 | 2.14 | 0.43 |
| SEB-042 | SEB | 526704 | 7.90 | 17837 | 890.7 | 3182.1 | 164.3 | 11.4 | 5.9 | 0.0 | 89.2 | 16414 | 3.3 | 14.74 | 40.87 | 10.08 | 5.15 | 0.94 |
| SEB-043 | SEB | 571693 | 4.45 | 7319 | 736.2 | 842.9 | 51.6 | 1.8 | 3.6 | 0.0 | 26.6 | 7046 | 0.0 | 5.05 | 11.07 | 0 | 1.39 | 0.24 |
| SEB-044 | SEB | 459044 | 6.94 | 42924 | 1138.6 | 1525.3 | 159.7 | 12.6 | 72.7 | 0.0 | 0.0 | 11206 | 12.8 | 20.22 | 51.02 | 10.67 | 5.83 | 0.97 |
| SEB-045 | SEB | 458501 | 8.17 | 30494 | 957.7 | 1529.3 | 150.5 | 11.5 | 64.9 | 0.0 | 0.0 | 10122 | 9.2 | 24.40 | 55.11 | 14.14 | 7.19 | 1.19 |
| SEB-046 | SEB | 453499 | 13.29 | 38922 | 1268.1 | 9820.2 | 557.0 | 22.2 | 17.9 | 0.0 | 959.9 | 13205 | 4.1 | 13.41 | 27.94 | 0 | 7.17 | 1.28 |
| SEB-047 | SEB | 488817 | 15.65 | 45812 | 1325.1 | 8012.4 | 466.3 | 21.3 | 20.8 | 0.0 | 643.1 | 11447 | 8.6 | 15.36 | 54.18 | 0 | 8.37 | 1.52 |
| SEB-048 | SEB | 458089 | 16.75 | 62564 | 1283.6 | 5717.2 | 220.4 | 16.0 | 39.3 | 0.0 | 230.5 | 18991 | 10.7 | 14.94 | 43.72 | 0 | 7.22 | 1.53 |
| SEB-049 | SEB | 640948 | 3.33 | 0 | 447.5 | 23.7 | 40.7 | 0.6 | 2.8 | 0.0 | 0.0 | 3676 | 0.0 | 2.26 | 5.87 | 0 | 0.29 | 0.05 |
| SEB-050 | SEB | 646910 | 3.31 | 0 | 422.3 | 24.4 | 41.2 | 0.6 | 2.8 | 0.0 | 0.0 | 4470 | 5.4 | 2.10 | 5.09 | 0 | 0.41 | 0 |
| SEB-051 | SEB | 573207 | 2.39 | 1468 | 346.3 | 19.1 | 30.7 | 0.6 | 1.5 | 0.0 | 0.0 | 7402 | 0.0 | 3.12 | 5.87 | 0 | 0.61 | 0.08 |
| SEB-052 | SEB | 681000 | 3.35 | 487 | 372.9 | 17.7 | 41.4 | 0.6 | 2.5 | 0.0 | 0.0 | 2659 | 0.0 | 2.03 | 3.81 | 0 | 0.22 | 0.02 |
| SEB-053 | SEB | 538922 | 2.88 | 102 | 369.0 | 56.8 | 39.0 | 0.6 | 2.7 | 0.0 | 0.0 | 6154 | 3.0 | 4.43 | 5.92 | 5.75 | 0.72 | 0.12 |
| SEB-054 | SEB | 348825 | 2.80 | 674 | 340.8 | 52.3 | 26.9 | 1.3 | 1.6 | 0.0 | 0.0 | 22327 | 0.0 | 3.81 | 7.17 | 0 | 0.67 | 0.11 |
| SEB-055 | SEB | 590432 | 4.75 | 4127 | 969.4 | 683.9 | 45.5 | 1.4 | 3.4 | 0.0 | 43.2 | 7053 | 0.0 | 3.25 | 4.81 | 0 | 0.91 | 0.14 |
| SEB-056 | SEB | 543535 | 5.57 | 4464 | 989.6 | 1101.5 | 52.0 | 2.2 | 3.8 | 0.0 | 75.0 | 7040 | 0.0 | 3.92 | 5.27 | 0 | 1.34 | 0.22 |
| TSO-131 | AC | 300787 | 5.98 | 29192 | 367.4 | 302.0 | 399.6 | 21.9 | 5.0 | 0.0 | 18.3 | 86143 | 10.2 | 95.61 | 182.53 | 65.78 | 11.75 | 1.84 |
| TSO-132 | AC | 461841 | 13.51 | 38479 | 470.6 | 427.5 | 593.0 | 31.6 | 8.4 | 0.0 | 32.2 | 28592 | 6.9 | 52.19 | 106.47 | 32.31 | 7.14 | 1.26 |
| TSO-133 | AC | 492063 | 11.63 | 37284 | 416.6 | 453.5 | 520.6 | 33.8 | 6.8 | 0.0 | 29.4 | 51131 | 7.3 | 47.59 | 98.20 | 30.12 | 6.64 | 1.28 |
| TSO-030 | BM | 384445 | 6.64 | 19882 | 295.5 | 448.2 | 472.8 | 24.8 | 4.7 | 0.0 | 20.8 | 52938 | 5.2 | 42.40 | 81.46 | 21.91 | 4.85 | 0.71 |
| TSO-161 | BM | 605537 | 3.64 | 2354 | 1476.6 | 123.6 | 110.6 | 8.9 | 0.2 | 0.0 | 0.0 | 21239 | 3.0 | 18.91 | 38.10 | 11.81 | 5.42 | 1.31 |
| TSO-162 | BM | 460464 | 5.74 | 24501 | 357.5 | 526.9 | 585.9 | 29.4 | 5.6 | 0.0 | 10.7 | 49422 | 4.8 | 33.96 | 65.79 | 28.70 | 4.37 | 0.63 |
| TSO-163 | BM | 490365 | 5.18 | 23705 | 351.5 | 553.0 | 620.6 | 30.9 | 6.5 | 0.0 | 12.2 | 38084 | 3.1 | 28.71 | 56.03 | 20.85 | 3.34 | 0.45 |
| TSO-164 | BM | 337987 | 6.16 | 52054 | 332.4 | 374.7 | 446.3 | 23.4 | 11.4 | 0.0 | 0.0 | 9513 | 6.6 | 67.10 | 107.79 | 35.31 | 6.45 | 1.17 |
| TSO-165 | BM | 412560 | 8.14 | 50387 | 313.5 | 458.6 | 451.2 | 28.5 | 10.6 | 0.0 | 0.0 | 9716 | 4.0 | 39.73 | 70.81 | 19.80 | 5.09 | 1.06 |
| TSO-166 | BM | 504469 | 5.90 | 21809 | 341.2 | 472.0 | 502.2 | 30.9 | 4.7 | 0.0 | 0.0 | 8433 | 4.4 | 59.73 | 99.86 | 26.44 | 6.48 | 1.33 |

Table 28 continued

| Sample ID | Mine | Tb | Dy | Yb | Lu | Th | U | Ta | Zr | Hf | Ca | Sr | Ba | Na | K | Rb | Cs |
|---|---|---|---|---|---|---|---|---|---|---|---|---|---|---|---|---|---|
| SEB-033 | SEB | 0 | 0.27 | 0.44 | 0.07 | 3.68 | 0.92 | 0.28 | 117 | 6.64 | 0 | 0 | 13 | 184 | 3256 | 95.8 | 0.5 |
| SEB-035 | SEB | 0 | 0.71 | 1.01 | 0.15 | 4.32 | 3.26 | 0.45 | 466 | 22.58 | 0 | 0 | 33 | 192 | 2265 | 88.2 | 0.6 |
| SEB-036 | SEB | 0 | 0.77 | 0.33 | 0.05 | 4.24 | 0.89 | 0.28 | 99 | 3.75 | 305 | 0 | 45 | 261 | 7066 | 164.6 | 1.1 |
| SEB-037 | SEB | 0 | 0.91 | 0.47 | 0.07 | 5.96 | 1.05 | 0.47 | 132 | 5.63 | 299 | 0 | 96 | 269 | 7546 | 215.8 | 1.1 |
| SEB-038 | SEB | 0 | 0.42 | 0.40 | 0.08 | 3.03 | 1.44 | 0.24 | 165 | 8.23 | 0 | 0 | 0 | 152 | 1396 | 51.9 | 0.0 |
| SEB-039 | SEB | 0 | 1.52 | 2.78 | 0.45 | 8.77 | 4.95 | 0.83 | 878 | 36.14 | 0 | 0 | 0 | 185 | 1677 | 58.4 | 0.5 |
| SEB-040 | SEB | 0 | 1.64 | 1.33 | 0.24 | 10.94 | 3.05 | 0.88 | 681 | 30.48 | 0 | 0 | 54 | 219 | 5704 | 133.7 | 0.6 |
| SEB-041 | SEB | 0.14 | 2.16 | 2.46 | 0.44 | 11.70 | 4.44 | 1.03 | 1344 | 57.69 | 0 | 0 | 48 | 210 | 4376 | 134.3 | 0.5 |
| SEB-042 | SEB | 0.32 | 4.06 | 6.54 | 1.29 | 32.64 | 13.73 | 3.57 | 3539 | 155.01 | 0 | 0 | 28 | 244 | 8178 | 212.0 | 1.3 |
| SEB-043 | SEB | 0 | 1.48 | 2.36 | 0.37 | 14.57 | 5.42 | 0.91 | 1081 | 48.63 | 0 | 0 | 8 | 175 | 2186 | 81.7 | 0.0 |
| SEB-044 | SEB | 0.65 | 6.18 | 9.36 | 1.70 | 35.13 | 27.43 | 5.98 | 5191 | 209.46 | 0 | 0 | 58 | 275 | 5583 | 82.7 | 0.6 |
| SEB-045 | SEB | 0.61 | 6.54 | 10.74 | 2.11 | 43.16 | 35.80 | 7.46 | 6701 | 269.81 | 0 | 0 | 56 | 239 | 3919 | 100.0 | 0.6 |
| SEB-046 | SEB | 0.80 | 8.66 | 14.61 | 2.55 | 60.99 | 33.35 | 6.43 | 7079 | 298.13 | 0 | 0 | 57 | 233 | 8469 | 142.4 | 0.7 |
| SEB-047 | SEB | 1.07 | 9.70 | 19.06 | 3.40 | 70.54 | 38.64 | 6.65 | 9530 | 396.97 | 0 | 0 | 0 | 251 | 6397 | 129.2 | 1.0 |
| SEB-048 | SEB | 0.93 | 10.10 | 14.00 | 2.51 | 54.91 | 34.92 | 7.76 | 8839 | 361.74 | 0 | 0 | 79 | 279 | 8908 | 201.4 | 1.1 |
| SEB-049 | SEB | 0 | 0 | 0 | 0 | 0.91 | 1.70 | 0 | 0 | 0.72 | 0 | 0 | 0 | 475 | 0 | 27.7 | 0.7 |
| SEB-050 | SEB | 0 | 0 | 0 | 0 | 1.03 | 2.49 | 0 | 0 | 2.52 | 0 | 0 | 0 | 278 | 0 | 23.1 | 0.8 |
| SEB-051 | SEB | 0 | 0.21 | 0 | 0 | 1.37 | 1.55 | 0.22 | 0 | 1.07 | 0 | 0 | 5 | 207 | 961 | 28.5 | 0.6 |
| SEB-052 | SEB | 0 | 0 | 0 | 0 | 0.89 | 1.76 | 0 | 0 | 0 | 0 | 0 | 0 | 155 | 0 | 0.0 | 0.5 |
| SEB-053 | SEB | 0 | 0.24 | 0 | 0.04 | 3.05 | 1.43 | 0 | 0 | 0.77 | 0 | 0 | 23 | 161 | 1545 | 40.6 | 0.5 |
| SEB-054 | SEB | 0 | 0.38 | 0.26 | 0.04 | 3.54 | 1.15 | 0.14 | 172 | 5.60 | 0 | 0 | 0 | 237 | 11346 | 327.8 | 2.2 |
| SEB-055 | SEB | 0.13 | 0.98 | 1.15 | 0.21 | 7.59 | 4.02 | 0.67 | 530 | 23.65 | 0 | 0 | 0 | 145 | 1089 | 60.9 | 0.6 |
| SEB-056 | SEB | 0 | 1.42 | 1.68 | 0.29 | 10.65 | 4.09 | 0.93 | 601 | 29.99 | 0 | 0 | 0 | 193 | 2715 | 108.7 | 0.5 |
| TSO-131 | AC | 0.88 | 5.69 | 2.45 | 0.51 | 50.32 | 11.50 | 12.44 | 631 | 22.48 | 0 | 139 | 0 | 162 | 0 | 0.0 | 0.0 |
| TSO-132 | AC | 1.07 | 11.32 | 4.54 | 1.02 | 49.67 | 16.70 | 15.14 | 1139 | 53.64 | 0 | 0 | 10 | 201 | 0 | 12.6 | 0.0 |
| TSO-133 | AC | 2.21 | 6.91 | 9.98 | 1.52 | 43.93 | 15.38 | 15.24 | 1253 | 50.33 | 0 | 0 | 0 | 197 | 2966 | 0.0 | 0.0 |
| TSO-030 | BM | 0.63 | 3.18 | 2.88 | 0.53 | 27.86 | 8.82 | 8.31 | 836 | 32.11 | 413 | 0 | 48 | 467 | 6849 | 48.3 | 0.5 |
| TSO-161 | BM | 0.56 | 3.46 | 2.06 | 0.25 | 43.57 | 1.43 | 0.84 | 296 | 11.90 | 0 | 0 | 0 | 297 | 2109 | 0.0 | 0.0 |
| TSO-162 | BM | 0.36 | 4.14 | 2.12 | 0.50 | 20.10 | 10.71 | 11.74 | 738 | 27.73 | 0 | 0 | 0 | 226 | 2371 | 0.0 | 0.0 |
| TSO-163 | BM | 0.39 | 2.51 | 0.63 | 0.36 | 20.16 | 8.56 | 11.70 | 463 | 18.61 | 0 | 0 | 0 | 258 | 3160 | 0.0 | 0.0 |
| TSO-164 | BM | 0.73 | 6.13 | 4.08 | 0.83 | 50.62 | 15.73 | 15.72 | 1246 | 45.65 | 0 | 92 | 0 | 260 | 3479 | 18.9 | 0.0 |
| TSO-165 | BM | 0.93 | 7.83 | 5.14 | 1.03 | 42.19 | 15.75 | 15.35 | 1463 | 56.91 | 0 | 0 | 99 | 243 | 2629 | 24.4 | 0.0 |
| TSO-166 | BM | 2.75 | 7.74 | 11.55 | 1.56 | 33.09 | 10.54 | 15.78 | 1039 | 39.97 | 0 | 0 | 0 | 255 | 2897 | 22.0 | 0.0 |

Table 28 continued

| Sample ID | Mine | Fe | Sc | Ti | V | Cr | Mn | Co | Sb | Ni | Zn | Al | As | La | Ce | Nd | Sm | Eu |
|---|---|---|---|---|---|---|---|---|---|---|---|---|---|---|---|---|---|---|
| TSO-167 | BM | 571856 | 9.58 | 37572 | 295.7 | 561.9 | 503.0 | 36.8 | 9.7 | 0.0 | 0.0 | 9687 | 2.1 | 50.58 | 77.65 | 26.01 | 5.02 | 1.05 |
| TSO-168 | BM | 543363 | 8.06 | 33993 | 306.3 | 538.4 | 490.7 | 34.7 | 8.0 | 0.0 | 0.0 | 6538 | 5.1 | 60.74 | 91.63 | 26.57 | 5.73 | 1.11 |
| TSO-008 | BS | 388037 | 6.67 | 17344 | 207.0 | 354.0 | 296.7 | 23.9 | 6.2 | 0.0 | 0.0 | 15016 | 3.7 | 55.61 | 142.80 | 33.94 | 8.56 | 1.45 |
| TSO-009 | BS | 398649 | 6.30 | 18390 | 217.3 | 358.4 | 307.9 | 24.6 | 6.5 | 0.0 | 0.0 | 10265 | 0.0 | 41.69 | 106.14 | 30.69 | 6.36 | 1.05 |
| TSO-010 | BS | 518539 | 8.33 | 24111 | 303.6 | 457.9 | 414.3 | 32.0 | 8.2 | 0.0 | 0.0 | 12074 | 4.5 | 64.59 | 159.71 | 51.49 | 9.18 | 1.58 |
| TSO-023 | BS | 582752 | 8.76 | 25304 | 313.8 | 525.5 | 455.5 | 36.1 | 8.1 | 0.0 | 12.5 | 7654 | 0.0 | 34.78 | 87.30 | 27.34 | 6.14 | 1.15 |
| TSO-024 | BS | 587780 | 8.87 | 26512 | 314.7 | 530.1 | 470.1 | 36.9 | 8.2 | 0.0 | 0.0 | 9702 | 0.0 | 43.37 | 103.36 | 30.25 | 6.99 | 1.20 |
| TSO-025 | BS | 536097 | 8.59 | 26200 | 295.5 | 497.4 | 422.1 | 32.7 | 8.8 | 0.0 | 0.0 | 12600 | 0.0 | 60.62 | 140.43 | 43.42 | 9.20 | 1.70 |
| TSO-026 | BS | 372062 | 6.05 | 24719 | 262.3 | 411.7 | 289.9 | 24.8 | 12.8 | 0.0 | 20.1 | 48308 | 6.9 | 54.69 | 115.05 | 30.21 | 6.52 | 1.18 |
| TSO-027 | BS | 463287 | 6.85 | 24533 | 349.2 | 482.0 | 371.4 | 26.9 | 8.5 | 0.0 | 0.0 | 55870 | 0.0 | 45.47 | 86.82 | 24.60 | 5.18 | 0.85 |
| TSO-134 | BS | 601971 | 3.01 | 1423 | 1204.5 | 20.2 | 47.8 | 4.6 | 0.0 | 0.0 | 0.0 | 5325 | 0.0 | 0.45 | 0 | 0 | 0.16 | 0.12 |
| TSO-135 | BS | 670488 | 2.75 | 1189 | 1314.2 | 12.2 | 41.6 | 3.7 | 0.0 | 0.0 | 0.0 | 3798 | 0.0 | 0.38 | 0 | 0 | 0.09 | 0 |
| TSO-136 | BS | 642648 | 3.25 | 1749 | 1214.2 | 24.6 | 52.0 | 5.1 | 0.0 | 0.0 | 0.0 | 6657 | 0.0 | 0.34 | 0 | 0 | 0.06 | 0 |
| TSO-137 | BS | 629895 | 2.40 | 1070 | 1181.6 | 11.1 | 40.6 | 3.2 | 0.2 | 0.0 | 0.0 | 6532 | 0.0 | 0.63 | 0 | 0 | 0.12 | 0 |
| TSO-138 | BS | 553521 | 5.18 | 8952 | 1162.3 | 121.2 | 102.0 | 12.5 | 3.9 | 120.3 | 0.0 | 8157 | 0.7 | 3.34 | 4.64 | 0 | 1.48 | 0.74 |
| TSO-012 | LM | 225002 | 11.64 | 29063 | 92.7 | 395.7 | 818.9 | 51.1 | 23.0 | 63.9 | 77.6 | 31639 | 12.3 | 41.23 | 90.34 | 40.32 | 6.50 | 1.01 |
| TSO-013 | LM | 405648 | 28.94 | 43029 | 119.1 | 758.1 | 1483.9 | 82.9 | 27.2 | 0.0 | 143.8 | 19326 | 16.3 | 53.45 | 113.35 | 29.05 | 7.51 | 1.11 |
| TSO-020 | LM | 381625 | 14.10 | 50670 | 118.8 | 648.5 | 1358.9 | 81.2 | 40.4 | 0.0 | 123.3 | 33385 | 25.8 | 122.59 | 268.13 | 92.75 | 16.86 | 2.50 |
| TSO-021 | LM | 331678 | 12.05 | 37119 | 123.4 | 553.8 | 1357.8 | 74.1 | 34.1 | 104.3 | 115.6 | 78360 | 32.4 | 115.78 | 243.59 | 80.23 | 15.79 | 2.67 |
| TSO-142 | LM | 462381 | 14.82 | 53322 | 145.2 | 765.1 | 1688.9 | 89.9 | 49.1 | 0.0 | 121.0 | 13670 | 28.0 | 118.95 | 241.40 | 78.21 | 13.60 | 1.79 |
| TSO-143 | LM | 489493 | 22.74 | 39966 | 98.0 | 913.1 | 1736.7 | 100.1 | 28.2 | 98.7 | 47.9 | 12358 | 17.2 | 43.94 | 94.76 | 26.05 | 7.29 | 1.16 |
| TSO-144 | LM | 246458 | 9.63 | 43504 | 136.0 | 424.2 | 1418.6 | 53.8 | 27.6 | 0.0 | 81.7 | 39893 | 43.0 | 60.96 | 126.94 | 49.60 | 9.06 | 1.34 |
| TSO-001 | MH | 229288 | 6.62 | 7916 | 362.3 | 45.3 | 542.8 | 30.1 | 0.9 | 0.0 | 26.7 | 26602 | 2.1 | 32.58 | 78.39 | 28.10 | 5.69 | 1.13 |
| TSO-002 | MH | 619028 | 11.08 | 32323 | 1275.6 | 53.5 | 1452.9 | 86.8 | 1.0 | 0.0 | 70.6 | 9209 | 0.0 | 1.00 | 0 | 0 | 0.16 | 0.05 |
| TSO-003 | MH | 422094 | 7.17 | 20712 | 220.9 | 392.7 | 313.5 | 25.9 | 7.4 | 0.0 | 37.0 | 18554 | 2.8 | 57.26 | 147.27 | 37.57 | 8.14 | 1.32 |
| TSO-004 | MH | 568112 | 8.94 | 22799 | 310.7 | 514.1 | 442.7 | 35.3 | 7.6 | 0.0 | 13.5 | 11443 | 0.0 | 42.39 | 112.49 | 28.57 | 7.56 | 1.37 |
| TSO-016 | MH | 591650 | 8.26 | 22267 | 292.0 | 530.8 | 452.6 | 36.5 | 6.8 | 0.0 | 13.7 | 15521 | 5.2 | 29.83 | 73.23 | 21.30 | 4.91 | 0.90 |
| TSO-017 | MH | 583941 | 8.89 | 24164 | 864.5 | 44.1 | 1312.6 | 72.0 | 1.3 | 0.0 | 67.1 | 5427 | 0.0 | 0.78 | 0 | 0 | 0.16 | 0 |
| TSO-018 | MH | 579679 | 10.39 | 31272 | 1161.0 | 39.3 | 1491.9 | 85.7 | 1.2 | 130.9 | 84.0 | 10943 | 0.0 | 3.37 | 2.89 | 8.18 | 0.74 | 0.12 |
| TSO-019 | MH | 521745 | 13.01 | 31391 | 925.0 | 227.4 | 939.3 | 82.6 | 9.6 | 117.6 | 62.3 | 28488 | 0.0 | 1.38 | 0 | 0 | 0.55 | 0.09 |
| TSO-022 | MH | 619950 | 11.23 | 34530 | 1176.2 | 29.0 | 1470.4 | 83.1 | 1.5 | 0.0 | 90.8 | 4591 | 0.0 | 0.66 | 0 | 0 | 0.18 | 0 |

Table 28 continued

| Sample ID | Mine | Tb | Dy | Yb | Lu | Th | U | Ta | Zr | Hf | Ca | Sr | Ba | Na | K | Rb | Cs |
|---|---|---|---|---|---|---|---|---|---|---|---|---|---|---|---|---|---|
| TSO-167 | BM | 1.21 | 4.28 | 7.37 | 1.31 | 34.54 | 13.82 | 12.61 | 1564 | 62.54 | 0 | 0 | 9 | 256 | 4511 | 17.4 | 0.0 |
| TSO-168 | BM | 0.57 | 4.78 | 3.28 | 0.72 | 39.21 | 13.95 | 13.69 | 1157 | 49.58 | 0 | 0 | 0 | 222 | 2658 | 0.0 | 0.0 |
| TSO-008 | BS | 0.83 | 5.14 | 3.57 | 0.58 | 34.69 | 12.16 | 9.75 | 867 | 33.20 | 0 | 0 | 52 | 333 | 3773 | 0.0 | 0.0 |
| TSO-009 | BS | 0.74 | 4.87 | 3.36 | 0.51 | 26.64 | 9.61 | 8.97 | 733 | 33.43 | 285 | 0 | 0 | 184 | 2021 | 0.0 | 0.0 |
| TSO-010 | BS | 1.09 | 6.79 | 4.25 | 0.76 | 45.85 | 13.68 | 12.01 | 1025 | 42.74 | 451 | 0 | 57 | 229 | 4172 | 0.0 | 0.0 |
| TSO-023 | BS | 0.92 | 7.40 | 4.23 | 0.81 | 29.67 | 15.90 | 14.84 | 1025 | 44.95 | 0 | 0 | 67 | 225 | 1895 | 0.0 | 0.0 |
| TSO-024 | BS | 0.93 | 7.60 | 4.92 | 0.86 | 33.26 | 14.96 | 12.74 | 1188 | 49.20 | 0 | 0 | 0 | 260 | 892 | 0.0 | 0.0 |
| TSO-025 | BS | 1.73 | 11.25 | 6.23 | 0.97 | 39.53 | 15.11 | 12.33 | 1259 | 51.17 | 0 | 0 | 0 | 266 | 1986 | 0.0 | 0.0 |
| TSO-026 | BS | 1.91 | 13.04 | 9.21 | 1.12 | 35.72 | 19.10 | 20.22 | 1304 | 53.28 | 740 | 0 | 58 | 563 | 7678 | 37.1 | 0.4 |
| TSO-027 | BS | 1.34 | 8.76 | 5.87 | 1.04 | 23.37 | 17.17 | 15.02 | 1091 | 47.23 | 1491 | 0 | 0 | 354 | 2367 | 23.5 | 0.0 |
| TSO-134 | BS | 0.30 | 6.59 | 0.33 | 0 | 1.75 | 0 | 0.52 | 0 | 0.64 | 0 | 0 | 0 | 226 | 744 | 0.0 | 0.0 |
| TSO-135 | BS | 0 | 0.22 | 0 | 0 | 0.98 | 0 | 0.43 | 0 | 0 | 0 | 0 | 0 | 196 | 0 | 0.0 | 0.0 |
| TSO-136 | BS | 0 | 0.38 | 0 | 0 | 0.99 | 0 | 0.49 | 0 | 0.27 | 0 | 0 | 0 | 211 | 683 | 0.0 | 0.0 |
| TSO-137 | BS | 0 | 0.32 | 0 | 0 | 1.00 | 0 | 0.39 | 0 | 0.46 | 0 | 0 | 14 | 200 | 1635 | 0.0 | 0.0 |
| TSO-138 | BS | 2.09 | 53.48 | 3.75 | 0.56 | 9.59 | 2.80 | 3.11 | 652 | 25.51 | 0 | 0 | 0 | 239 | 2263 | 0.0 | 0.0 |
| TSO-012 | LM | 0.58 | 4.48 | 2.17 | 0.56 | 15.41 | 14.01 | 5.51 | 359 | 12.79 | 0 | 0 | 143 | 703 | 7619 | 57.8 | 2.7 |
| TSO-013 | LM | 0.80 | 4.36 | 2.07 | 0.66 | 26.46 | 16.90 | 7.23 | 554 | 21.59 | 519 | 0 | 126 | 441 | 4502 | 31.1 | 0.8 |
| TSO-020 | LM | 1.32 | 6.49 | 4.53 | 0.76 | 31.75 | 24.91 | 10.86 | 562 | 20.00 | 0 | 0 | 0 | 527 | 0 | 34.8 | 1.3 |
| TSO-021 | LM | 1.60 | 7.74 | 4.35 | 0.83 | 43.84 | 17.13 | 8.18 | 527 | 18.43 | 2000 | 0 | 0 | 606 | 0 | 25.5 | 0.9 |
| TSO-142 | LM | 0.83 | 5.56 | 3.37 | 0.97 | 33.66 | 20.65 | 11.05 | 943 | 35.26 | 0 | 0 | 0 | 430 | 4006 | 19.1 | 1.3 |
| TSO-143 | LM | 0.77 | 3.21 | 2.80 | 0.62 | 51.53 | 13.82 | 6.69 | 569 | 20.36 | 0 | 0 | 32 | 535 | 5256 | 32.8 | 1.0 |
| TSO-144 | LM | 0.84 | 7.73 | 3.62 | 0.80 | 16.94 | 14.53 | 7.60 | 876 | 31.21 | 0 | 0 | 69 | 371 | 4331 | 30.4 | 2.2 |
| TSO-001 | MH | 0.86 | 5.10 | 2.82 | 0.41 | 12.18 | 0 | 0.13 | 142 | 4.68 | 1061 | 0 | 65 | 340 | 1837 | 16.2 | 0.3 |
| TSO-002 | MH | 0 | 0 | 0 | 0 | 0.43 | 0 | 0 | 0 | 0 | 0 | 0 | 0 | 161 | 0 | 0.0 | 0.0 |
| TSO-003 | MH | 0.89 | 5.32 | 3.50 | 0.57 | 33.15 | 12.44 | 10.52 | 831 | 35.04 | 0 | 0 | 0 | 270 | 3815 | 14.6 | 0.0 |
| TSO-004 | MH | 1.01 | 7.03 | 4.75 | 0.71 | 36.40 | 10.06 | 11.15 | 1109 | 43.60 | 0 | 0 | 0 | 262 | 2692 | 0.0 | 0.0 |
| TSO-016 | MH | 0.77 | 4.98 | 3.25 | 0.55 | 23.65 | 10.27 | 10.76 | 1065 | 43.12 | 0 | 0 | 0 | 262 | 992 | 0.0 | 0.0 |
| TSO-017 | MH | 0 | 0 | 0 | 0 | 0.52 | 0 | 0.79 | 0 | 1.64 | 0 | 0 | 0 | 243 | 0 | 0.0 | 0.0 |
| TSO-018 | MH | 0 | 0 | 0 | 0 | 0.56 | 0 | 0 | 0 | 0.44 | 0 | 0 | 0 | 213 | 0 | 0.0 | 0.0 |
| TSO-019 | MH | 0.28 | 0.69 | 2.06 | 0.36 | 2.15 | 4.79 | 1.13 | 704 | 29.79 | 0 | 0 | 0 | 1080 | 0 | 16.1 | 0.0 |
| TSO-022 | MH | 0 | 0 | 0 | 0 | 0.27 | 0 | 0 | 0 | 0.27 | 0 | 0 | 0 | 155 | 0 | 0.0 | 0.0 |

Table 28 continued

| Sample ID | Mine | Fe | Sc | Ti | V | Cr | Mn | Co | Sb | Ni | Zn | Al | As | La | Ce | Nd | Sm | Eu |
|---|---|---|---|---|---|---|---|---|---|---|---|---|---|---|---|---|---|---|
| TSO-154 | MH | 446079 | 9.04 | 23018 | 927.5 | 13.4 | 1157.1 | 60.6 | 0.8 | 133.8 | 12.4 | 6367 | 3.7 | 322.85 | 505.45 | 247.31 | 50.99 | 10.18 |
| TSO-155 | MH | 457493 | 14.55 | 57939 | 640.6 | 773.1 | 861.2 | 51.7 | 61.7 | 0.0 | 19.4 | 35097 | 0.0 | 19.28 | 43.49 | 0 | 2.79 | 0.58 |
| TSO-156 | MH | 351482 | 12.60 | 33595 | 486.3 | 352.1 | 804.0 | 95.0 | 58.8 | 0.0 | 78.6 | 81768 | 3.3 | 58.55 | 149.44 | 48.10 | 9.42 | 2.04 |
| TSO-157 | MH | 428439 | 25.89 | 47742 | 690.9 | 125.7 | 658.3 | 18.6 | 9.3 | 0.0 | 0.0 | 16088 | 24.7 | 75.30 | 130.53 | 62.35 | 11.95 | 3.21 |
| TSO-158 | MH | 464500 | 21.67 | 46330 | 206.1 | 683.7 | 3073.0 | 97.1 | 38.6 | 0.0 | 44.0 | 34190 | 18.2 | 18.72 | 41.85 | 15.91 | 3.19 | 0.49 |
| TSO-159 | MH | 557844 | 10.56 | 43926 | 698.3 | 526.6 | 817.4 | 58.9 | 32.2 | 154.8 | 22.9 | 22964 | 0.0 | 79.60 | 100.38 | 32.95 | 6.22 | 1.33 |
| TSO-160 | MH | 641458 | 10.25 | 29197 | 1070.0 | 26.0 | 1362.0 | 74.6 | 0.7 | 179.6 | 50.5 | 5368 | 0.0 | 0.57 | 0 | 0 | 0.17 | 0 |
| TSO-122 | MM | 563850 | 11.58 | 30923 | 374.7 | 522.7 | 726.6 | 38.4 | 7.4 | 0.0 | 28.7 | 10947 | 6.3 | 50.00 | 93.81 | 29.74 | 6.93 | 1.06 |
| TSO-123 | MM | 570057 | 15.08 | 36617 | 411.1 | 543.1 | 777.4 | 38.8 | 13.4 | 0.0 | 27.9 | 5262 | 4.7 | 42.36 | 79.31 | 21.34 | 5.35 | 0.82 |
| TSO-124 | MM | 439049 | 15.45 | 38628 | 398.7 | 452.5 | 715.4 | 30.1 | 8.8 | 0.0 | 29.5 | 21792 | 9.0 | 66.94 | 129.32 | 38.15 | 8.55 | 1.30 |
| TSO-125 | MUR | 594239 | 9.88 | 28165 | 322.2 | 543.9 | 466.3 | 36.5 | 9.0 | 0.0 | 11.3 | 6664 | 4.2 | 50.57 | 118.20 | 36.64 | 7.16 | 1.41 |
| TSO-126 | MUR | 614664 | 7.22 | 25081 | 309.7 | 560.8 | 463.5 | 38.2 | 7.9 | 68.3 | 11.1 | 7233 | 3.9 | 33.98 | 80.52 | 23.18 | 5.06 | 0.93 |
| TSO-127 | MUR | 603278 | 7.60 | 24905 | 325.1 | 561.3 | 464.5 | 37.4 | 9.4 | 0.0 | 0.0 | 5656 | 5.0 | 53.29 | 122.71 | 36.78 | 6.41 | 1.01 |
| TSO-028 | NS | 491514 | 6.79 | 4555 | 319.1 | 73.9 | 645.1 | 31.4 | 0.1 | 99.0 | 20.1 | 47540 | 0.0 | 141.59 | 248.62 | 55.26 | 8.39 | 1.61 |
| TSO-032 | NS | 418127 | 8.34 | 4519 | 319.2 | 69.0 | 565.4 | 25.9 | 0.2 | 0.0 | 22.4 | 64056 | 0.0 | 181.99 | 334.76 | 73.48 | 12.35 | 3.07 |
| TSO-169 | NS | 547042 | 6.73 | 4426 | 296.0 | 45.9 | 696.9 | 30.1 | 0.0 | 87.6 | 9.5 | 24825 | 3.7 | 89.57 | 153.70 | 34.61 | 8.70 | 3.20 |
| TSO-170 | NS | 504927 | 7.99 | 4060 | 336.4 | 46.6 | 673.9 | 31.2 | 0.3 | 189.6 | 88.0 | 27633 | 14.2 | 72.03 | 139.91 | 13.75 | 23.49 | 18.39 |
| TSO-171 | NS | 230288 | 12.33 | 3567 | 319.0 | 90.7 | 454.7 | 16.3 | 0.4 | 273.1 | 28.7 | 88472 | 0.0 | 4450.66 | 5714.90 | 348.41 | 174.12 | 23.02 |
| TSO-172 | NS | 437599 | 8.17 | 4735 | 328.9 | 68.9 | 688.1 | 26.7 | 0.2 | 0.0 | 13.4 | 35865 | 4.3 | 140.46 | 228.24 | 45.42 | 8.39 | 1.90 |
| TSO-139 | RHI | 626937 | 4.68 | 1976 | 243.0 | 13.1 | 614.1 | 22.4 | 0.1 | 0.0 | 11.0 | 7512 | 0.0 | 2.23 | 0 | 0 | 0.22 | 0.05 |
| TSO-140 | RHI | 216553 | 8.61 | 24374 | 153.1 | 217.0 | 1381.6 | 23.0 | 23.7 | 0.0 | 27.9 | 99189 | 30.9 | 39.02 | 87.28 | 28.39 | 6.05 | 1.12 |
| TSO-141 | RHI | 324710 | 5.90 | 39577 | 339.5 | 261.0 | 1292.3 | 37.2 | 41.9 | 0.0 | 25.4 | 56745 | 23.5 | 40.10 | 87.13 | 32.68 | 5.98 | 0.99 |
| TSO-145 | UEM | 422435 | 25.88 | 29556 | 22.6 | 264.4 | 3293.2 | 67.3 | 32.8 | 0.0 | 48.2 | 36924 | 17.3 | 51.43 | 92.17 | 31.18 | 5.48 | 0.97 |
| TSO-147 | UEM | 442570 | 22.32 | 42679 | 102.8 | 280.2 | 3354.1 | 95.9 | 37.0 | 130.4 | 94.4 | 52993 | 19.9 | 20.59 | 38.66 | 18.29 | 4.14 | 1.04 |
| TSO-148 | UEM | 464752 | 19.80 | 43784 | 45.1 | 293.1 | 3274.3 | 84.8 | 29.3 | 0.0 | 49.4 | 24843 | 12.3 | 17.86 | 36.55 | 14.22 | 2.87 | 0.49 |
| TSO-149 | UEM | 282964 | 16.66 | 31965 | 32.1 | 200.2 | 2731.2 | 50.5 | 25.6 | 0.0 | 59.7 | 83367 | 32.8 | 36.77 | 85.60 | 24.68 | 5.21 | 0.98 |
| TSO-153 | UEM | 335672 | 20.61 | 33824 | 46.8 | 209.3 | 2762.4 | 48.6 | 28.7 | 0.0 | 43.1 | 16386 | 6.0 | 25.69 | 57.49 | 18.58 | 3.95 | 0.75 |
| TSO-128 | WH | 634160 | 6.16 | 3134 | 1023.0 | 158.1 | 153.0 | 6.2 | 0.7 | 0.0 | 5.5 | 14808 | 0.0 | 143.18 | 222.86 | 63.45 | 7.69 | 1.75 |
| TSO-129 | WH | 647113 | 6.05 | 4293 | 1226.3 | 349.1 | 180.5 | 6.0 | 0.5 | 90.5 | 100.4 | 6046 | 8.8 | 32.16 | 47.46 | 13.44 | 2.96 | 0.84 |
| TSO-130 | WH | 666053 | 6.14 | 9925 | 1793.3 | 71.9 | 517.1 | 25.5 | 0.3 | 0.0 | 11.3 | 8715 | 0.0 | 0.86 | 2.20 | 0 | 0.26 | 0.07 |

Table 28 continued

| Sample ID | Mine | Tb | Dy | Yb | Lu | Th | U | Ta | Zr | Hf | Ca | Sr | Ba | Na | K | Rb | Cs |
|---|---|---|---|---|---|---|---|---|---|---|---|---|---|---|---|---|---|
| TSO-154 | MH | 4.33 | 18.43 | 1.39 | 0.15 | 206.46 | 2.64 | 0 | 187 | 0.59 | 0 | 0 | 70 | 151 | 0 | 0.0 | 0.0 |
| TSO-155 | MH | 0.92 | 6.69 | 10.18 | 1.84 | 13.69 | 23.12 | 25.88 | 2099 | 77.90 | 524 | 181 | 397 | 875 | 17977 | 71.6 | 0.9 |
| TSO-156 | MH | 1.01 | 7.37 | 3.45 | 0.70 | 26.50 | 16.21 | 18.05 | 845 | 32.08 | 0 | 0 | 0 | 249 | 0 | 0.0 | 0.0 |
| TSO-157 | MH | 1.42 | 6.36 | 1.16 | 0.25 | 13.97 | 3.01 | 3.50 | 388 | 13.30 | 1120 | 793 | 451 | 471 | 0 | 0.0 | 0.0 |
| TSO-158 | MH | 0.40 | 5.97 | 2.10 | 0.59 | 6.54 | 17.57 | 8.48 | 336 | 11.03 | 0 | 0 | 0 | 141 | 0 | 0.0 | 0.0 |
| TSO-159 | MH | 1.19 | 7.88 | 6.15 | 0.99 | 22.72 | 9.22 | 7.27 | 829 | 30.83 | 0 | 0 | 0 | 208 | 0 | 0.0 | 0.0 |
| TSO-160 | MH | 0 | 0 | 0 | 0 | 0.12 | 0 | 0.54 | 0 | 0 | 0 | 0 | 44 | 189 | 0 | 0.0 | 0.0 |
| TSO-122 | MM | 0.81 | 6.85 | 3.91 | 0.59 | 59.77 | 11.22 | 16.15 | 818 | 38.69 | 0 | 0 | 0 | 211 | 0 | 0.0 | 0.0 |
| TSO-123 | MM | 1.35 | 3.25 | 6.47 | 1.11 | 39.59 | 13.91 | 16.96 | 1216 | 57.93 | 0 | 0 | 0 | 168 | 735 | 0.0 | 0.0 |
| TSO-124 | MM | 0.88 | 10.18 | 4.92 | 0.84 | 55.88 | 15.33 | 20.65 | 1305 | 60.82 | 0 | 0 | 0 | 203 | 0 | 0.0 | 0.0 |
| TSO-125 | MUR | 3.01 | 6.03 | 7.84 | 1.23 | 27.67 | 12.03 | 12.35 | 1049 | 49.49 | 0 | 0 | 0 | 178 | 1246 | 0.0 | 0.0 |
| TSO-126 | MUR | 1.10 | 3.15 | 3.10 | 0.61 | 24.50 | 11.66 | 12.63 | 539 | 24.34 | 0 | 0 | 0 | 205 | 1580 | 0.0 | 0.0 |
| TSO-127 | MUR | 0.54 | 2.91 | 1.40 | 0.30 | 26.77 | 14.19 | 12.52 | 790 | 34.71 | 0 | 0 | 0 | 181 | 1345 | 0.0 | 0.0 |
| TSO-028 | NS | 1.06 | 6.82 | 4.70 | 0.67 | 85.23 | 3.70 | 0.70 | 183 | 10.09 | 0 | 0 | 169 | 875 | 20830 | 102.6 | 1.5 |
| TSO-032 | NS | 4.30 | 28.71 | 14.17 | 1.94 | 122.01 | 7.00 | 0.76 | 308 | 10.99 | 0 | 0 | 253 | 1023 | 31848 | 122.2 | 2.4 |
| TSO-169 | NS | 3.92 | 25.81 | 7.76 | 0.93 | 52.22 | 4.63 | 0.26 | 150 | 2.34 | 0 | 0 | 138 | 386 | 10450 | 48.4 | 0.7 |
| TSO-170 | NS | 44.18 | 305.81 | 105.49 | 11.80 | 63.91 | 15.58 | 0.28 | 676 | 13.14 | 0 | 0 | 0 | 519 | 11993 | 82.8 | 1.1 |
| TSO-171 | NS | 8.37 | 55.19 | 0 | 0 | 1239.98 | 0 | 0.34 | 1133 | 20.34 | 805 | 392 | 309 | 1462 | 44892 | 206.3 | 4.3 |
| TSO-172 | NS | 0.86 | 3.84 | 1.20 | 0.12 | 54.53 | 3.93 | 0.49 | 162 | 7.09 | 0 | 0 | 96 | 580 | 17193 | 127.5 | 2.4 |
| TSO-139 | RHI | 0 | 0 | 0 | 0 | 0.38 | 0 | 0 | 0 | 0.12 | 0 | 0 | 0 | 143 | 0 | 0.0 | 0.0 |
| TSO-140 | RHI | 0.96 | 7.91 | 2.84 | 0.54 | 14.74 | 9.12 | 3.79 | 282 | 8.60 | 0 | 171 | 0 | 237 | 0 | 0.0 | 0.0 |
| TSO-141 | RHI | 0.36 | 3.89 | 1.44 | 0.40 | 15.51 | 11.84 | 7.40 | 271 | 10.62 | 0 | 0 | 0 | 289 | 1637 | 0.0 | 0.8 |
| TSO-145 | UEM | 0.87 | 7.46 | 3.41 | 0.80 | 17.09 | 11.86 | 17.04 | 685 | 27.64 | 0 | 0 | 0 | 189 | 0 | 5.2 | 0.0 |
| TSO-147 | UEM | 1.06 | 8.66 | 4.23 | 0.77 | 11.12 | 6.86 | 6.18 | 321 | 12.87 | 0 | 0 | 95 | 231 | 0 | 0.0 | 0.0 |
| TSO-148 | UEM | 0.52 | 5.20 | 2.39 | 0.45 | 12.15 | 7.31 | 6.85 | 467 | 17.52 | 0 | 0 | 0 | 278 | 0 | 0.0 | 0.0 |
| TSO-149 | UEM | 0.90 | 5.24 | 4.26 | 0.63 | 14.93 | 4.66 | 5.47 | 214 | 8.76 | 0 | 0 | 0 | 235 | 0 | 0.0 | 0.3 |
| TSO-153 | UEM | 0.60 | 4.25 | 3.11 | 0.73 | 27.93 | 12.22 | 16.33 | 746 | 30.53 | 0 | 0 | 0 | 219 | 0 | 0.0 | 0.5 |
| TSO-128 | WH | 1.07 | 4.38 | 2.77 | 0.38 | 20.51 | 2.59 | 2.48 | 280 | 12.67 | 0 | 0 | 0 | 269 | 1919 | 0.0 | 0.0 |
| TSO-129 | WH | 0.62 | 7.28 | 1.74 | 0.28 | 11.01 | 0 | 1.27 | 173 | 9.57 | 0 | 0 | 0 | 215 | 477 | 0.0 | 0.0 |
| TSO-130 | WH | 0 | 0 | 0 | 0 | 0.39 | 0 | 0 | 0 | 0 | 0 | 0 | 0 | 164 | 0 | 0.0 | 0.0 |

Table 29. Summary of sample descriptions done during preparation for INAA. Footnotes on page final page of table.

| Sample | Region | Mine | Rock Fabric | HMC (Yes/No) | Light Mineral Contribution | Hand Sample Mineralogy | | | |
|---|---|---|---|---|---|---|---|---|---|
| | | | | | | Hem | Qtz | Mica | Others |
| TSO-001 | Tsodilo | Upper Male | Schist/Vein Crystals | N | | +++ | +++ | + | |
| TSO-002 | Tsodilo | Upper Male | Vein Crystals | N | | +++++ | + | - | |
| TSO-003 | Tsodilo | Upper Male | Schist/Vein Crystals | N | | +++ | +++ | +++ | |
| TSO-004 | Tsodilo | Upper Male | Schist | N | | +++++ | + | + | |
| TSO-005 | Tsodilo | Upper Male | Vein Crystals | N | | +++++ | + | + | |
| TSO-006 | Tsodilo | Upper Male | Schist/Vein Crystals | N | | +++ | +++ | +++ | |
| TSO-007 | Tsodilo | Upper Male | Schist | N | | ++ | + | +++++ | |
| TSO-008 | Tsodilo | Below Sex | Schist/Vein Crystals | N | | +++ | +++ | + | |
| TSO-009 | Tsodilo | Below Sex | Schist/Vein Crystals | N | | +++ | +++ | + | |
| TSO-010 | Tsodilo | Below Sex | Schist | N | | +++++ | + | + | |
| TSO-011 | Tsodilo | Lower Male | Schist | N | | ++++ | +++ | ++ | |
| TSO-012 | Tsodilo | Lower Male | Schist | N | | ++++ | ++ | ++ | |
| TSO-013 | Tsodilo | Lower Male | Schist | N | | +++++ | - | ++ | |
| TSO-014 | Tsodilo | Big Mine | Schist | N | | +++ | +++ | +++ | |
| TSO-015 | Tsodilo | Big Mine | Schist | N | | ++ | ++++ | +++ | |
| TSO-016 | Tsodilo | Upper Male | Schist | Y | | +++++ | ++ | - | |
| TSO-017 | Tsodilo | Upper Male | Vein Crystals | Y | | ++ | ++++ | - | |
| TSO-018 | Tsodilo | Upper Male | Vein Crystals | Y | | ++++ | ++ | - | |
| TSO-019 | Tsodilo | Upper Male | Vein Crystals | Y | | +++++ | ++ | - | |
| TSO-020 | Tsodilo | Lower Male | Schist | Y | | +++ | +++ | +++ | |
| TSO-021 | Tsodilo | Lower Male | Vein Crystals | Y | | +++ | +++ | +++ | |
| TSO-022 | Tsodilo | Upper Male | Vein Crystals | Y | | +++++ | + | + | |
| TSO-023 | Tsodilo | Below Sex | Schist | Y | | +++++ | ++ | + | |
| TSO-024 | Tsodilo | Below Sex | Schist | Y | | +++++ | ++ | + | |

Table 29 continued

| Sample | Region | Mine | Rock Fabric | HMC (Yes/No) | Light Mineral Contribution | Hand Sample Mineralogy | | | |
|---|---|---|---|---|---|---|---|---|---|
| | | | | | | Hem | Qtz | Mica | Others |
| TSO-025 | Tsodilo | Below Sex | Schist | Y | | +++++ | ++ | + | |
| TSO-026 | Tsodilo | Below Sex | Schist | Y | | ++ | +++++ | + | |
| TSO-027 | Tsodilo | Below Sex | Schist | Y | | ++ | +++++ | + | |
| TSO-028 | Tsodilo | Near Sex | Schist | Y | | ++++ | ++ | +++ | |
| TSO-029 | Tsodilo | Big Mine | Schist | Y | | +++ | +++ | +++ | |
| TSO-030 | Tsodilo | Big Mine | Schist | Y | | ++ | ++++ | + | |
| TSO-031 | Tsodilo | Big Mine | Schist | Y | | ++ | ++++ | ++ | |
| TSO-032 | Tsodilo | Near Sex | Schist | Y | | +++ | + | +++ | |
| SEB-033 | Sebilong | | Equigranular | Y | | +++ | ++ | + | |
| SEB-034 | Sebilong | | Equigranular | Y | | +++ | ++ | + | |
| SEB-035 | Sebilong | | Equigranular | Y | | +++ | ++ | + | |
| SEB-036 | Sebilong | | Equigranular | Y | | ++++ | ++ | - | |
| SEB-037 | Sebilong | | Equigranular | Y | | ++++ | ++ | - | |
| SEB-038 | Sebilong | | Porphyritic | Y | | ++++ | ++ | - | |
| SEB-039 | Sebilong | | Porphyritic | Y | | +++ | +++ | - | |
| SEB-040 | Sebilong | | Equigranular | Y | | +++++ | + | - | |
| SEB-041 | Sebilong | | Equigranular | Y | | +++++ | + | - | |
| SEB-042 | Sebilong | | Equigranular | Y | | +++ | +++ | + | |
| SEB-043 | Sebilong | | Equigranular | Y | | ++++ | +++ | + | |
| SEB-044 | Sebilong | | Equigranular | Y | Much | ++ | ++++ | + | |
| SEB-045 | Sebilong | | Equigranular | Y | Much | ++ | ++++ | + | |
| SEB-046 | Sebilong | | Equigranular | Y | Much | +++ | ++++ | + | |
| SEB-047 | Sebilong | | Equigranular | Y | Much | +++ | ++++ | + | |
| SEB-048 | Sebilong | | Equigranular | Y | Much | +++ | ++++ | + | |

Table 29 continued

| Sample | Region | Mine | Rock Fabric | HMC (Yes/No) | Light Mineral Contribution | Hand Sample Mineralogy | | | |
|---|---|---|---|---|---|---|---|---|---|
| | | | | | | Hem | Qtz | Mica | Others |
| SEB-049 | Sebilong | | Vein Crystals | Y | Little | +++ | ++++ | - | |
| SEB-050 | Sebilong | | Vein Crystals | Y | Little | +++ | ++++ | - | |
| SEB-051 | Sebilong | | Vein Crystals | Y | Little | +++ | ++++ | - | |
| SEB-052 | Sebilong | | Breccia | Y | Very Little | +++ | ++++ | - | |
| SEB-053 | Sebilong | | Breccia | Y | Much | +++ | ++++ | - | |
| SEB-054 | Sebilong | | Breccia | Y | Little | ++ | +++++ | - | |
| SEB-055 | Sebilong | | Breccia | Y | Very Little | ++ | ++++ | - | |
| SEB-056 | Sebilong | | Breccia | Y | Little | +++ | ++++ | - | |
| SEB-057 | Sebilong | | Breccia | Y | Little | +++ | ++++ | - | |
| SEB-058 | Sebilong | | Breccia | Y | Little | +++ | ++++ | - | |
| DIK-059 | Dikgatlampi | | Porphyritic | Y | Much | ++ | ++++ | - | |
| DIK-060 | Dikgatlampi | | Porphyritic | Y | Very little | ++ | ++++ | - | |
| DIK-061 | Dikgatlampi | | Porphyritic/Vein Crystals | Y | Little | ++ | +++++ | - | |
| DIK-062 | Dikgatlampi | | Porphyritic/Vein Crystals | Y | Little | ++ | +++++ | - | |
| DIK-063 | Dikgatlampi | | Equigranular | Y | Little | ++ | +++++ | - | |
| DIK-064 | Dikgatlampi | | Equigranular | Y | Little | ++ | +++++ | - | |
| DIK-065 | Dikgatlampi | | Equigranular | Y | Very Little | ++ | +++++ | - | |
| DIK-066 | Dikgatlampi | | Vein Crystals | Y | Little | ++ | +++++ | - | |
| DIK-067 | Dikgatlampi | | Vein Crystals | Y | Much | ++ | +++++ | - | |
| DIK-068 | Dikgatlampi | | Vein Crystals | Y | Little | ++ | +++++ | - | |
| DIK-069 | Dikgatlampi | | Vein Crystals | Y | Very Little | ++ | +++++ | - | |
| DIK-070 | Dikgatlampi | | Vein Crystals | Y | Little | ++ | +++++ | - | |
| DIK-071 | Dikgatlampi | | Breccia | Y | Very Little | +++++ | + | - | |
| DIK-072 | Dikgatlampi | | Breccia | Y | Little | +++++ | + | - | |

Table 29 continued

| Sample | Region | Mine | Rock Fabric | HMC (Yes/No) | Light Mineral Contribution | Hand Sample Mineralogy | | | |
|---|---|---|---|---|---|---|---|---|---|
| | | | | | | Hem | Qtz | Mica | Others |
| DIK-073 | Dikgatlampi | | Vein Crystals | Y | Much | + | +++++ | - | Possible traces of magnetite |
| BKK-074 | Blinkklipkop | | Equigranular | Y | Little | +++ | +++ | - | |
| BKK-075 | Blinkklipkop | | Equigranular | Y | Much | +++ | +++ | - | Very weathered, no heavy minerals remained after HMC |
| BKK-076 | Blinkklipkop | | Equigranular | Y | Little | +++ | +++ | - | |
| BKK-077 | Blinkklipkop | | Equigranular | Y | Some | +++ | +++ | - | |
| BKK-078 | Blinkklipkop | | Equigranular | Y | Little | +++ | +++ | - | |
| BKK-079 | Blinkklipkop | | Equigranular | Y | Very Little | ++++ | +++ | - | |
| BKK-080 | Blinkklipkop | | Equigranular | Y | Very Little | ++++ | +++ | - | |
| BKK-081 | Blinkklipkop | | Equigranular | Y | Very Little | ++++ | +++ | - | |
| BKK-082 | Blinkklipkop | | Equigranular | Y | Very Little | ++++ | +++ | - | |
| BKK-083 | Blinkklipkop | | Equigranular | Y | Little | ++++ | +++ | - | |
| BKK-084 | Blinkklipkop | | Equigranular | Y | Very Little | +++++ | + | - | |
| BKK-085 | Blinkklipkop | | Equigranular | Y | Very Little | +++++ | + | - | |
| BKK-086 | Blinkklipkop | | Equigranular | Y | Little | +++++ | + | - | |
| BKK-087 | Blinkklipkop | | Equigranular | Y | Little | +++++ | + | - | |
| BKK-088 | Blinkklipkop | | Equigranular | Y | Very Little | +++++ | + | - | |
| BKK-089 | Blinkklipkop | | Equigranular | Y | Very Little | +++++ | + | - | |
| BKK-090 | Blinkklipkop | | Equigranular | Y | Very Little | +++++ | + | - | |
| BKK-091 | Blinkklipkop | | Vein Crystals | Y | Much | +++ | ++++ | - | |
| BKK-092 | Blinkklipkop | | Vein Crystals | Y | Much | +++ | ++++ | - | |
| BKK-093 | Blinkklipkop | | Equigranular | Y | Little | ++++ | ++ | - | |
| BKK-094 | Blinkklipkop | | Equigranular | Y | Some | ++++ | ++ | - | Some yellow powder in sample after separation |
| BKK-095 | Blinkklipkop | | Vein Crystals | Y | Little | +++ | +++ | - | |
| BKK-096 | Blinkklipkop | | Vein Crystals | Y | Much | ++++ | +++ | - | |

Table 29 continued

| Sample | Region | Mine | Rock Fabric | HMC (Yes/No) | Light Mineral Contribution | Hand Sample Mineralogy | | | |
|---|---|---|---|---|---|---|---|---|---|
| | | | | | | Hem | Qtz | Mica | Others |
| BKK-097 | Blinkklipkop | | Vein Crystals | Y | Much | ++++ | +++ | - | Some yellow powder in sample after separation |
| BKK-098 | Blinkklipkop | | Vein Crystals | Y | Much | ++++ | +++ | - | Some yellow powder in sample after separation |
| BKK-099 | Blinkklipkop | | Vein Crystals | Y | Much | ++++ | +++ | - | Some yellow powder in sample after separation |
| BKK-100 | Blinkklipkop | | Vein Crystals/Equigranular | Y | Much | ++++ | +++ | - | Some yellow powder in sample after separation |
| MAT-101 | Matsiloje | | Equigranular | Y | Little | ++ | ++++ | - | |
| MAT-102 | Matsiloje | | Equigranular | Y | Little | ++ | ++++ | - | |
| MAT-103 | Matsiloje | | Equigranular | Y | Little | ++ | ++++ | - | |
| MAT-104 | Matsiloje | | Equigranular | Y | Some | ++ | ++++ | - | |
| MAT-105 | Matsiloje | | Equigranular | Y | Much | +++ | +++ | - | Some possible magnetite |
| MAT-106 | Matsiloje | | Equigranular | Y | Much | +++ | +++ | - | |
| MAT-107 | Matsiloje | | Porphyritic | Y | Some | +++ | +++ | - | Some possible magnetite |
| MAT-108 | Matsiloje | | Vein Crystals /Equigranular | Y | Much | +++ | +++ | - | Some possible magnetite |
| MAT-109 | Matsiloje | | Porphyritic/Equigranular | Y | Some | +++ | +++ | - | |
| MAT-110 | Matsiloje | | Vein Crystals /Equigranular | Y | Much | +++ | ++++ | - | |
| MAT-111 | Matsiloje | | Vein Crystals | Y | Much | ++ | ++++ | - | |
| MAT-112 | Matsiloje | | Vein Crystals /Equigranular | Y | Very Little | +++ | +++ | - | |
| MAT-113 | Matsiloje | | Vein Crystals /Equigranular | Y | Much | +++ | +++ | - | |
| MAT-114 | Matsiloje | | Vein Crystals /Equigranular | Y | Little | +++ | +++ | - | |
| MAT-115 | Matsiloje | | Vein Crystals /Equigranular | Y | Little | +++ | +++ | - | |
| MAT-116 | Matsiloje | | Vein Crystals /Equigranular | Y | Some | +++ | +++ | - | |
| MAT-117 | Matsiloje | | Vein Crystals | Y | Some | +++ | +++ | - | |
| MAT-118 | Matsiloje | | Breccia | Y | Much | +++ | +++ | - | |
| MAT-119 | Matsiloje | | Breccia | Y | Much | +++ | +++ | - | |

Table 29 continued

| Sample | Region | Mine | Rock Fabric | HMC (Yes/No) | Light Mineral Contribution | Hand Sample Mineralogy | | | |
|---|---|---|---|---|---|---|---|---|---|
| | | | | | | Hem | Qtz | Mica | Others |
| MAT-120 | Matsiloje | | Breccia | Y | Much | +++ | +++ | - | |
| MAT-121 | Matsiloje | | Breccia | Y | Little | +++ | +++ | - | |
| TSO-122 | Tsodilo | Mike Main | Equigranular | Y | Some | ++++ | +++ | + | |
| TSO-123 | Tsodilo | Mike Main | Equigranular | Y | Some | ++++ | +++ | + | |
| TSO-124 | Tsodilo | Mike Main | Equigranular | Y | Some | ++++ | +++ | + | |
| TSO-125 | Tsodilo | Murphy | Equigranular | Y | Some | ++++ | +++ | + | |
| TSO-126 | Tsodilo | Murphy | Equigranular | Y | Some | ++++ | +++ | + | |
| TSO-127 | Tsodilo | Murphy | Equigranular | Y | Some | ++++ | +++ | + | |
| TSO-128 | Tsodilo | Water Hole | Schist | Y | Some | +++ | +++ | + | |
| TSO-129 | Tsodilo | Water Hole | Schist | Y | Little | ++++ | +++ | + | |
| TSO-130 | Tsodilo | Water Hole | Equigranular | N | None | +++++ | - | - | |
| TSO-131 | Tsodilo | Alec Campbell | Equigranular | Y | Much | ++ | ++++ | - | |
| TSO-132 | Tsodilo | Alec Campbell | Equigranular | Y | Some | +++ | +++ | - | |
| TSO-133 | Tsodilo | Alec Campbell | Equigranular | Y | Much | +++ | +++ | - | |
| TSO-134 | Tsodilo | Below Sex | Vein Crystals | Y | Some | ++++ | ++ | - | |
| TSO-135 | Tsodilo | Below Sex | Equigranular | Y | Very Little | +++++ | + | - | |
| TSO-136 | Tsodilo | Below Sex | Equigranular | Y | Some | +++++ | + | - | |
| TSO-137 | Tsodilo | Below Sex | Equigranular | Y | Some | +++++ | + | - | |
| TSO-138 | Tsodilo | Below Sex | Equigranular | Y | Some | ++++ | ++ | + | |
| TSO-139 | Tsodilo | Rhino Cave | Vein Crystals | N | Some | +++++ | + | - | |
| TSO-140 | Tsodilo | Rhino Cave | Schist | Y | Much | ++ | ++++ | + | Possible traces of kyanite |
| TSO-141 | Tsodilo | Rhino Cave | Schist | Y | Much | ++ | ++++ | + | |
| TSO-142 | Tsodilo | Lower Male | Schist | Y | Much | ++ | ++++ | + | |
| TSO-143 | Tsodilo | Lower Male | Schist | N | Some | +++++ | + | - | |

Table 29 continued

| Sample | Region | Mine | Rock Fabric | HMC (Yes/No) | Light Mineral Contribution | Hand Sample Mineralogy | | | |
|---|---|---|---|---|---|---|---|---|---|
| | | | | | | Hem | Qtz | Mica | Others |
| TSO-144 | Tsodilo | Lower Male | Schist | Y | Much | ++ | ++++ | + | |
| TSO-145 | Tsodilo | Upper Elephant | Equigranular | Y | Some | ++ | ++++ | - | |
| TSO-146 | Tsodilo | Upper Elephant | Equigranular/Vein Quartz | Y | Much | ++ | ++++ | + | Traces of kyanite present and possibly contaminated by mortar and pestle |
| TSO-147 | Tsodilo | Upper Elephant | Equigranular | Y | Some | ++ | ++++ | + | Traces of kyanite |
| TSO-148 | Tsodilo | Upper Elephant | Equigranular | Y | Much | ++ | ++++ | ++ | |
| TSO-149 | Tsodilo | Upper Elephant | Equigranular | Y | Some | ++ | ++++ | + | Traces of kyanite |
| TSO-150 | Tsodilo | Upper Elephant | Equigranular | Y | Some | ++ | ++++ | + | Traces of kyanite |
| TSO-151 | Tsodilo | Upper Elephant | Equigranular | Y | Much | ++ | ++++ | + | |
| TSO-152 | Tsodilo | Upper Elephant | Vein Quartz | Y | Much | +++ | +++ | + | Traces of kyanite |
| TSO-153 | Tsodilo | Upper Elephant | Equigranular | N | Much | +++++ | + | - | |
| TSO-154 | Tsodilo | Upper Male | Vein Quartz | N | Little | +++++ | + | - | |
| TSO-155 | Tsodilo | Upper Male | Schist | N | Much | ++++ | + | + | |
| TSO-156 | Tsodilo | Upper Male | Vein Quartz | N | Some | ++++ | + | - | Traces of kyanite |
| TSO-157 | Tsodilo | Upper Male | Equigranular | Y | Some | +++ | +++ | - | |
| TSO-158 | Tsodilo | Upper Male | Schist | Y | Some | +++ | +++ | + | |
| TSO-159 | Tsodilo | Upper Male | Equigranular | Y | Some | ++ | ++++ | + | |
| TSO-160 | Tsodilo | Upper Male | Vein Quartz | N | Very Little | +++++ | + | - | |
| TSO-161 | Tsodilo | Big Mine | Equigranular | Y | Some | +++ | +++ | + | |
| TSO-162 | Tsodilo | Big Mine | Schist | Y | Much | +++ | +++ | + | |
| TSO-163 | Tsodilo | Big Mine | Schist | Y | Some | ++ | +++ | + | |
| TSO-164 | Tsodilo | Big Mine | Schist | Y | Some | +++ | +++ | + | |
| TSO-165 | Tsodilo | Big Mine | Schist | Y | Some | +++ | +++ | + | |

Table 29 continued

| Sample | Region | Mine | Rock Fabric | HMC (Yes/No) | Light Mineral Contribution | Hand Sample Mineralogy | | | |
|---|---|---|---|---|---|---|---|---|---|
| | | | | | | Hem | Qtz | Mica | Others |
| TSO-166 | Tsodilo | Big Mine | Schist | Y | Little | +++ | +++ | ++ | |
| TSO-167 | Tsodilo | Big Mine | Equigranular | Y | Little | +++ | +++ | - | |
| TSO-168 | Tsodilo | Big Mine | Equigranular | Y | Little | +++ | +++ | + | |
| TSO-169 | Tsodilo | Near Sex | Schist | Y | Some | +++ | ++ | +++ | |
| TSO-170 | Tsodilo | Near Sex | Schist | Y | Much | ++ | ++ | +++ | |
| TSO-171 | Tsodilo | Near Sex | Schist | Y | Much | ++ | ++ | +++ | |
| TSO-172 | Tsodilo | Near Sex | Schist | Y | Much | ++ | ++ | +++ | |

HMC is whether Heavy Mineral Concentration was performed on the sample. Relative hand sample mineralogy was done by eye before crushing of sample and under 45x binocular microscope after crushing the sample but before heavy mineral concentration. (+++++) = mineral is <90% of the sample; (++++) = 50-89 %; (+++) = 20-49%; (++) = 5-19%; (+) = Trace amounts present; (-) = Not present or visible with binocular microscope.

During sample preparation, only Quartz, Hematite, Muscovite, and Kyanite were identifiable. Garnet that was visible in petrographic slides was not visible at these scales.

Rock Fabric indicates the general rock type or fabric at the scale of the sample. Some samples include parts of Vein crystals and adjacent matrix rock. At Tsodilo, Dikgatlampi, and Sebilong the equigranular rock type is a quartzite or meta-sandstone while at Blinkklipkop and Matsiloje the equigranular rock type is a metamorphosed Banded Iron Formation rhythmite. At Blinkklipkop, all samples are brecciated at larger scales, but some samples are from single clasts of BIF.

Light mineral contribution is the subjective and relative contribution of light (non-hematite) minerals to the powdered sample after heavy mineral concentration. Very Little and None indicate only traces of other minerals in the rock were visible to the naked eye and the powder was very dark red or purple. Some indicates that there were some other minerals visible to the eye and the powder had a purple/red appearance that was not as dark as a very pure sample. Much indicates that there was a large contribution of lighter minerals visible to the naked eye and the powder was a reddish or purplish gray to white color. This factor was only judged systematically for the samples indicated.